

**EFFECTS OF EVAPORATOR GEOMETRY AND
WORKING FLUIDS ON THE PERFORMANCE OF A
TWO-PHASE LOOP THERMOSYPHON**

A Thesis



Submitted by

NAZMOON NAHER

A Thesis

Submitted to the Department of Mechanical Engineering
In Partial Fulfillment of the Requirements for the Degree of
MASTER OF SCIENCE IN MECHANICAL ENGINEERING



DEPARTMENT OF MECHANICAL ENGINEERING
BANGLADESH UNIVERSITY OF ENGINEERING & TECHNOLOGY

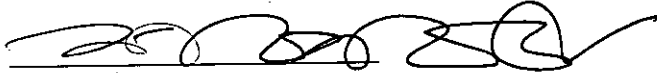
Dhaka – 1000, Bangladesh

March, 2009

RECOMMENDATION OF THE BOARD OF EXAMINERS

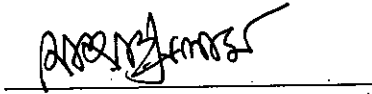
The thesis titled '**EFFECTS OF EVAPORATOR GEOMETRY AND WORKING FLUIDS ON THE PERFORMANCE OF A TWO-PHASE LOOP THERMOSYPHON**', submitted by Nazmoon Naher, Roll No. 040310033F, Session: April 2003, has been accepted as satisfactory in partial fulfillment of the requirement for the degree of **Master of Science in Mechanical Engineering** on March 8, 2009.

BOARD OF EXAMINERS



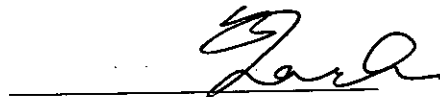
Dr. M. A. Rashid Sarkar
Professor
Department of Mechanical Engineering
BUET, Dhaka

Chairman
(Supervisor)



Dr. Md. Ashraful Islam
Professor
Department of Mechanical Engineering
BUET, Dhaka

Member



Dr. Abu Rayhan Md. Ali
Professor and Head
Department of Mechanical Engineering
BUET, Dhaka

Member
(Ex - officio)




Dr. Mohammad Alauddin
Professor
Department of Mechanical Engineering
DUET, Dhaka

Member
(External)

CERTIFICATE OF RESEARCH

This is to certify that the work presented in this thesis is carried out by the author under the supervision of Dr. M. A. Rashid Sarkar, Professor of Department of Mechanical Engineering, Bangladesh University of Engineering & Technology, Dhaka.



Dr. M. A. Rashid Sarkar



Nazmoon Naher

CANDIDATE'S DECLARATION

It is hereby declared that this thesis or any part of it has not been submitted elsewhere for the award of any degree or diploma.

Naher

Nazmoon Naher

Roll No. 040310033F

ACKNOWLEDGMENT

The author wishes to express the sincerest gratitude and indebtedness to Dr. M. A. Rashid Sarkar, Professor, Department of Mechanical Engineering, Bangladesh University of Engineering & Technology (BUET), Dhaka, for his continuous guidance, inspiration and supervision support throughout this research work. Special thanks are due to Professor Dr. Md. Ashrafur Islam for his constructive suggestions and kindly examining the manuscript and offering valuable comments.

The author gratefully acknowledges the contribution of Rayhan Ahmed and Sharif Md. Yousuf Bhuiyan for their cooperation at the all stages of this research works.

The author acknowledges his gratefulness to the Mechanical Department for providing required facilities. The author is thankful to Mr. Alauddin Fakhir, Heat Transfer Lab, BUET for his cooperation.

ABSTRACT

A two-phase loop thermosyphon had been experimented with a view to cooling electronic components that dissipate high heat flux. Loop thermosyphon is a device consisting of an evaporator, condenser, reservoir, two check valves and forward and return lines connecting the evaporator and condenser. Experiments were conducted to assess the effects of working fluids and evaporator geometry on the performance of a two-phase loop thermosyphon. Three different working fluids were used in this study, namely water, ethanol and methanol. Boiling heat transfer was studied for different geometry of evaporator surfaces. The evaporator surface temperature, condenser inlet and outlet temperatures and cycle time were measured at a regular interval of 10 second in this study for different working fluids.

The experimental results are obtained at different heat input levels which are varied from 120W to 300W with an increment of 15W for the filling volume of approximately 100%. The temperatures of evaporator surfaces and heat fluxes on the basis of heat surface area are measured, determined and discussed.

NOMENCLATURE

A_e	Evaporator surface area, m^2
C_{pl}	Specific heat of saturated liquid, $J/kg \cdot ^\circ C$
C_{sf}	Coefficient for various liquid surface combinations
g	Gravitational acceleration, m/s^2
h	Boiling heat transfer coefficient, $W/m^2 \cdot ^\circ C$
h_{fg}	Enthalpy of vaporization, J/kg
k	Thermal conductivity of material, $W/m \cdot ^\circ C$
Pr_l	Prandtl number of saturated liquid
Q	Heat input, W
q	Heat flux, W/cm^2
q_{conv}	Heat loss by convection, W
q_{radi}	Heat loss by radiation, W
q_L	Total heat loss, W
q_{crit}	Critical heat flux, W/m^2
q_E	Heat flux per unit area after deducting heat loss, W/cm^2
q_R	Heat flux from Rohsenow correlation, W/cm^2
r	Radius, cm
R	Thermal resistance, $^\circ C/W$
t	Time, Sec
t_{ct}	Cycle completion time, Sec
T_a	Ambient temperature, $^\circ C$
T_{Cin}	Condenser inlet temperature, $^\circ C$
T_{Cout}	Condenser outlet temperature, $^\circ C$
T_E	Evaporator surface temperature, $^\circ C$
T_{sat}	Saturation temperature of working fluids, $^\circ C$
ΔT_{sat}	Wall superheat or temperature excess, $^\circ C$
μ_l	Liquid viscosity, $kg/m \cdot s$
ρ_l	Density of saturated liquid, kg/m^3
ρ_v	Density of saturated vapor, kg/m^3
σ	Surface tension of liquid-vapor interface, N/m
U_t	Overall heat-transfer coefficient, $W/m^2 \cdot ^\circ C$

ABBREVIATION

AC	Alternating Current
ALPHA	American Loop Heat Pipe
CHF	Critical Heat Flux
CPL	Capillary pumped Loop
CPU	Central Processing Unit
LHP	Loop Heat Pipe
LT	Loop Thermosyphon
MAP	Maximum Applicable Power
ODP	Ozone Depleting Potential
PC	Personal Computer
THTT	Thermoloop Heat Transfer Technology
TPLT	Two-Phase Loop Thermosyphon

CONTENTS

Declaration	iv
Acknowledgement	v
Abstract	vi
Nomenclature	vii
List of Tables	xi
List of Figures	xii
CHAPTER-1 INTRODUCTION	1
1.1 General	1
1.2 Motivation	2
1.3 Objectives	4
CHAPTER-2 LITERATURE REVIEW	5
2.1 Background	5
2.2 Regimes of Subject Matter	8
2.2.1 Pool Boiling	8
2.2.2 Boiling Curve	8
2.2.3 Rohsenow Correlation	10
2.2.4 Kutateladze Correlation	10
2.3 Two-Phase Loop Thermosyphon	11
2.3.1 Different Types of Cooling Devices	12
2.3.2 Application	16
2.4 Loop Thermosyphon Compared to Heat Pipe	17
2.4.1 Heat Pipe	18
2.4.2 Loop Thermosyphon	18
2.5 Considerations When Choosing Working Fluid	18
CHAPTER-3 EXPERIMENTAL SETUP AND WORKING PROCEDURE	21
3.1 Experimental Apparatus	22
3.1.1 Loop Thermosyphon	22
3.1.1(i) Evaporator	22
3.1.1(ii) Forward Tube	24

3.1.1(iii) Condenser	25
3.1.1(iv) Reservoir	26
3.1.1(v) In-valve	27
3.1.1(vi) Out-valve	27
3.1.1(vii) Return tube	27
3.1.2 Measuring Apparatus	28
3.1.3 Copper Block	29
3.1.4 Heaters	29
3.2 Working Fluid	30
3.3 Experimental Procedure	31
3.4 Performance Parameter	34
CHAPTER-4 RESULTS AND DISCUSSION	35
4.1 Heat Transport Characterization	36
4.2 Effect of Input Power on Performance Limit	38
4.3 Effect of Working Fluid on Various Parameters	40
4.3.1 Heat Transport Time	40
4.3.2 Thermal Resistance	40
4.3.3 Overall Heat Transfer Co-Efficient	41
4.3.4 Evaporator Surface Temperature	41
4.3.5 Condenser Wall Temperatures	42
4.4 Enhancement of Heat-Transfer in the Evaporator Part of Thermosyphon	42
4.5 Various Effects on the System	44
4.5.1 Non-Return Valves	44
4.5.2 Liquid Fill Volume	44
4.6 Exceptional Behavior of Working Fluid Methanol	45
CHAPTER-5 CONCLUSIONS AND RECOMMENDATIONS	65
5.1 Conclusions	65
5.2 Recommendations	66
REFERENCES	67
APPENDIX-A Sample Calculations	A1-A6
APPENDIX-B Experimental Data	B1-B7

LIST OF TABLES

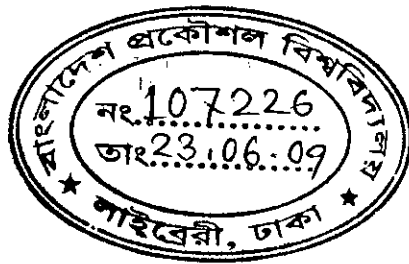
Table 3.1	The dimension and geometric features of the evaporators used in the experiment	23
Table 3.2	Dimension and geometric features of the forward tube	25
Table 3.3	Dimension and geometric features of the condenser	25
Table 3.4	Dimension and geometric features of the return tube	28
Table 3.5	Dimension of the copper block	29
Table 3.6	Details information of the heaters used in the experiment	30
Table 3.7	Boiling point and latent heat of vaporization for three working fluids	30
Table 3.8	Important properties of the working fluids at atmospheric pressure	32
Table 4.1	Average evaporator surface temperature and cycle completion time for different evaporator surface geometry and water as the working fluid	36
Table 4.2	Thermal performance data for Geometry-1 and Water as working fluid	38
Table 4.3	Thermal performance data for Geometry-1 and Ethanol as working fluid	39
Table 4.4	Thermal performance data for Geometry-1 and Methanol as working fluid	39
Table 4.5	The heat fluxes per unit area after deducting heat loss and from Rohsenow Correlation	43

LIST OF FIGURES

Figure 2.1	General pool boiling curve	9
Figure 2.2	Two-phase loop thermosyphon	12
Figure 2.3	Schematic of a wicked tubular heat pipe	13
Figure 2.4	Schematic of a wickless pulsating heat pipe	14
Figure 2.5	Schematic of a wickless tubular thermosyphon	15
Figure 2.6	Schematic of an indirect thermosyphon loop	15
Figure 2.7	Schematic of an immersion thermosyphon loop	16
Figure 2.8	Pressure along the distance of heat pipe and loop thermosyphon	17
Figure 3.1	Experimental setup	21
Figure 3.2	Evaporators used for (a) Geometry-1 (b) Geometry-2 (c) Geometry-3	24
Figure 3.3	Evaporator surface (geometry-1)	24
Figure 3.4	Condenser	26
Figure 3.5	Reservoir	27
Figure 3.6	In-Valve and Out-Valve	27
Figure 3.7	Copper block- heater assembly	29
Figure 3.8	Heaters	30
Figure 4.1	Variation of evaporator wall temperature with time for different working fluid with a input power of 150W (Geometry: 1)	47
Figure 4.2	Variation of evaporator wall temperature with time for different working fluid with a input power of 150W (Geometry:2)	47
Figure 4.3	Variation of evaporator wall temperature with time for different working fluid with a input power of 150W (Geometry:3)	48
Figure 4.4	Variation of evaporator wall temperature for different evaporator surface geometry with water as the working fluid	48
Figure 4.5	Variation of evaporator wall temperature for different evaporator surface geometry with ethanol as the working fluid	49
Figure 4.6	Variation of evaporator wall temperature for different evaporator surface geometry with methanol as the working fluid	49
Figure 4.7	Comparison of cycle completion time for different working fluid (water, ethanol, methanol) at input powers of 210W & 240W (Geometry:1)	50

Figure 4.8	Temperatures during five consecutive cycles (6 to 10) for geometry-1 and water as the working fluid	50
Figure 4.9	Temperatures during five consecutive cycles (6 to 10) for geometry-1 and ethanol as the working fluid	51
Figure 4.10	Temperatures during five consecutive cycles (6 to 10) for geometry-1 and methanol as the working fluid	51
Figure 4.11	Variation of average evaporator wall temperature with input power for three working fluids (Geometry: 2)	52
Figure 4.12	Effect of input power on cycle time for different working fluid (Geometry: 1)	52
Figure 4.13	Effect of input power on cycle time for different working fluid (Geometry: 2)	53
Figure 4.14	Effect of input power on cycle time for different working fluid (Geometry:3)	53
Figure 4.15	Effect of working fluid on overall heat transfer coefficient for geometry-1	54
Figure 4.16	Effect of working fluid on overall heat transfer coefficient for geometry-2	54
Figure 4.17	Effect of maximum evaporator wall temperature on different working fluid and different evaporator surface geometry for input power of 180W	55
Figure 4.18	Variation of evaporator wall temperature with time for different input power with ethanol as the working fluid (Geometry:2)	55
Figure 4.19	Variation of evaporator wall temperature with time for different input power with methanol as the working fluid (Geometry:2)	56
Figure 4.20	Variation of evaporator wall temperature with time for different input power with water as the working fluid (Geometry:2)	56
Figure 4.21	Effect of working fluid on condenser wall temperatures for geometry-1	57
Figure 4.22	Effect of working fluid on condenser wall temperatures for Geometry-2	57
Figure 4.23	Effect of working fluid on condenser wall temperatures for	58

	geometry-3	
Figure 4.24	Effect of input power on cycle time for different evaporator surface geometry with ethanol as the working fluid	58
Figure 4.25	Effect of input power on cycle time for different evaporator surface geometry with methanol as the working fluid	59
Figure 4.26	Effect of input power on cycle time for different evaporator surface geometry with water as the working fluid	59
Figure 4.27	Effect of input power on thermal resistance for geometry-1 and water as the working fluid	60
Figure 4.28	Effect of input power on thermal resistance for geometry-1 and methanol as the working fluid	60
Figure 4.29	Effect of input power on thermal resistance for geometry-1 and ethanol as the working fluid	61
Figure 4.30	Variation in the maximum condenser inlet temperature with increasing input power for different working fluids (Geometry:2)	61
Figure 4.31	Effect of working fluids on first cycle time for geometry-1	62
Figure 4.32	Variation in the maximum condenser outlet temperature with increasing input power for different working fluids (Geometry:2)	62
Figure 4.33	Temperature diagram for ethanol, 120W as heat power rate (Geometry:2)	63
Figure 4.34	Effect of average evaporator wall temperature on different evaporator surface geometry with ethanol as the working fluid	63
Figure 4.35	Effect of temperatures on time for working fluid methanol at a input power of 240W (Geometry:2)	64



INTRODUCTION

1.1 GENERAL

Advances in the field of semiconductor electronics have resulted in a significant increase in the number of active devices per unit chip area. The dissipated heat flux from these electronic devices has correspondingly increased. The current heat dissipation rate for some desktop computers is 20 W/cm^2 . It is expected that microprocessor chips for some of the next generation workstations would dissipate $50\text{-}100 \text{ W/cm}^2$ [1]. Developments of efficient thermal management schemes are essential to dissipate these high heat fluxes. Liquid cooling, with phase change, is a very efficient heat transfer process and is a good alternative to existing air-cooled designs. The direct immersion cooling has been considered as a promising method for such application because it removes a large amount of heat effectively. However, application of such cooling method to the high-speed microprocessor is not as easy task because of difficulties in maintenance and reliability. As an alternative, an ingenious air cooled thermosyphon module and an indirect liquid-cooling thermosyphon have been proposed for cooling high-density electronic packaging. A historical overview on thermal control of electronic components by heat pipes and two-phase closed thermosyphon was presented by Rossi and Polasek [2].

Modern electronic components are generally air-cooled by either free or forced convection. Fans attached to the central processing unit are the most popular cooling devices for low power dissipation systems. They are popular because of reliability, cost, efficiency and ease of manufacturing and implementation. However, for higher frequency chips (above 1000 MHz), the air-cooled heat sinks have some limitations due to its size, noise and insufficient cooling performance. As a result, current practice of dense packaging of electronics in compact spaces demands novel ways of heat dissipation [3], which will be able to dissipate as much as 100 W/cm^2 at chip levels while maintaining the device at acceptable temperatures, typically below 85°C . One of the proposed solutions [4] for dissipating high heat fluxes is the use of liquid cooling techniques. Two-phase heat transfer is a very attractive liquid cooling process, as high

heat fluxes can be removed through vaporization of the fluid in an evaporator attached to or enclosing the heat source, but the added process of condensing the vapor and bringing it back to the evaporator adds complexity in the system.

The increasing importance of thermal energy transfer technology is dedicated by the broadening of areas of its application including: cooling semiconductor devices, fuel-cells, electrical and electronic devices, air conditioning, solar energy collection, motor and engine cooling, manufacturing processes, heat recovery and thermal management in outer-space structures. These application looks for a common requirement, which is to facilitate and control thermal energy transportation at higher heat flux level over longer distance while maintaining a moderate device temperature. In the phase-change heat transfer devices, the motive power behind the condensate return has been derived mainly by one of two natural forces: Gravity, used in Thermosyphon and Force of capillary action, used in heat pipe. Both systems have advantages including: self-starting, self-regulating, passive, no moving parts, and very quiet while in operation. Thermosyphon has a major limitation as its operation and performance is dependent on gravity and relative position of its components. The major constrain of heat pipe is the relative weakness of capillary force, which can pull condensate through capillary passageway only very slowly, limiting the rate of thermal energy transfer.

Two-phase loop thermosyphon is a newly invented and improved heat transfer technology [5] to address high-end electronics cooling and cooling needs for other industries. A two-phase loop thermosyphon is a passive, self-actuating and very highly efficient heat transfer device that necessarily can overcome the above performance limitations of phase change heat transfer devices.

1.2 MOTIVATION

The quick growth in the use of electronic packaging has created critical values on the maximum heat flux dissipation, in comparison with the devices cooled by forced air. Heat pipes, LHPs, and CPLs are really the most efficient cooling devices, but their high cost can limit their use in commercial devices. Recent innovations, in loop thermosyphons design, have had a relevant impact on the electronic equipment thermal control for high-density desktop computers, but one of the most critical topics of this device is the gravity dependence on its heat transfer properties. For this reason some

particular devices, named Two-Phase Loop Thermosyphons, operating against gravity with the use of passive systems are developed. The main advantages, with the use of passive systems for heat transport devices are: energy saving, Safety (in case of use of toxic fluids), lower maintenance due to the absence of rotating elements, a possible miniaturization of the device.

Thermosyphon loops, where the evaporator is connected to the condenser by a couple of individual channels, one for the liquid flow and the other for the vapor flow. Loop thermosyphon does not use capillary pump or gravity for condensate return. Pressure increase due to evaporation and pressure decrease due to condensation inside the device is mechanically utilized for vapor transfer and condensate return in a closed loop path for thermal energy transportation. This device is able to overcome some of the major performance limitations (that is mentioned previously) of existing passive phase-change heat transfer devices, and significantly increase heat transfer capacity. A typical heat flux of a Loop Thermosyphon device useful for electronics cooling is in the range of $500\text{-}1000\text{ W/cm}^2$, compared to $50\text{-}100\text{ W/cm}^2$ of a comparable heat pipe. Nucleate pool boiling takes place inside evaporator of this device at constant pressure, so the device is able to maintain almost constant evaporator temperature at variable thermal loads. Due to strong vapor transfer and condensate return force, this device can operate almost independent of gravity and orientation, and can transfer heat over longer distance with lower temperature drop.

To design effective devices for heat transfer augmentation and temperature control, scientists all over the world have been paying their attention for many years on different types of geometric arrangements. Among those devices, thermosyphon is the one, which has been being studied since the middle of last century due to its high effective heat transfer co-efficient. Some highlighted studies are being described here and remaining works about thermosyphon will be described more elaborately in the Chapter-2. Mudawar and Anderson [6] performed pool boiling studies using structures with multiple levels of enhancement and dielectric fluorinerts as the working fluid (FC-72 and FC-87). The maximum heat flux attained with the same structure, with a surface temperature below 85°C was $\sim 105\text{ W/cm}^2$. Most recently, Rahman et al. [7] analyzed the performance of a pulsated two-phase loop thermosyphon that operates against gravity. The fill ratio tested were 30%, 50% and 60%. Those results showed that the

liquid fill volume has negligible effect on the boiling performance of enhanced structure.

1.3 OBJECTIVES

The objectives of the present research work are as follows:

- a) To study the effect of evaporator geometry on the performance of the loop thermosyphon.
- b) To study the effects of different working fluids (water, ethanol and methanol) on the performance of thermoloop.
- c) To compare the results of this experiment with those of similar previous works.

LITERATURE REVIEW

In recent years, the two-phase heat transfer devices used for heat dissipation and homogeneous temperature of computer and numerous electronic instruments has displayed its remarkable effect. So a thorough investigation on two-phase heat transfer device is indispensable for further development and improvement of its performance.

2.1 BACKGROUND

During the 1980s, direct liquid cooling emerged as one of the most promising thermal management techniques for electronic systems. Many observers were believed that, direct liquid cooling with inert, dielectric liquids will become the method of choice for the thermal management of advanced computers. A clear understanding of the available empirical data and relevant heat transfer theories is an essential prerequisite for successful application of this technique. Following a brief survey of electronic packaging trends, attention is turned to the many options indirect liquid cooling and to the selection of coolants for electronic systems. Next, single-phase natural and forced convection, including impinging and streaming flow are reviewed and the best available correlations presented.

The wide spread acceptance of water-cooled mainframe computers and the continuing rise in component heat dissipation has spurred extensive research and development of advanced thermal control techniques for microelectronics. While many distinct approaches are under investigation, much of the activity is focused on [8],[9] the minimization of thermal "contact" resistances at lightly loaded, solid-solid interfaces and [10] the elimination of these resistances through the use of direct liquid cooling. Despite the large thermal management capability of water-cooled systems, it has become apparent that the chip and board-level heat fluxes, as well as the functional and thermal density projected for computing platforms, pose serious challenges to indirect liquid cooling technology. While considerable momentum, know-how, and design experience has been gained, very substantial improvements in cold-plate and thermal interface designs, as well as in the manufacturing and assembly procedures for multi-

chip modules, required if water cooling is to continue to dominate the thermal management of high-performance computers.

Katto et al. [11] examined the effect of placing a plate parallel to the boiling surface, at very close distances (0.2-10mm), with saturated distilled water as the working fluid. The boiling surface was a 11mm diameter horizontally oriented copper plate with a parallel coaxial glass plate. They found degradation in the heat transfer performance with reduction of vapor space. Nowell et al. [12] conducted a similar study with a micro configured heat sink (1 cm² base area) in FC-72. Their heat sink was etched in silicon and was oriented vertically. The parallel plate was also made of silicon and the distance was varied from 1-6mm. Results showed an improvement in heat transfer performance with a reduction in the gap. For the 1mm gap, the performance was very similar to pool boiling. They attributed this improvement to a local thermosyphon effect, where some of the vapor generated was condensed at the parallel plate.

Githinji and Sabersky [13] found that the pool boiling performance improved with an increase in the inclination angle of the heater surface. Nishikawa et al. [14] tested the boiling performance of a copper surface in water, in the range of inclination from 0° to 175° from horizontal. In 1996, Palm and Tengblad [8] tested several prototypes of thermosyphons with single and multiple evaporators. To accommodate the higher heat fluxes, enhancement schemes have been used in the evaporator section. Webb et al. [15] have used enhance surfaces in the evaporator and condenser sections of a thermosyphon for cooling the hot side of thermoelectric coolers. Using a "bent-fin" structure, they have achieved a heat flux of about 18 W/cm² in refrigerant R-134a.

Ramaswamy et al. [1] studied the combined effects of pressure and sub-cooling on the performance of two- chamber thermosyphons with gradually increasing heat fluxes. Yuan et al. [16] took the concept further and studied the effects of imposed circulation and location of condenser on the performance of a two-phase thermosyphon in a confined space.

A lot of cooling equipment based on two phase heat transfer devices have been developed in a recent past [17], [18]. For example Xie et al. [19] proposed a heat pipe to connect the Pentium processors surface with a cooling plate surface located on the

back of the video in a notebook. Other solutions with cylindrical heat pipes have been recently studied in [20].

Miniature flat heat pipe applications have been studied by Krustalev and Faghri [21], Kaya and Hoang [22] and Ponappan [23]. In particular the last one shows the performance of 12.7X6.35X107.9mm heat pipe able to dissipate a heat flux of 142 W/cm² with a temperature difference evaporator-condenser of 22K.

Recently micro heat pipes have been studied and applied for the chip cooling by Peterson et al. [24], Wu et al. [25] and Shen et al. [26]. The typical diameter of a micro heat pipe is 10-100 μ m but the maximum heat transfer rate is 0.3 W. A review of this innovative technique is reported in [27], while some critical aspects are well described in [28].

Other devices as Loop Heat Pipes and Capillary Pumped Loops, developed for low gravity applications, are proposed at the moment for terrestrial application too, because they have good heat transfer performance any way located respect to the gravity. Some interesting application of LHPs are reported in [29]-[30] while CPLs applications in [31].

In 2001 Chen and Lin [32] showed a CPL to cool a Pentium processor using FC 72 as working fluid instead of water. This solution allows an approach with direct cooling technique, which presents lower thermal resistances. The maximum heat transfer rate is 30W (2W/cm²) with the condenser at the same level of the evaporator. However, in this case, the temperature of the chip grows up till a value of 115^oC.

Garner and Patel [33] looked into the applications of loop thermosyphon in high-density packaging. Webb and Yamauchi [34] demonstrated a system capable of dissipating 100W from a single CPU system. Pal et al. [35] experimentally investigated the effect of working fluids and the inclination of the thermosyphons for the cooling of a Pentium-4 microprocessor in a Hewlett Packard Vetra PC with a peak heat dissipation of 80W.

Alam [36] performed few experimental tests identifying the key performance parameters and named it the thermoloop. The result of these works showed the prospect of loop thermosyphon as the future solution of high-density electronics cooling in the respect of cost competitiveness, heat dissipation capacity and flexibility of design.

Most recently, Rahman [37] analyzed the performance of a pulsated two-phase loop thermosyphon that operates against gravity. Rahman experimentally investigated how the variation of liquid fill ratio of the evaporator and convection condition of the condenser influence the performance of the thermoloop. He also reported that the time for the completion of heat transport cycle increases with evaporator fill ratio and that the maximum temperature of the evaporator does not vary considerably. The maximum pressure developed within the system increases with increasing evaporator fill ration for both type of condenser convection (natural/forced) conditions.

2.2 REGIMES OF SUBJECT MATTER

2.2.1 Pool Boiling

Boiling at the surface of a body immersed in an extensive pool of motionless liquid is generally referred to as pool boiling. This type of boiling process is encountered in a number of applications, including metallurgical quenching processes, flooded tube and shell evaporators, immersion cooling of electronic components and boiling of water in a pot on the burner of a stove. The nature of pool boiling process varies considerably depending on the conditions at which boiling occurs. The level of heat flux, the thermo physical properties of the liquid and vapor, the surface material and finish and the physical size of the heated surface all may have an effect on the boiling process.

2.2.2 Boiling Curve

The regimes of pool boiling are most easily understood in terms of the boiling curve; a plot of heat flux q versus wall superheat $T_E - T_{sat}$ for the circumstances of interest. The different regions of boiling are indicated in Fig.2.1 where heat-flux data from an electrically heated platinum wire submerged in water are plotted against wall superheat. In region I free convection currents are responsible for motion of the fluid near the

surface. In this region the liquid near the heated surface is superheated slightly and it subsequently evaporates when it rises to the surface. In region II bubbles begin to form on the surface of the wire and are dissipated in the liquid after breaking away from the surface. This region indicates the beginning of nucleate boiling. As the temperature excess is increased further bubbles form more rapidly and rise to the surface of the liquid where they are dissipated. This is indicated in region III. Eventually, bubbles are formed so rapidly that they blanket the heating surface and prevent the inflow of fresh liquid from taking their place. At this point the bubbles coalesce and form a vapor film, which covers the surface. The heat must be conducted through this film before it can reach the liquid and affect the boiling process. The thermal resistance of this film causes a reduction in heat flux, and this phenomenon is illustrated in region IV, the film-boiling region. This region represents a transition from nucleate boiling to film boiling and is unstable. Stable film boiling is eventually encountered in region V. The surface temperatures required to maintain stable film boiling are high and once this condition is attained, a significant portion of the heat loss by the surface may be the result of thermal radiation, as indicated in region VI.

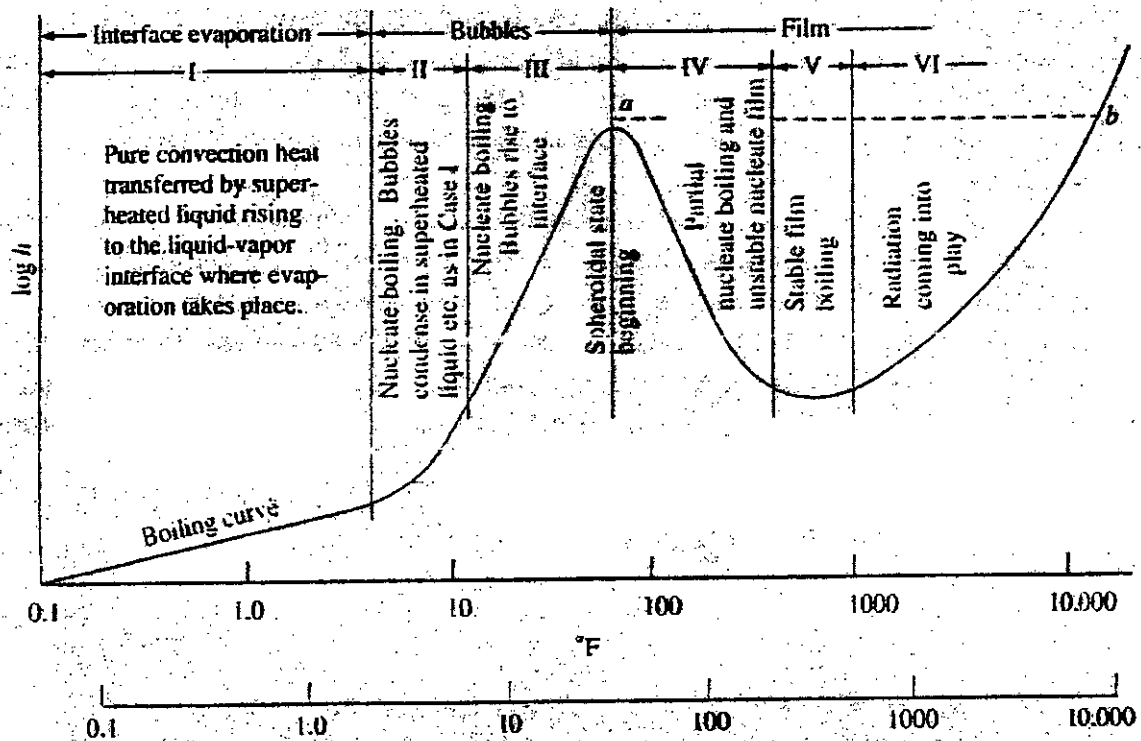


Figure 2.1: Boiling Curve

2.2.3 Rohsenow Correlation

Many of the very early models of the nucleate boiling process were based on the assumption that the process of bubble growth and release induced motion of the surrounding liquid facilitated convective transport of heat from the adjacent surface. Perhaps the most successful application of this approach was made by Rohsenow, who postulated that heat flows from the surface first to the adjacent liquid, as in any single phase convection process and that the high heat transfer coefficient associated with nucleate boiling is a result of local agitation due to liquid flowing behind the wake of dependent bubbles. Rohsenow (1955) correlated experimental data for nucleate pool boiling as follows.

$$\frac{C_{p,l} \Delta T_{sat}}{h_{fg} Pr,l^n} = C_{s,f} \left[\frac{q_R}{\mu_l h_{fg}} \sqrt{\frac{\sigma}{g(\rho_l - \rho_v)}} \right]^{0.33}$$

Where, $C_{p,l}$ = specific heat of saturated liquid, J/kg.K

ΔT_{sat} = wall superheat = $T_E - T_{sat}$, °C

h_{fg} = enthalpy of vaporization, J/kg

Pr,l = Prandtl number of saturated liquid

n = 1.0 for water and 1.7 for other liquids

$C_{s,f}$ = coefficient for various liquid surface combinations

q_R = heat flux from Rohsenow correlation, W/m².

μ_l = liquid viscosity, kg/m.s

σ = surface tension of liquid-vapor interface, N/m

g = gravitational acceleration, m/s²

ρ_l = density of saturated liquid, kg/m³

ρ_v = density of saturated vapor, kg/m³

2.2.4 Kutateladze Correlation

Kutateladze (1948) apparently was among the first investigators to note the similarity between flooding phenomena in distillation columns and the CHF condition in pool boiling. He used dimensional analysis arguments to derive the following relation for the maximum heat flux.

$$q_{crit} = C_k \rho_v^{1/2} h_{fg} [g(\rho_l - \rho_v)\sigma]^{1/4}$$

Where q_{crit} = critical heat flux, W/m^2

ρ_v = density of saturated vapor, kg/m^3

h_{fg} = enthalpy of vaporization, J/kg

σ = Surface tension of liquid-vapor interface, N/m

g = gravitational acceleration, m/s^2

ρ_l = density of saturated liquid, kg/m^3

$C_k = 0.16$, constant for pool boiling

2.3 TWO-PHASE LOOP THERMOSYPHON

Two-phase loop thermosyphons are devices that use gravity to maintain the two-phase fluid circulation when a thermosyphon is operating. Sasin et al. [38] was first realized the idea of a loop thermosyphon, a particular pump-less heat transfer device operating against gravity without any capillary structure. It is necessary for some electronic applications (for example, server boards) to have loop thermosyphons operating in strictly horizontal orientation with the evaporator at the same level with the condenser and horizontal transport lines. While the fluid flow through the transport lines is maintained due to the difference between the liquid levels in the evaporator and condenser, the present study relates to an apparatus which allows operation of loop thermosyphons in horizontal orientation and independent on gravity.

Two-phase loop thermosyphon uses liquid as a working fluid for indirect and direct cooling. The loop thermosyphon as shown in Fig 2.2 consists of an evaporator chamber, a vapor outlet tube called the forward tube, a condenser and a return tube connecting the condenser outlet with the evaporator inlet. The evaporator chamber houses a boiling enhancement structure soldered to the inside surface of the evaporator bottom. It is a closed loop with water or a fluid similar to ethanol or methanol as its working fluid. The system removes the heat from the electronics by interfacing through the bottom of the evaporator chamber causing the working fluid to heat up and reach boiling conditions where vapor bubbles start to form. The working fluid vapor then travels to the top of the evaporator chamber and into the condenser via the forward tube where it gets condensed and returns to the evaporator chamber via the return tube and the cycle continues.

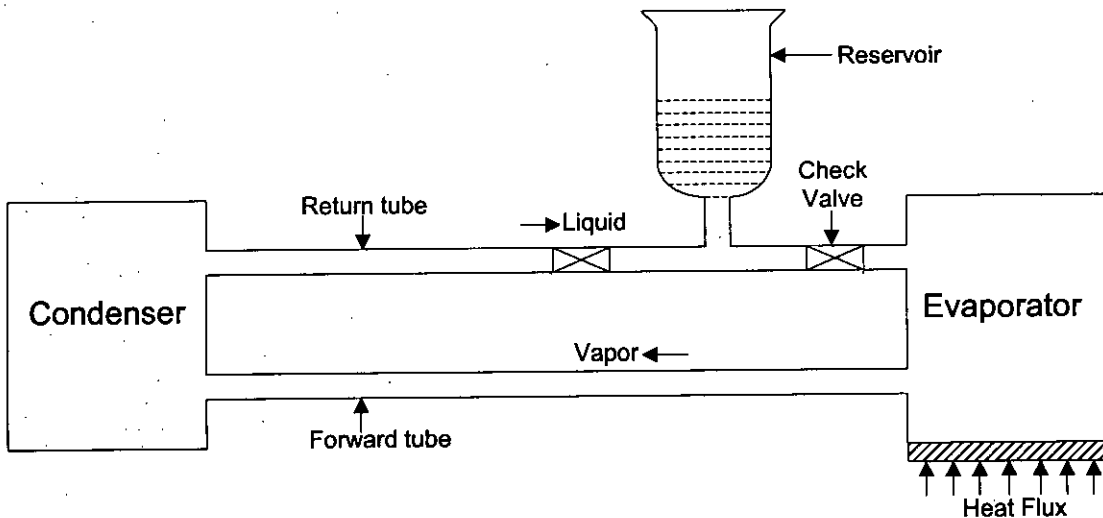


Figure 2.2: Two-phase Loop Thermosyphon

2.3.1 Different types of cooling devices

Cooling systems based on the principle of two-phase change (evaporation/boiling, condensation) of a heat transfer medium in a closed space are progressively eroding the use of standard air and liquid (one-phase) coolers in the thermal control of electronic equipment. These two-phase heat transfer element fall into two families

A. Pumped liquid coolers; where a pump supplies an evaporator with the liquid. They usually feature either forced liquid evaporation or boiling in their evaporator part. Such coolers can be further designed as

1. Indirect coolers, when the electronic equipment is attached to the outer surface of the evaporator part (usually called cold plates).
2. Immersion coolers, when the electronic equipment is directly submerged in the liquid in the evaporator part.

B. Passive coolers (without any forced pumping action), with film evaporation or pool boiling of the liquid in the evaporator part. These passive two-phase heat transfer scaled elements are divided into three groups according to the return of the liquid from the cooled part (condenser) to the evaporator [39].

1. Wicked heat pipes, where a wick on the inner wall of the cooler serves as a capillary pump (Fig. 2.3)

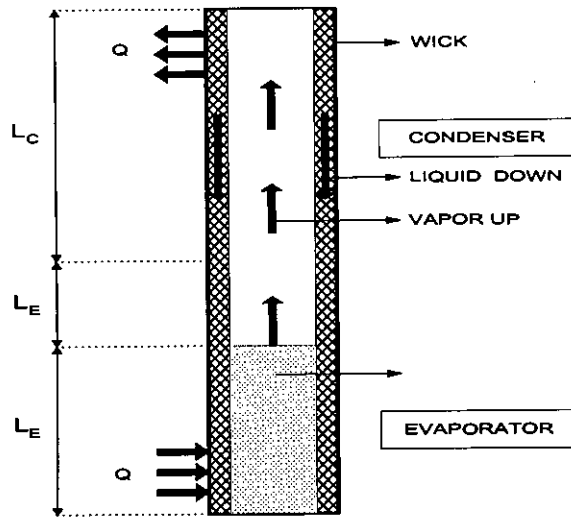
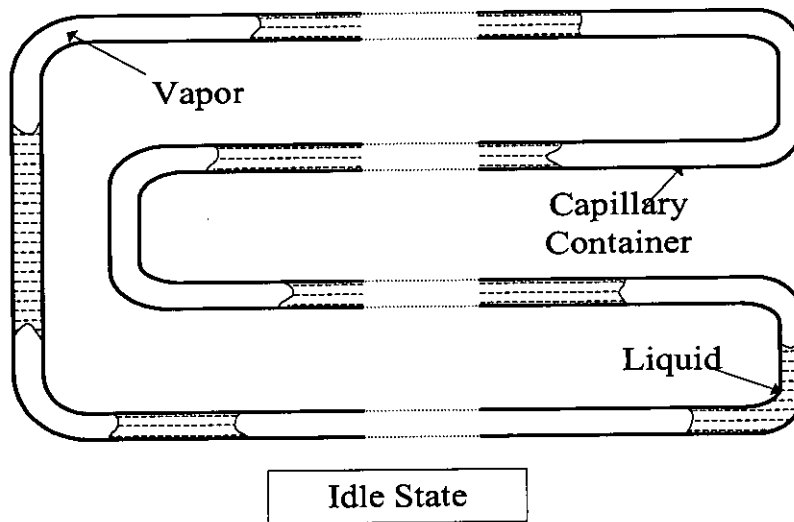


Figure 2.3: Schematic of a wicked tubular heat pipe

2. Wickless pulsating (oscillating) heat pipe (Fig. 2.4), in which the working fluid does not circulate between the evaporator and the condenser in the form of counter current liquid-vapor flow, but rather axially oscillated in the bundle of turns of capillary tubes. This oscillation movement of the working fluid is created by the bubble-boiling phenomenon in the evaporator zone [39].



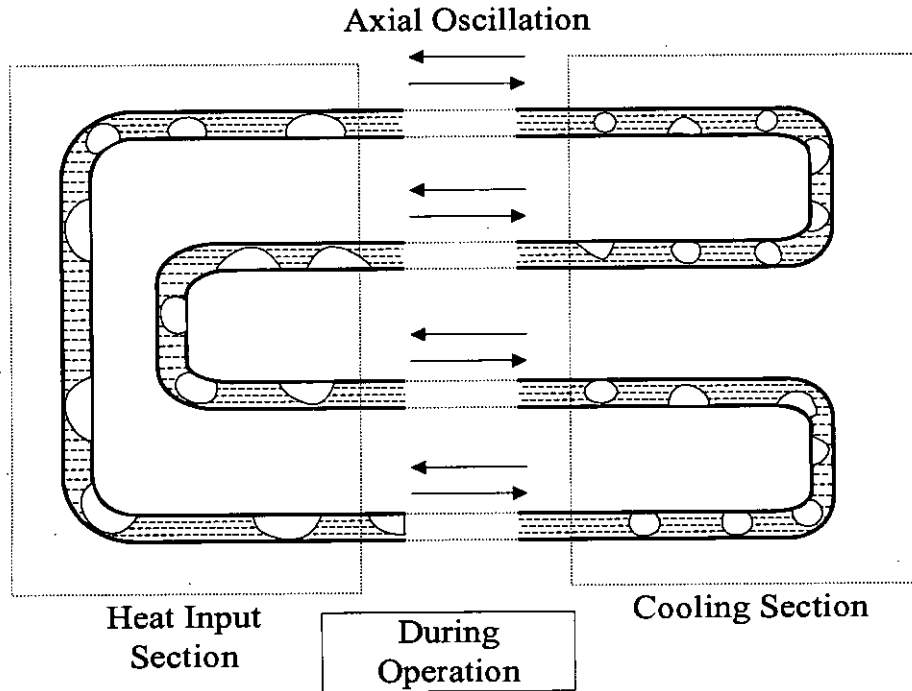


Figure 2.4: Schematic of a wickless pulsating heat pipe

3. Wickless two-phase closed thermosyphons, in which gravity is used for returning the liquid, form the condenser to the evaporator. Thermosyphon coolers can be designed as:
- tubular thermosyphon coolers (Fig. 2.5), both with counter-current flow of the liquid and the vapor, or as:
 - Thermosyphon loops, where the evaporator is connected to the condenser by a couple of individual channels, one for the liquid flow and the other for the vapor flow. Thermosyphon loops, but in general all passive coolers (heat pipes and thermosyphons), can be constructed as:
 - indirect coolers, when the electronic equipment is attached to the outer surface of the evaporator part (Fig. 2.6) or as immersion coolers, where the electronic equipment is submerged directly in the liquid in the evaporator part (Fig 2.7)

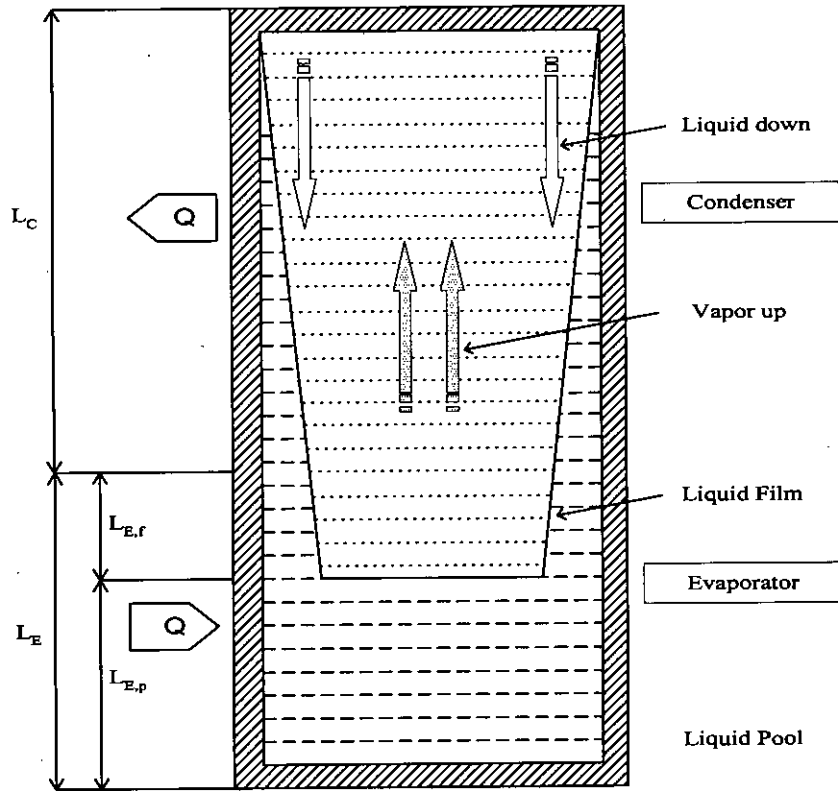


Figure 2.5: Schematic of a wickless tubular thermosyphon

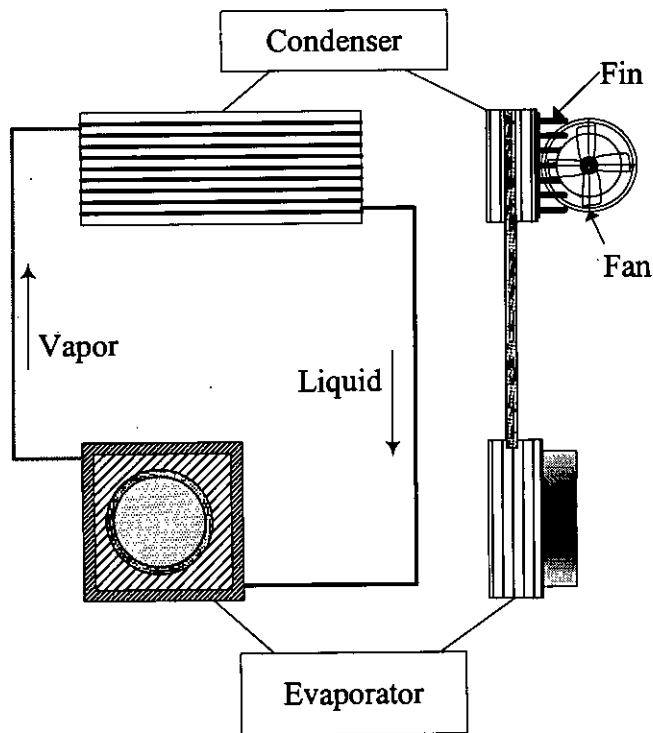


Figure 2.6: Schematic of an indirect thermosyphon loop

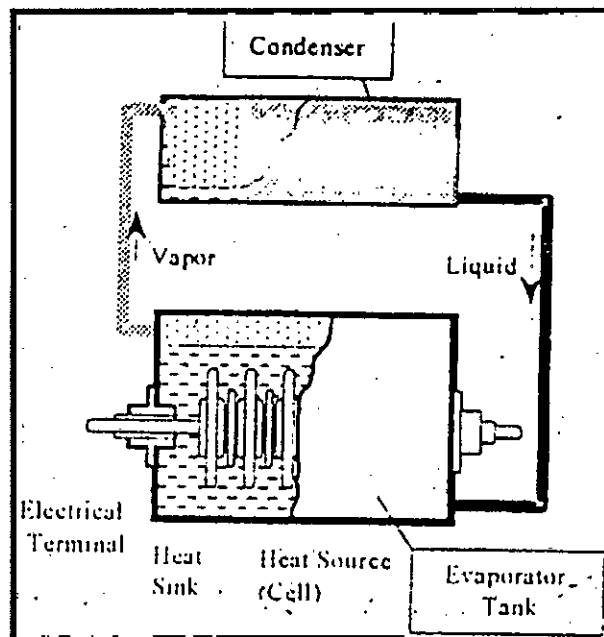


Figure 2.7: Schematic of an immersion thermosyphon loop

2.3.2 Application

The increasing importance of thermal energy transfer technology is generally dictated by the broadening of areas of its application including:

- Cooling semiconductor devices
- Cooling fuel-cells
- Cooling electrical and electronic devices
- Air conditioning
- Solar energy collection
- Motor and engine cooling
- Manufacturing processes heat recovery
- Thermal management in outer-space structures.

All applications mentioned above looks for a common requirement, which is to facilitate and control thermal energy transportation at higher heat flux level over longer distance while maintaining a moderate device temperature. Up until now, considering all known phase-change heat transfer devices, the motive power behind the condensate return has been derived mainly by one of two natural forces:

- Gravity, used in Thermosyphon
- Force of capillary action, used in heat pipe.

Both systems mentioned have numerous advantages including: Self-starting, Self-regulating, passive, no moving parts, and very quiet while in operation. However, each has specific disadvantages of its own. Thermosyphon has a major limitation as its operation and performance is dependent on gravity and relative position of its components. The major constrain of heat pipe is the relative weakness of capillary force, which can pull condensate through capillary passage way only very slowly, limiting the rate of thermal energy transfer. From years of effort, researchers have very limited success in improving this limitation and improving overall heat flux capacity.

Thermoloop Heat Transfer Technology (THTT) is a promising technology capable of dealing with very high heat flux requirement for electronics cooling and other high heat flux applications. Thermoloop device is a simple, passive, self-actuating, self regulating and very highly efficient heat transfer device that has been proven to overcome some of the major performance limitations of phase-change heat transfer devices. With the help of flow controller and reservoir, this device can produce much stronger vapor transport and condensate return force, and therefore enables very high heat flux capacity. Unlike heat pipe or thermosyphon, thermoloop device has moving parts, which includes: two self regulated flow controllers (check valves) and one self regulated reservoir.

2.4 LOOP THERMOSYPHON COMPARED TO HEAT PIPE

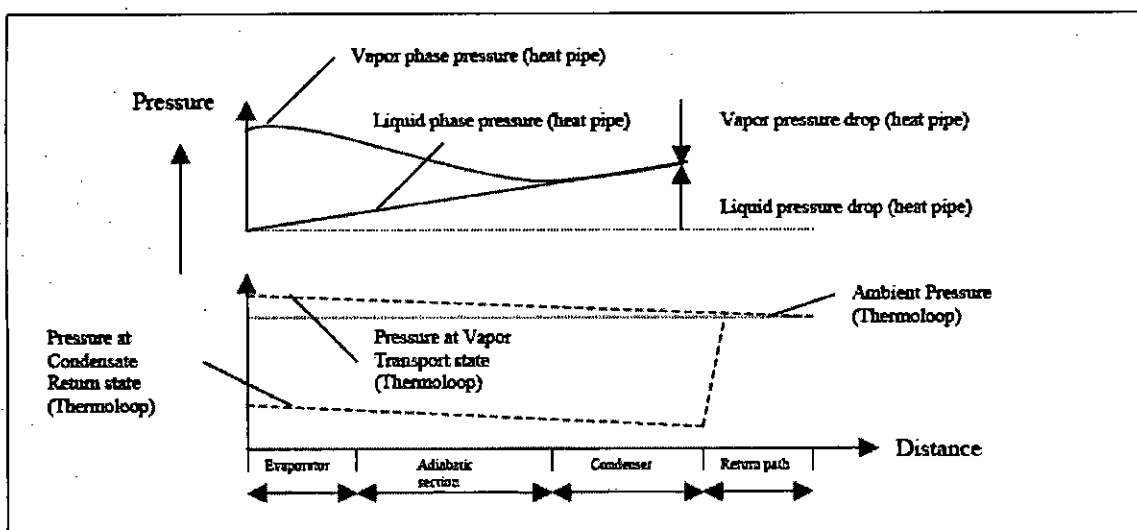


Figure 2.8: Pressure along the distance of heat pipe and loop thermosyphon

2.4.1 Heat pipe

- a) Both vapor transfer and condensate return takes place simultaneously.
- b) Both vapor phase pressure and liquid phase pressure decrease along the distance from evaporator to condenser resulting reduced vapor flow, and thus reduced heat transfer.
- c) Capillary forces pulls condensate back to evaporator is a weak natural force. For a heat pipe with effective wick pore radius of 0.03mm, the driving force for condensate return due to capillary force is 1.3 KN/m^2 for acetone, and 3.9 KN/m^2 for water.
- d) Due to this weak vapor driving force and weak liquid return force, heat transfer capacity of heat pipe is low. Typical heat flux for a heat pipe useful for electronics cooling is in the range of $50\text{-}100\text{W/cm}^2$.

2.4.2 Loop Thermosyphon

- a) Vapor transfer and condensate return takes place alternately.
- b) Vapor pressure inside evaporator above ambient pressure is the driving force for vapor transportation, and pressure drop inside condenser below ambient pressure is the driving force for condensate return.
- c) Small pressure increase can cause large vapor transportation (condenser other end is always at air pressure).
- d) Due to large volume of vapor transportation and strong condensate return force, the heat transfer capacity of thermolooop device is very high. Typical heat flux for a thermolooop device useful for electronics cooling is in the range of $500\text{-}1000\text{W/cm}^2$.
- e) Vapor transfer and condensate return force for loop thermosyphon is very strong. Therefore the device is expected to operate almost independent of gravity and orientation.

2.5 CONSIDERATIONS WHEN CHOOSING WORKING FLUID

Speaking to designers of electronic equipment it is difficult to get a straight answer as to which fluids should be chosen, i.e., which of the requirements are absolute and which could be set aside. It is the author's experience that the concern is, first, the risk

of damage due to a leak, and, second, what the customer believes would happen in case of a leak. It is also the experience, that the designers are very aware of the environmental issues concerning man-made fluids and that natural working fluids are preferred, both due to concern of the environment and because green products have advantage on the market.

Some present and most future electronic equipment have heat fluxes in the range from 20 up to 200 W/cm², so that only certain liquids are able to meet their demanding requirements. Upgrading the heat fluxes by means of the previous mentioned enhanced and extended surfaces is the today main task for many engineers: for example, the critical heat flux at pool boiling of FC liquids is only from 10 to 20 W/cm².

The boiling point and latent heat of the fluid governs the device performance. For normal operation, depending on thermal load the evaporator temperature is expected to oscillate above and below the boiling point of the working fluid. In the present experiment water and the two fluids are tested, i.e., ethanol and methanol. High latent heat and high wettability are desired for these working fluids. Table 2.1 shows the boiling point and latent heat of vaporization for above three working fluids.

One of the advantages of using a thermosyphon loop instead of immersion boiling is that the fluid may be chosen more freely as the fluid is not in direct contact with the components during normal operation. One may thus choose a fluid which needs small diameters of tubing and which gives low temperature differences in boiling and condensation and allows high heat fluxes in the evaporator. A thermosyphon may also be hermetically and permanently sealed which reduces the risk of leakage and allows the use of fluids with higher vapor pressures. The high-pressure fluids give better performance and more compact designs as high-pressure results in higher boiling heat transfer coefficients and smaller necessary tube diameter.

Apart from the properties related to the performance of the loop thermosyphon (pressure drop, heat transfer coefficients of boiling, condensation heat transfer etc.), there are several other requirements which should be met:

1. The fluid should not be harmful to people during production, normal operation or in case of a breakdown (sudden leak, fire, etc).
2. It should not be harmful to the equipment in which it is installed. This means that it should not be explosive or flammable, not corrosive or otherwise incompatible with the materials of the equipment.
3. It should not be harmful to the global environment. This means that it should have zero ozone depleting potential (ODP), it should not contribute to the greenhouse effect, not be hazardous to animals or plants or have decomposition products, which have such effects. Preferably, it should be a naturally occurring substance to eliminate the risk of unknown environmental effects.
4. From an operational point of view, the fluid should be able to withstand the environment of the equipment for a long period of time without decomposing.
5. Finally it should have a low price and be readily available.

It is necessary to make some kind of compromise as no fluid meets all these requirements. This is done by considering various geometric and functional parameters of the system such as size, material, amount of heat to be transferred, application etc.

EXPERIMENTAL SETUP AND WORKING PROCEDURE

In order to study the heat transfer characteristics of two-phase loop thermosyphon, various functional parameters are measured. Three different evaporator geometries of the device of varying evaporator bottom surfaces were chosen and experimented using different working fluids with 100% fill ratio. A schematic of the test facility is shown in Fig. 3.1. The detailed description of experimental apparatus and experimental procedure are presented in the subsequent sections of this chapter.

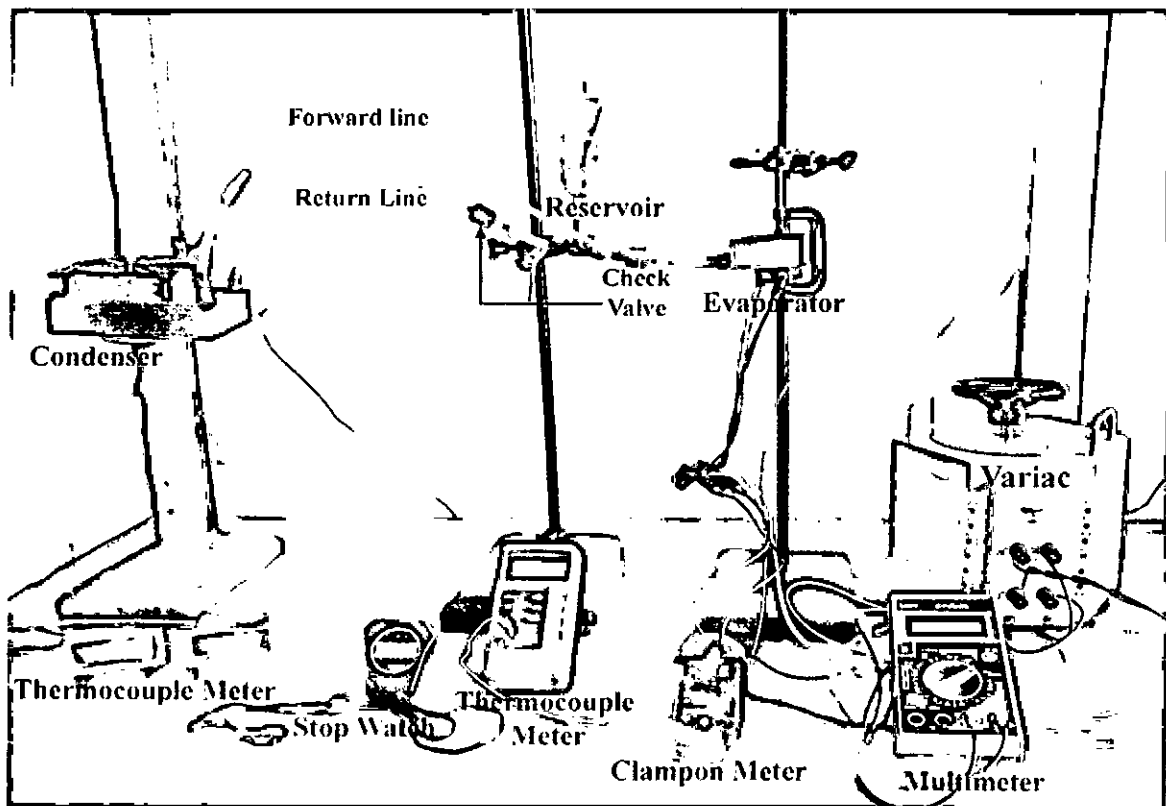


Figure 3.1: Experimental setup

3.1 EXPERIMENTAL APPARATUS

The experimental apparatus are as follows

1. Loop thermosyphon

- (i) Evaporator
- (ii) Forward tube
- (iii) Condenser
- (iv) Reservoir
- (v) In-valve
- (vi) Out-valve
- (vii) Return tube

2. Measuring apparatus

- i) Thermocouple
- ii) Multimeter
- iii) Thermocouple meter

3. Copper Block

3.1.1 Loop Thermosyphon

Thermosyphon is such a device, which successfully implements two-phase liquid cooling by indirect contact with electronics. Loop thermosyphon consists of the followings as shown in Fig. 3.1.

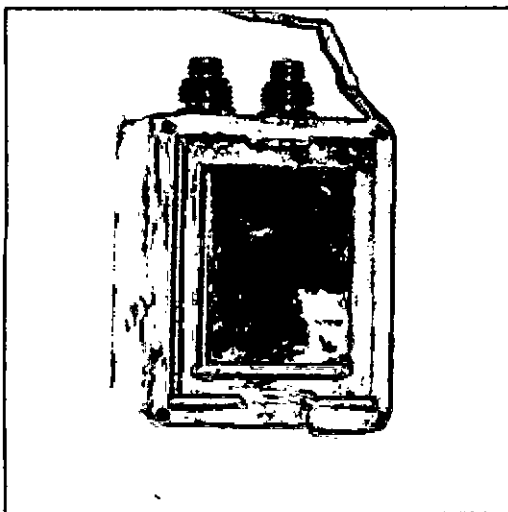
3.1.1 (i) Evaporator

Evaporator is a metal chamber made of copper or aluminum, having empty space inside to contain phase change fluid for boiling. Evaporator is thermally connected to the heat-producing source to receive thermal energy. The work analyses the effect of different evaporator geometry on the performance of the two-phase loop thermosyphon. All of the evaporators had a flat bottom surface to attach the copper block, which contained the heaters. Copper block was used as a good conductor and loss of heat by conduction was negligible. The internal surfaces of the evaporators were grooved and plain. To enhance the boiling heat transfer features the grooved surface gave better performance

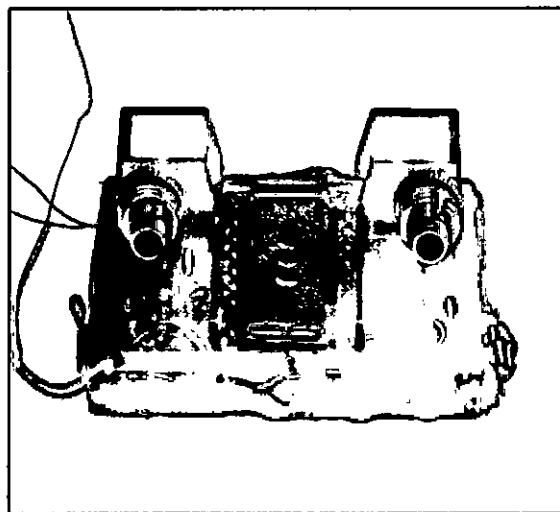
compared to the plain surface. The shape and dimension of all of the evaporators were chosen to ensure that they are compact and can be miniaturized for the practical application in electronics cooling. Considerable thought was given in their design to make measurement and instrumentation easier. Proper care was taken in perfectly sealing the evaporators to ensure that they can withstand the high pressure developed inside during the evaporation of the fluid. To measure the evaporator wall temperature, one thermocouple was connected to the bottom surface of the evaporator. The dimension and other geometric features of the evaporator used in the experiment are summarized in table 3.1.

Table 3.1: The dimension and geometric features of the evaporators used in the experiment are summarized

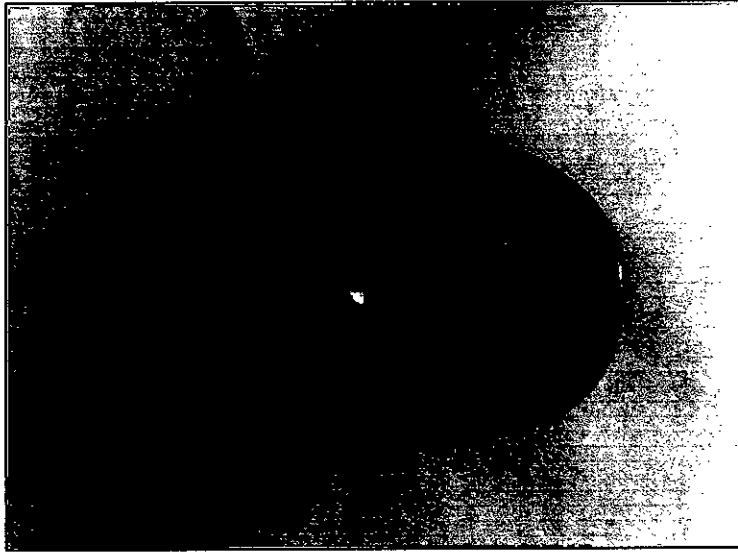
Dimension	Geometry-1	Geometry-2	Geometry-3
Material	Aluminum	Copper	Copper
Internal Surface	Grooved	Grooved	Plain
Inside volume of the evaporator (cc)	75.0	30.0	15.0
Outside dimension (mm)	72.5X60X20	77X65X8	50X50X10
Contact area with Heaters (mm)	35X45	35X45	35X45



(a)



(b)



(c)

Figure 3.2: Evaporators used for (a) Geometry-1 and (b) Geometry-2 (c) Geometry-3

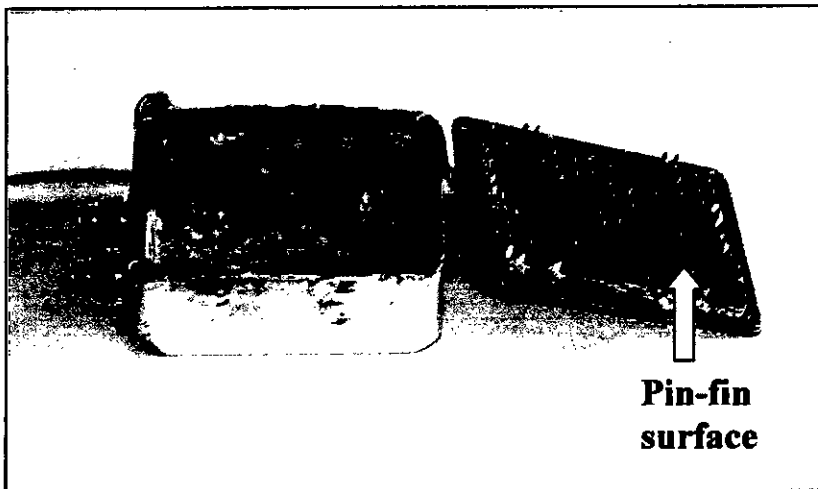


Figure 3.3: Evaporator surface (geometry-1)

3.1.1 (ii) Forward Tube

Forward tube connects evaporator to condenser. This tube may be made of metal/non-metal tubes. In this work non-metal tube, which was made of transparent poly-ethylene material (capable of withstanding high temp & pressure) was chosen. So, the flow of the fluid through the tube was possible to observe visually. Forward tube transports the vapor from the evaporator to the condenser. This tube is also called vapor line.

Table 3.2: Dimension and geometric features of the forward tube

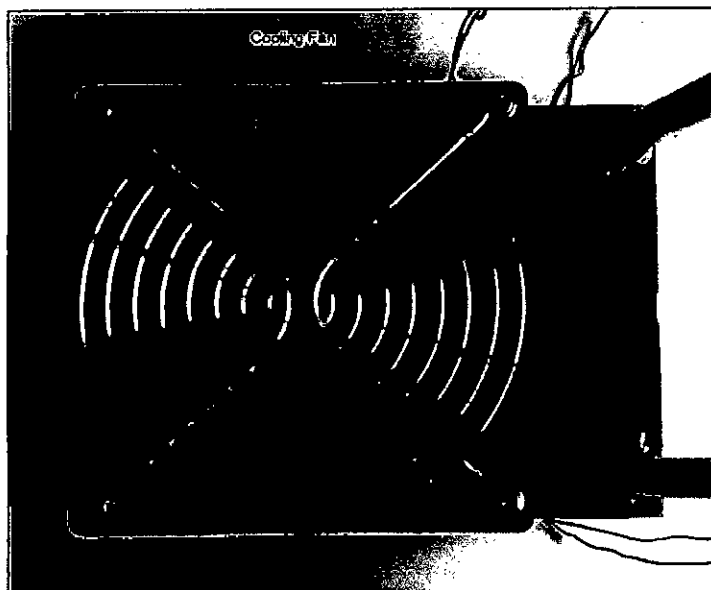
Features	Forward tube
Volume (CC)	8.8
Outside Diameter (mm)	6.4
Length (mm)	700
Thickness (mm)	1.02

3.1.1 (iii) Condenser

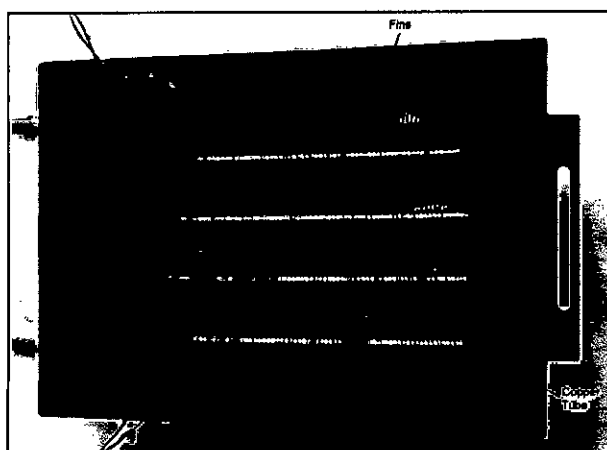
In thermolooop device the cooling performance is completely dependent on the condenser. So, condenser is the most important part of this system. In this experimental work condenser was made of heat conductive metal (copper) tubes with added fins. The condenser was connected to the forward and return tubes with copper connectors, making the joint firm and leak-free. Condenser inlet and outlet temperatures of the fluids were measured by the thermocouples connected to the condenser. The convection condition of the condenser was forced convection by employing a forced draft fan. Forced convection increases the rate of heat dissipation from the condenser compared to the natural convection.

Table 3.3: Dimension and geometric features of the condenser

Features	Condenser
Volume (CC)	30
Diameter of condenser tube (mm)	73
Length of condenser tube (mm)	1600
Condenser tube material	Copper



(a)



(b)

Figure 3.4: Condenser used (a) Top view (b) Bottom view

3.1.1 (iv) Reservoir

This is a flexible reservoir made of rubber that is able to provide variable volume without change in pressure. The reservoir is capable of holding up to 70 cm^3 liquid while inflated and had the dimension of 5.35 cm in diameter and 10.7 cm in height. Two non-return valves were placed into the return line on both sides of the reservoir. The pressure inside the reservoir was always atmospheric. The cold liquid collected in the reservoir moves towards the evaporator and the height of the cold liquid was visible from outside, as the reservoir was transparent.

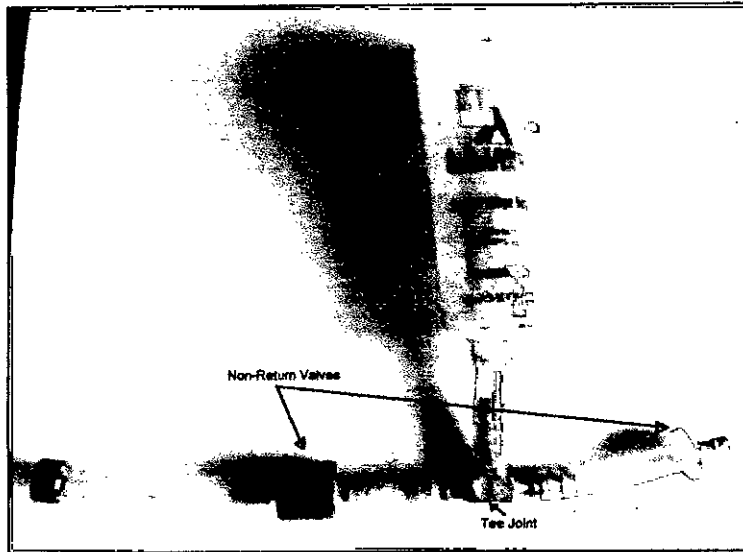


Figure 3.5: Reservoir

3.1.1 (v) In-valve

This is a one-way check valve. This allows liquid to flow only from condenser to reservoir.

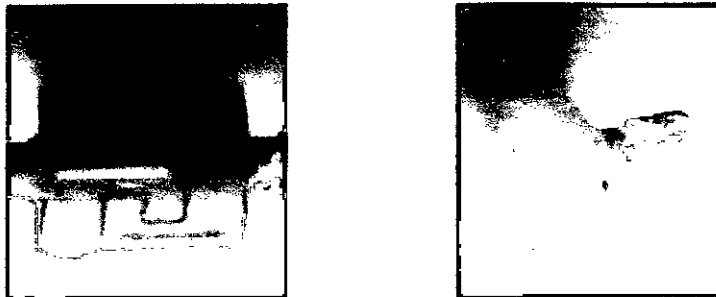


Figure 3.6: In-Valve and Out-Valve

3.1.1 (vi) Out-valve

This is also one-way check valve (similar kind of in-valve) and allows liquid to flow only reservoir to evaporator.

3.1.1 (vii) Return tube

Return tube transports the cold liquid from the condenser to the evaporator and this tube is also called liquid line. This tube was made of transparent poly-ethylene

material, capable of withstanding high temperature and pressure and the fluid flow through the tube was possible to observe visually.

Table 3.4: Dimension and geometric features of the return tube

Features	Return tube
Volume (CC)	8.4
Outside Diameter (mm)	6.4
Length (mm)	600
Thickness (mm)	1.02

3.1.2 Measuring Apparatus

To measure the important parameters such as evaporator surface temperature, condenser inlet and outlet temperatures were recorded by standard measuring devices.

3.1.2. (i) Thermocouple

One K-type (ϕ 0.18mm) thermocouple was glued to the bottom surface of the evaporator for measuring the evaporator surface temperature. Condenser inlet and outlet temperatures were measured by similar kind of two T-type thermocouples.

3.1.2. (ii) Multimeter

The multimeter was used to record the input voltage. This meter is shown in Fig.3.1

3.1.2. (iii) Clampon meter

The clampon meter was used to record the input current. This meter is shown in Fig.3.1

3.1.2. (iv) Thermocouple Meter

Condenser inlet and outlet temperatures were recorded in the two thermocouple meter of this loop thermosyphon system. Fig. 3.1 shows the thermocouple meter.

3.1.3 Copper block

This block was made of copper and holds two heaters. The copper was chosen because it is very good heat conductor. This copper block was attached to the bottom of the evaporator part.

Table 3.5: Dimension of the copper block

Features	Copper block
Length (mm)	45
Width (mm)	34.5
Height (mm)	19
Diameter (mm)	10



Figure 3.7: Copper block- heater assembly

3.1.4 Heaters

In this experimental work, two AC heaters of same type were assembled to the evaporator part. These heaters were used to supply the required input power to the system. Two heaters were resistive heating elements whose output can be controlled by connecting them to the electric line through a variac. Both these heaters were connected in parallel for higher input power. With the help of C-clamp, the heaters were attached to the evaporator. As the evaporator surface is flat, these two round heaters were pressed into a rectangular copper block with flat surface to facilitate the connection with the evaporator.

Table 3.6: Details information of the heaters used in the experiment

Features	Heater
Number of heaters	2
Material	MS
Heating Surface	Flat
Heating Capacity (W)	483
Length (mm)	44

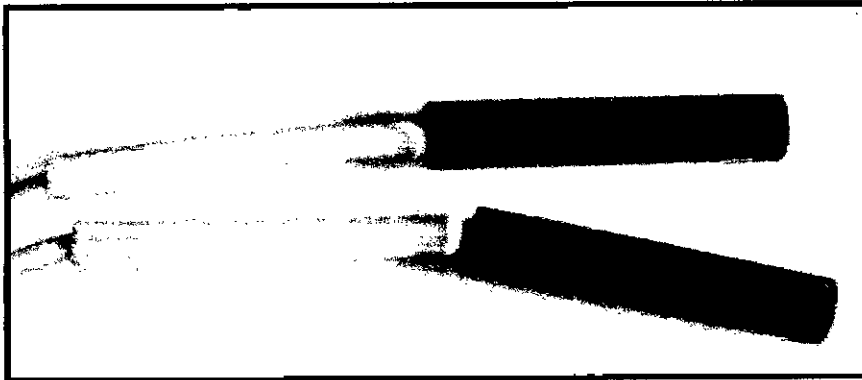


Figure 3.8: Heaters

3.2 WORKING FLUID

Thermal performance of a TPLT (two-phase loop thermosyphon) is primarily dependent on the phase-change fluid used. During normal operation, the evaporator temperature is expected to oscillate above and below the boiling point of the phase-change fluid. High latent heat and high wettability are desired for selected phase-change fluid. In this study water, ethanol and methanol are selected as the phase-change fluids (working fluids). The following are the some important properties of these three working fluids:

Table 3.7: Boiling point and latent heat of vaporization for three working fluids

Working fluid	Boiling point ($^{\circ}\text{C}$)	Latent heat of vaporization(kJ/kg)
Water	100	2256
Ethanol	78	963
Methanol	65	1101

Water: Water is non-toxic and inexpensive. It has high specific heat, and a very low viscosity, making it easy to pump. It has also high latent heat and has a relatively low boiling point. At atmospheric pressure the boiling point and freezing point of water are 100°C and 0°C respectively. It can also be corrosive if its P^{H} value (acidity/alkalinity level) is not maintained at a neutral level. Water with a high mineral content can cause mineral deposits to form in collector tubing and plumbing.

Ethanol: Ethanol or ethyl alcohol ($\text{C}_2\text{H}_5\text{OH}$) can be produced by fermentation of carbohydrates, which occur naturally and abundantly in some plants like sugarcane and from starchy materials like corn and potatoes. All the alcohols have common feature. Their molecular structure includes an OH, or hydroxyl radical, which gives them certain characteristics, high solubility in water. It boils at 78.3°C and latent heat of vaporization is 963.0kJ/kg at atmospheric pressure. Ethanol due to its very high heat of vaporization is used in racing cars.

Methanol: Methanol or wood alcohol (CH_3OH), a colorless, flammable liquid that is miscible with water in all proportions. Methanol is a monohydric alcohol. It melts at -97.8°C , boils at 64.7°C and the latent heat of the vaporization of it is 1101kJ/kg at atmospheric pressure [40]. The commercial use of methanol has sometimes been prohibited. Methanol is used as a solvent for varnishes and lacquers as an antifreeze and as a gasoline extender in the production of gasohol. Large amounts of it are used in the synthesis of formaldehyde. Methanol is often called wood alcohol because it was once produced chiefly as a by-product of the destructive distillation of wood. Methanol or methyl alcohol can be produced from coal, a relatively abundant fossil fuel. Methanol and ethanol are also used as fuels in SI Engines. Alcohols are mainly used as blends. Important properties of these three working fluids are given in Table 3.6.

3.3 EXPERIMENTAL PROCEDURE

A TPLT consists of an evaporator, a condenser located at the same level to the evaporator and a reservoir. The evaporator is connected with the condenser through a vapor line and with the reservoir through a liquid return line. The line connecting the condenser with the reservoir is named liquid line. Two check valves drive the flow in a fixed direction. A diagram of a TPLT is shown in Fig. 2.2.

Table 3.8: Important properties of the working fluids at atmospheric pressure:

Name of working fluid	Density of liquid at T_{sat} , ρ_l (kg/m^3)	Density of vapor at T_{sat} , ρ_v (kg/m^3)	Boiling point T_{sat} , $^{\circ}\text{C}$	Specific heat of liquid at T_{sat} , C_{pl} (kJ/kg.K)	Specific heat of vapor at T_{sat} , C_{pv} (kJ/kg.K)	Latent heat of vaporization at T_{sat} , h_{fg} (kJ/kg)	Liquid viscosity, μ_l ($\mu\text{Ns/m}^2$)	Vapor viscosity, μ_v ($\mu\text{Ns/m}^2$)	Prandtl number of liquid, Pr_l	Surface tension of vapor liquid interface, σ (mN/m)
Water	958.3	0.597	100.0	4.22	2.03	2256.7	277.53	12.55	1.72	58.91
Ethanol	757.0	1.435	78.3	3.00	1.83	963.0	428.7	10.4	8.37	17.7
Methanol	751.0	1.222	64.7	2.88	1.55	1101.0	326.0	11.1	5.13	18.75

In the present study, experiments are performed keeping the 100% liquid fill volume of the evaporator and water, ethanol, methanol are used as the working fluid for three different evaporator surface geometry. Heat flux is supplied to the evaporator wall, liquid vaporizes and evaporator pressure increases according to an isovolumic transformation. The vapor is pushed through the vapor line to the condenser, because the return line is closed by a check valve. The evaporator pressured is lower and the condensed liquid is motionless.

As soon as the evaporator pressure increases and the condensed liquid moves into the reservoir, the evaporator is gradually emptying and the reservoir is filling. To make possible the return of the liquid collected in the reservoir, the pressure difference between evaporator and reservoir must invert its sign.

The return operation starts as the evaporator is empty, so that the pressure inside decreases till to the saturation pressure at environmental temperature. The evaporator pressures reaches a value lower than the pressure inside the reservoir, the cold liquid collected in the reservoir moves towards the evaporator, closing the cycle. The same procedure is followed again and again.

Before starting the experiment the whole system is examined for leak proof and care must be taken to eliminate the formation of bubble or gas pockets in the forward and return lines and also in the condenser. To avoid the back flow of the phase-change fluid all the devices are kept clean.

Important parameters such as evaporator surface temperature, condenser inlet and outlet temperatures are measured at a regular interval of 10 second. Total time is recorded for every cycle. To understand the physics of the system, the change of the fluid is carefully observed during the experiment.

3.4 PERFORMANCE PARAMETER

Overall thermal resistance, R ($^{\circ}\text{C}/\text{W}$), which is defined in equation (1)

$$R = \frac{T_e - T_c}{Q_c} \quad (1)$$

Overall heat transfer coefficient of condensation, U_t ($\text{W}/\text{m}^2\text{ }^{\circ}\text{C}$) is obtained from Eq. (2) as follows

$$U_t = \frac{Q_c}{A_e(T_e - T_c)} \quad (2)$$

Overall thermal resistance will be required in the determination of the effectiveness of various components and in identifying the means to minimize their limitations. The thermal resistance of condenser, evaporator and reservoir can be calculated using Eq. (1) and search can be made for minimizing those resistances. So, the determination of the total thermal resistance of loop thermosyphon is necessary to increase the thermal efficiency of the device.

RESULTS AND DISCUSSION

The effects of various operational parameters such as charging fluids (water, ethanol and methanol) for three different evaporator surface geometry as shown in Fig.3.3 are experimentally determined. Performances are compared between the different charging fluids, evaporator surface geometry and also the results are compared with previous relevant studies.

The experimental results are obtained at thirteen different power levels which are varied from 120W to 300W with an increment of 15W for the filling volume of the evaporator is approximately 100%. The forward and return tubes and also the condenser are filled by liquid. At the filling the vacuum/bubble formation is eliminated inside the loop, so that the liquid into the evaporator is at the saturation condition at the starting time. At this moment a heat power rate is supplied to the copper block (this block is firmly attached with the bottom surface of the evaporator) and the thermal behavior is observed with time. As the heat power is supplied to the copper block, the evaporator surface temperature (wall temperature) and liquid temperature of the evaporator increase as the pressure. A heat and mass transport is realized from the evaporator to the condenser where condensation is occurred for forced convection condition of the condenser.

The present device has shown a stabilized periodic functioning. Figure 4.33 shows that the start up temperature trends of the component of the loop for an input power of 120W and ethanol as the working fluid. The functioning of the device reaches quickly (after about 570s) a stabilized periodic regime. Figure 4.1 shows a stabilized periodic regime for different working fluid and an input power of 150W. From Fig. 4.1 it is seen that the temperature of the evaporator surface increases gradually up to a temperature of 102⁰C and boiling initiates when water is used as the working fluid. These temperatures are 75.8⁰C and 71.8⁰C for ethanol and methanol. The respective temperatures drop to a value of 73.6⁰C, 65.6⁰C and 67⁰C for water, ethanol and methanol. The temperature drops for methanol is lower than that for water and ethanol.

Figure 4.2 and Fig. 4.3 shows the same temperature trends for geometry-2 and geometry-3 with an input power of 150W. From Fig. 4.2 and 4.3 it can also be observed that the temperature drops for methanol is lower than that for water and ethanol for the same heat input. For geometry-3, the device takes short time for completing the cycle but the maximum evaporator surface temperature is lower. The evaporator surface temperature and the cycle time are shown in Table 4.1.

Table 4.1: Average evaporator surface temperature, T_e (avg.) and cycle completion time, t_{ct} for different evaporator surface geometry and water as the working fluid (Input power: 150W).

Cycle Number	Geometry -1		Geometry-2		Geometry-3	
	$t_{ct}(\text{Sec})$	$T_e(\text{avg.})^{\circ}\text{C}$	$t_{ct}(\text{Sec})$	$T_e(\text{avg.})^{\circ}\text{C}$	$t_{ct}(\text{Sec})$	$T_e(\text{avg.})^{\circ}\text{C}$
1	294	65.3	284	69.5	185	60.3
2	114	87.7	132	102.3	54	93.5
3	134	89.4	138	96.1	60	89.6
4	128	89.8	124	96.8	63	92.4
5	128	89.3	116	97.3	55	89
6	114	91.5	119	97.4	62	87.9
7	127	90.2	121	95.4	60	91.2
8	109	90.9	135	94.5	62	93.4
9	118	90.4	134	97	58	90.6
10	106	90.2	130	98.2	59	90

4.1 HEAT TRANSPORT CHARACTERIZATION

All the experimental tests have been carried out for four/five hours and the TPLT have showed a very stable functioning with constant mean heat transport cycle temperatures and a periodic stabilized regime reached after five/six heat transport cycles (in most cases). The start up operation mode is very fast and the device reaches quickly a stabilized periodic heat transport regime. As soon as the periodic regime is reached the behavior of the apparatus can be illustrated by the temperatures trend of the different

component of the loop during a whole transfer cycle. The temperatures during five consecutive cycles with water as the working fluid and an input power of 240W are shown in Fig. 4.8. Similar trends are shown in Fig. 4.9 and Fig. 4.10 for ethanol and methanol as the working fluid respectively. When water is used as the working fluid the device reaches quickly a steady value than methanol and ethanol, but water takes more time for completing the cycle compare to the other two fluids. The pressure trends of the fluid inside the evaporator and the reservoir are qualitatively similar to the temperature one, being the fluid at the saturation condition during all the cycle.

For this experimented TPLT, the transfer cycle consists of two operations: a transport and a return one. The first one starts when the cold liquid from the reservoir enters into the evaporator. This operation is divided in three consecutive parts, characterized by the vapor evaporator behavior: compression, expansion and a constant transport operation. The last operation is characterized by constant temperature and the mass flow rate circulating in the entire loop. Vapor transfer begins when boiling initiates inside evaporator. Elevated pressure due to vaporization starts pushing liquid out from forward tube and condenser tube into reservoir, crossing the In-Valve. Out-Valve remains closed at this time due to opposite pressure direction. Thus, the forward tube and part of condenser tube gets filled in with saturated vapor replacing existing liquid. Now condensation rate increases, which also starts reducing vapor pressure at condenser. Pushing out liquid and replacing liquid with vapor continues until vapor volume inside condenser is high enough, so that the vapor pressure decreasing rate (which also follows condensation rate at the condenser) becomes equal to the vapor pressure increasing rate (which also follows evaporation rate at evaporator).

At the end of vapor transfer, all liquid from evaporator gets vaporized and therefore steady state pressure increase inside evaporator suddenly comes to an end. On the other hand, pressure reduction rate in the condenser remains the same as the condenser and forward tube still remains filled with saturated vapor and condensation continues. Due to much higher condensation rate than evaporation rate, pressure suddenly drops inside condenser. This low pressure quickly propagates to forward tube and evaporator. Pressure at the reservoir on the other hand still remains at ambient pressure. Due to this pressure difference, liquid gets pushed out from reservoir into evaporator, forward tube and condenser tube, filling out the entire system with liquid again. Both operations

continue to repeat as long as the device is in operation. The device automatically adjusts its functionality (cycle frequency, heat absorption and dissipation rate) depending on the thermal load at evaporator, and the heat removal rate from condenser.

4.2 EFFECT OF INPUT POWER ON PERFORMANCE LIMIT

From Fig. 4.11, it is shown that all average evaporator temperatures increase about linearly with increasing heat input, then they increase rapidly near 150W for water & ethanol and 165W for methanol due to the occurrence of dry-out and they reaches a steady value near 210W for water & ethanol and 220W for methanol. Also it is shown that the influence of gravity is a practically negligible (the device is placed at horizontal position); all the experimental tests are performed for three different evaporator surface geometry. It can be seen from Fig. 4.27, Fig. 4.28 and Fig. 4.29 that all thermal resistances decrease with increasing heat load, till a minimum is reached at about 195 W for water, 180 W for ethanol and methanol. Then the thermal resistances increase again, especially sharply at 200W, 185W, and 190W (dry-out) for water, ethanol and methanol respectively. Thermal performance data (heat load, thermal resistance, evaporator and condenser wall temperatures, heat flux) are summarized in Table 4.2, 4.3 and 4.4 for all three working fluids.

Table 4.2: Thermal performance data for Geometry-1 and Water as working fluid

Heat Load (W)	R ($^{\circ}\text{C}/\text{W}$)	T _E ($^{\circ}\text{C}$)	T _{Cin} ($^{\circ}\text{C}$)	T _{Cout} ($^{\circ}\text{C}$)	q (W/cm^2)
135	0.38	83.7	49.5	31.8	8.5
150	0.33	84.6	50.2	33.8	9.5
165	0.31	86.4	51	35	10.4
180	0.29	89.1	51.9	35.2	11.4
195	0.27	90	52.3	35.9	12.3
210	0.26	91.3	53	36.2	13.3

Table 4.3: Thermal performance data for Geometry-1 and Ethanol as working fluid

Heat Load (W)	R ($^{\circ}\text{C}/\text{W}$)	$T_E(^{\circ}\text{C})$	$T_{\text{Cin}}(^{\circ}\text{C})$	$T_{\text{Cout}}(^{\circ}\text{C})$	$q(\text{W}/\text{cm}^2)$
135	0.24	65.9	48.4	33.1	8.5
150	0.22	67.7	56.9	33.8	9.5
165	0.20	68.9	51.4	34.7	10.4
180	0.18	67.5	50.7	34.8	11.4
195	0.18	71	49.9	35.9	12.3
210	0.15	69.6	43.9	37.8	13.3

Table 4.4: Thermal performance data for Geometry-1 and Methanol as working fluid

Heat Load (W)	R ($^{\circ}\text{C}/\text{W}$)	$T_E(^{\circ}\text{C})$	$T_{\text{Cin}}(^{\circ}\text{C})$	$T_{\text{Cout}}(^{\circ}\text{C})$	$q(\text{W}/\text{cm}^2)$
135	0.27	70.3	49.7	33.2	8.5
150	0.21	66.8	50.7	33.9	9.5
165	0.20	69.4	49	35.5	10.4
180	0.17	66.7	50.5	35.8	11.4
195	0.17	69.4	52	35.8	12.3
210	0.15	69.6	54.1	37.3	13.3

The time required for one complete cycle is known as cycle time. It can be noted that the cycle time decreases with increase in input power as shown in Fig. 4.12. From Fig. 4.7 it is seen that the cycle time reaches a steady value after six/seven cycles, in most cases, for all the working fluids. For water the cycle time is higher compare to the other two fluids and ethanol takes minimum time to complete the cycle.

The TPLT has been considered as a thermal machine operating among three different levels of temperature and exchanging heat with three different sources: hot (evaporator), cold (condenser) and intermediate (reservoir) with natural circulation of fluid. The variation in the maximum condenser inlet temperature with increasing input power is shown in Fig. 4.30 for all of the working fluids and evaporator surface geometry-2.

The performance of the thermosyphon to a large extent depends on the ability to cool the condenser section. The cooling capacity increases with decreasing condenser outlet temperature. From Fig 4.32 it is seen that for water and ethanol the condenser performance is better for heat input of 150-165W and for methanol it is 180-210W.

Dissipation of large heat fluxes at relatively small temperature differences is possible in systems utilizing boiling phenomenon as long as the heated wall remains wetted with the liquid. With the wetted wall condition at the heated surface, heat is transferred by a combination of two mechanisms: (i) bubbles are formed at the active nucleation cavities on the heated surface, and heat is transferred by the nucleate boiling mechanism, and (ii) heat is transferred from the wall to the liquid film by convection and goes into the bulk liquid or causes evaporation at the liquid-vapor interface. In the present LT device, the second mechanism is followed. As the heat flux increases, both the evaporator temperature and, more importantly, the fluid temperature increase gradually, causing a decrease of surface tension and latent heat.

4.3 EFFECT OF WORKING FLUID ON VARIOUS PARAMETERES

4.3.1 Heat Transport Time

Figure 4.31 shows the effect of working fluids on the first cycle time required for evaporator surface geometry-1. It is seen that the first cycle time decreases rapidly with increasing thermal load, they reaches a steady value near 225W.

After the first cycle the liquid from the reservoir returns into the evaporator, it is already at a very high temperature. So the liquid is evaporated very quickly and the pressure develops in the system rapidly. The cycle time is reduced after the first cycle and attains a steady value after five/six cycles (in most cases) as shown in Fig. 4.7.

4.3.2 Thermal Resistance

To improve the performance of the LT, it is necessary to minimize all the thermal resistance associated with LT operation. The decreased thermal resistance is achieved by increasing the surface area available for condensation and increasing heat load. The

effect of thermal resistance on different working fluids for three different evaporator geometries is shown in Fig. 4.27.

4.3.3 Overall Heat Transfer Co-efficient

Overall heat transfer coefficient increases with increasing input power as shown in Fig. 4.15 and Fig. 4.16 for three different working fluids. For water heat transfer coefficient has been increased very smoothly with input power compare to ethanol and methanol. The difference between evaporator surface temperature and condenser outlet temperature decreases with increasing heat load and hence increases the overall heat transfer coefficient. From the above figure it is shown that the overall heat transfer coefficient for methanol is higher than water and ethanol. At a heat input of 240W, the overall heat transfer coefficient for water, ethanol and methanol are $373.8\text{W/m}^2\text{ }^\circ\text{C}$, $643\text{W/m}^2\text{ }^\circ\text{C}$ and $660\text{W/m}^2\text{ }^\circ\text{C}$ respectively. Overall heat transfer coefficient decreases with increasing surface area. From Fig. 4.15 & Fig. 4.16 it is also seen that the overall heat transfer coefficient for geometry-2 is greater than geometry-1 because the surface area of geometry-2 is smaller than geometry-1.

4.3.4 Evaporator Surface Temperature

The variation of average evaporator wall temperature for different working fluids is shown in Fig. 4.11. The average wall temperature of the evaporator is nearly constant for the same heat input but it varies with increasing heat input and different working fluids (shown in Fig. 4.11) and also different evaporator surface geometry (shown in Fig. 4.34). From Fig. 4.11 it is observed that the maximum evaporator wall temperature increases nearly to 210W, this temperature becomes steady after 210W for water & ethanol and nearly 225W for methanol.

The maximum and minimum wall temperatures are the very important parameter because these temperatures indicate the range within which the temperature of the various equipments to be cooled will oscillate. Figure 4.17 has shown the variation of maximum wall temperature for different working fluids and different evaporator surface geometry. From figure it can be seen that after the initial unsteadiness, the wall temperature of the evaporator attains nearly a steady value after five/six heat and mass

favor of its applicability for electronics cooling, especially when the electronic component to be cooled is in operation for a long time.

From Fig. 4.18, Fig. 4.19 and Fig. 4.20 shows the variation of evaporator wall temperature with time for different input power and three working fluids. The evaporator wall temperature varies smoothly (in most cases) with time when ethanol as the working fluid. The maximum temperature of the evaporator wall and the condenser outlet for water, ethanol & methanol are respectively 103.4°C , 75.4°C & 75.3°C and 36.8°C , 40.5°C & 41.8°C at a input power of 180W (shown in Fig. 4.17 and Fig. 4.32). In this manner, when water as the working fluid, the device dissipates more heat compare to ethanol and methanol.

4.3.5 Condenser Wall Temperatures

Temperatures during five consecutive cycles (6 to 10) for geometry-1 and water, ethanol & methanol as the working fluid are respectively shown in Fig. 4.8, Fig. 4.9 & Fig. 4.10. It is seen that, for working fluid water the device reaches quickly a steady value. The variation of condenser inlet temperature is similar in nature to the evaporator wall temperature and condenser outlet temperature is almost constant for all the cycles.

Figure 4.23 shows the effect of working fluids on condenser wall temperatures for geometry-3. When working fluid is water, the heat and mass transport cycle is completed very smoothly. The performance of ethanol is medium and methanol is poorer than that of water & ethanol. The condenser outlet temperature is also lower for water. Similar trends are shown in Fig. 4.21 and Fig. 4.22 for geometry-1 and geometry-2.

4.4 ENHANCEMENT OF HEAT-TRANSFER IN THE EVAPORATOR PART OF THERMOSYPHON

The critical point in most applications in electronics is the evaporator part, due to increasing heat fluxes, which are usually non-uniform and unsteady, from electronic equipment to the cooler. In the evaporator part, three main characteristics of heat

transfer can be pointed out: heat transfer coefficient at evaporation or boiling, critical heat flux and temperature overshoot at boiling incipience of highly wetting liquids.

In the present study one plain and two enhanced and extended surfaces in the form of grooves (geometry-1 and geometry-2, shown in Fig. 3.2(a) and 3.2(b) respectively) are tested. Figure 4.15 shows the effects of overall heat transfer coefficient on evaporator surface geometry-1 for three different working fluids. The overall heat transfer coefficient for methanol is varied in a similar manner like ethanol and the maximum heat transfer coefficient is $519.5\text{W/m}^2\text{ }^\circ\text{C}$ for both of them. The variation of overall heat transfer coefficient with heat input for evaporator surface geometry-2 is shown in Fig. 4.16. In both cases the overall heat transfer coefficient is lower for water with compare to ethanol and methanol.

The heat fluxes are calculated from Rohsenow correlation (see table 4.5) for heat input 225W, which is maximum 2.56W/cm^2 for water, 0.26W/cm^2 for ethanol and 2.83W/cm^2 for methanol.

Table 4.5: The heat fluxes per unit area after deducting heat loss and from Rohsenow correlation

Working fluid	Geometry-1		Geometry-2		Geometry-3	
	$q_R(\text{W/cm}^2)$	$q_E(\text{W/cm}^2)$	$q_R(\text{W/cm}^2)$	$q_E(\text{W/cm}^2)$	$q_R(\text{W/cm}^2)$	$q_E(\text{W/cm}^2)$
Ethanol	0.26	14.02	0.205	14.03	0.078	14.03
Methanol	2.83	14	2.18	14	0.59	14.02
Water	2.56	14.02	2.05	14.03	0.12	14.03

Experimental results of heat fluxes for water, ethanol and methanol as working fluids are presented in table 4.5. From the comparison of the calculated results for heat fluxes on plain surface and the experimental results form the two extended surfaces, it is clear that the evaporator surfaces of geometry-1 and geometry-2 increase the heat fluxes than geometry-3(plain surface).

The variation of evaporator wall temperature for different evaporator surface geometry with water as the working fluid is shown in Fig. 4.4. Similar trends are shown in Fig.

4.5 and Fig. 4.6 for ethanol and methanol as the working fluid. Evaporator wall temperature varies almost equally for geometry-1 and two when working fluid is ethanol. From the above figure, it is seen that the evaporator surface geometry-3 (plain surface) shows worst performance in terms of heat dissipation capacity.

4.5 VARIOUS EFFECTS ON THE SYSTEM

4.5.1 Non-Return Valves

The proper functioning of the LT is almost dependent on the non-return valves which are placed on either side of the reservoir. In the present study, two non-return valves (in-valve & out-valve) are used to maintain the flow of the working fluid in the desired directions which is previously mentioned.

Back flow is one of the most important problems in the operating system. Back flow from the reservoir through the non-return valve to the condenser occurred, which is in complete disagreement with the working principle of the LT. To avoid the back flow within the non-return valves, care must be taken when charging the fluid that all of the components of the device and the working fluid are properly cleaned. Back flow is mainly occurs due to the dirt inside the loop thermosyphon device.

Also back flow occurred due to continuous use of the same non-return valves for a number of tests. This was true especially for the case of the one way non-return valves that had to be change after a few tests as they failed after continuous operation for a number of tests. In the experiment, the plastic non-return valves were used. Depending on the working fluid and pressure in the system, stronger and proper metal non-return valves with the optimum opening pressure should be selected.

4.5.2 Liquid Fill Volume

Fantozzi et al. [41] observed that the maximum evaporator wall temperature increases with an increase in the evaporator fill volume and also showed that the cycle time is also increased with increasing evaporator fill volume. Murthy [42] reported that the two-phase spreader performance was fairly insensitive to the variation in liquid fill

volume. Ramaswamy et al. [43] noticed a similar trend in their study on the performance of a compact two-chamber two-phase thermosyphon.

Rahman [37] showed the influence of evaporator fill volume on the maximum temperature of the evaporator wall at two heat inputs (100W and 250W). For the heat input of 250W, wall temperature is maximum for 50% fill volume which is about 2^oC higher than the maximum wall temperature for 30% and 60% fill volumes. But for the heat input of 100W, evaporator wall temperature is the maximum for 60% fill volume, whereas the wall temperature is nearly equal for 30% and 50% fill ratios. The variation in the maximum wall temperature is again less than 2^oC for this case. Rahman reported that at a given load, the maximum temperature of the evaporator wall is fairly insensitive to the variation of evaporator fill volume.

As previously illustrated also for this experimented TPLT, all the experimental tests were performed with 100% fill volume for different heat inputs and the loop thermosyphon was showed a stable functioning with constant mean heat transport cycle temperatures.

4.6 EXCEPTIONAL BEHAVIOR OF WORKING FLUID METHANOL

From the present experiment it is observed that methanol shows exceptional behavior at a input power of 250W for evaporator surface geometry-2. In this case the heat and mass transport cycle was not completed and a small portion of liquid was entered into the evaporator. After entering, methanol becomes vaporized so rapidly that the pressure inside the evaporator is higher than the pressure of the liquid inside the reservoir (which maintains atmospheric pressure). So that, rest of the liquid is not entered into the evaporator, and the heat transport characterization is failed. Then the vapor from the evaporator flows in the forward tube to the condenser tube, until the pressure inside the evaporator is lower than the atmospheric pressure. After decreasing the pressure in the evaporator, again a small portion of liquid was entered into the evaporator and the pressure inside the evaporator was suddenly increased. In this way, the process was repeating.

Figure 4.35 shows that the evaporator wall temperature is almost constant (varies from 74^oC to 74.7^oC). The variation of condenser inlet temperature is similar in nature as the

evaporator wall temperature. From Fig. 4.35 it is also seen that the condenser outlet temperature is nearly same to the condenser inlet temperature after 270S. Similar trends are shown at a input power of 210W for evaporator surface geometry-3 and methanol as the working fluid. Here, the evaporator wall temperature is also almost constant (varies from 67.1°C to 67.7°C).

Methanol performs better at low input power, up to 225W for geometry-2 (enhance evaporator surface) and 160W for geometry-3 (plain surface). The enhanced structure used demonstrates almost 1.4 times increase in the heat transfer compared to the plain surface. Above these heat inputs the system shows inconsistent performance.

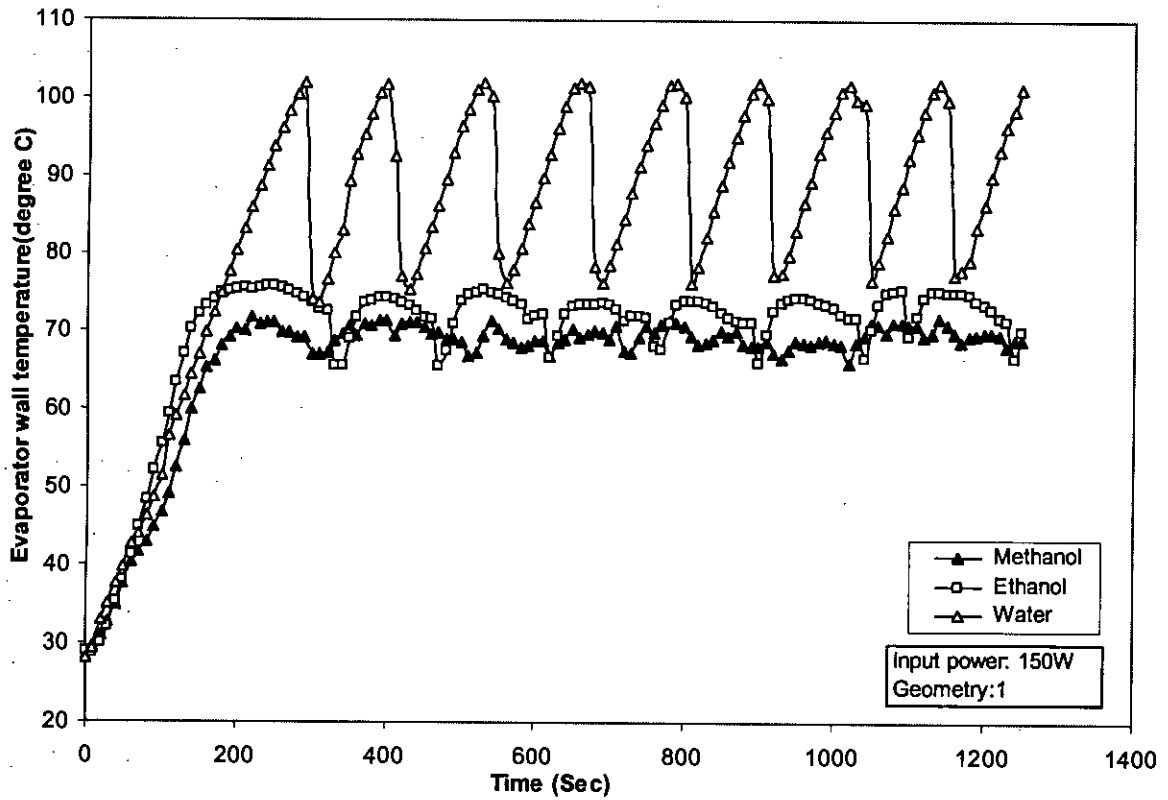


Figure 4.1: Variation of evaporator wall temperature with time for different working fluid with a input power of 150W (Geometry: 1)

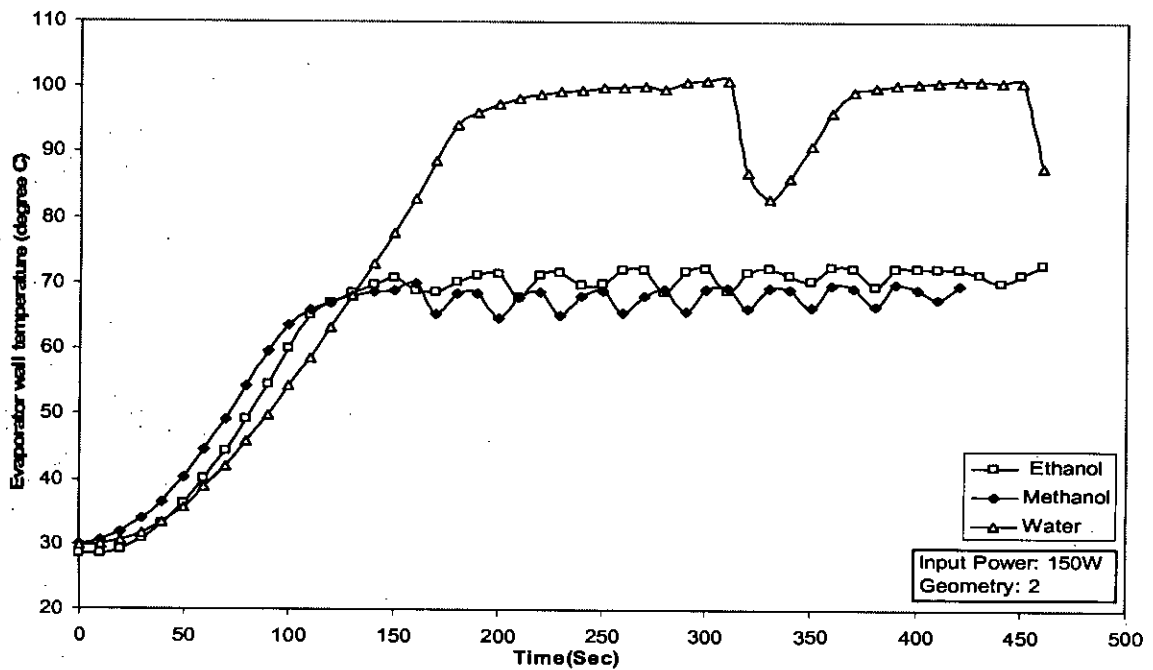


Figure 4.2: Variation of evaporator wall temperature with time for different working fluid with a input power of 150W (Geometry: 2)

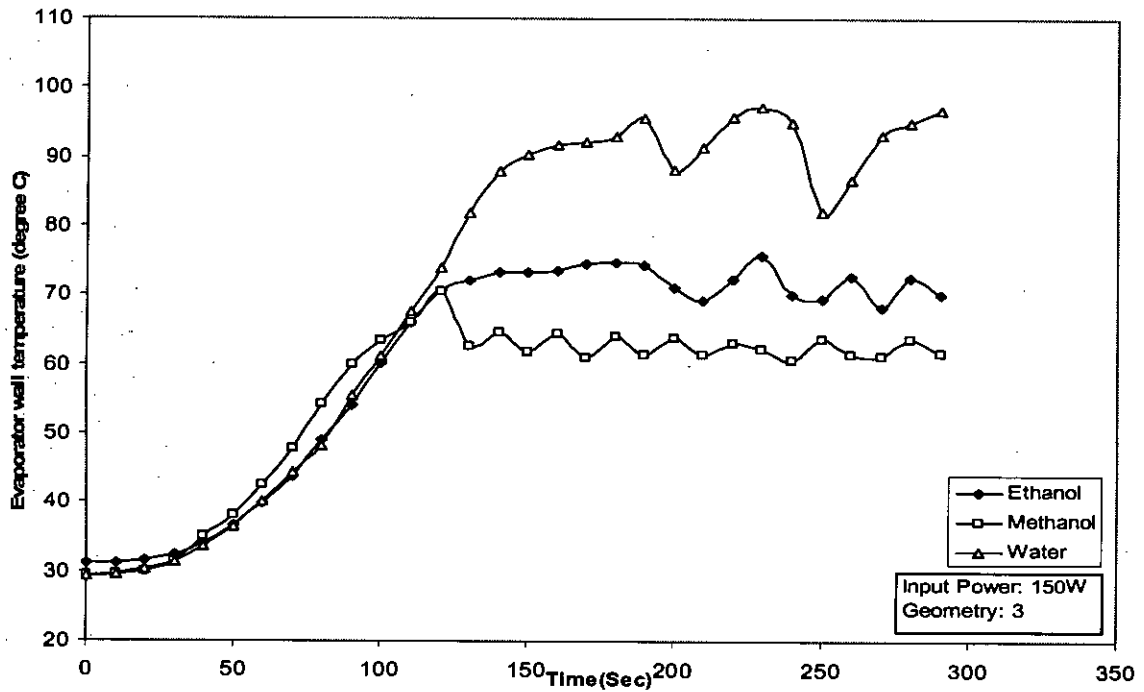


Figure 4.3: Variation of evaporator wall temperature with time for different working fluid with a input power of 150W (Geometry:3)

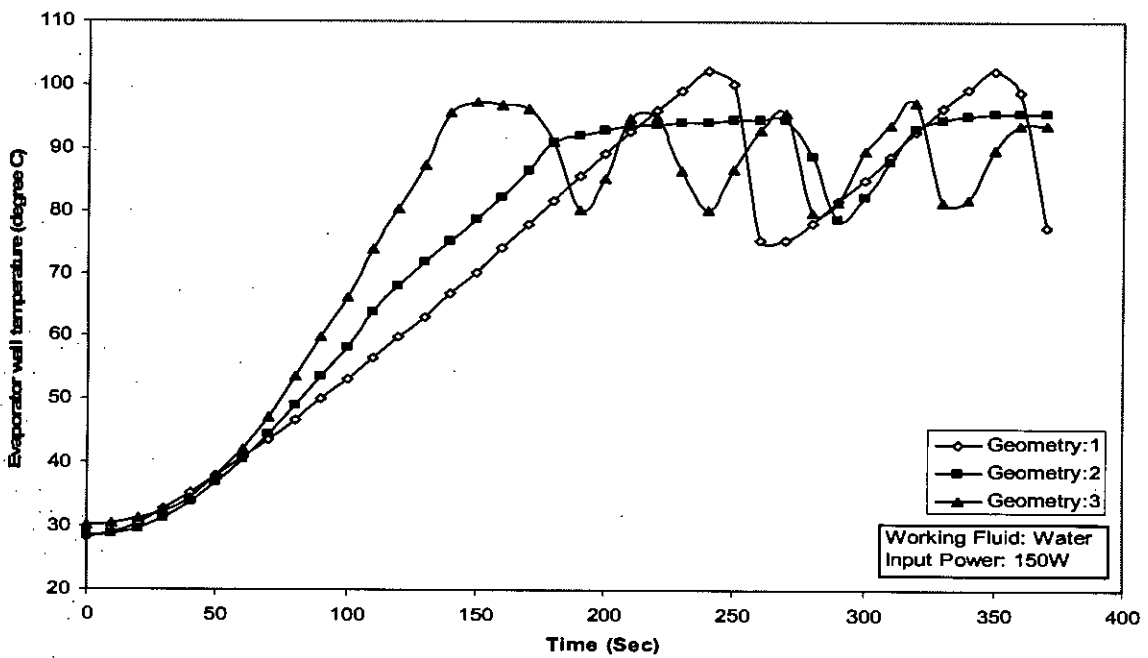


Figure 4.4: Variation of evaporator wall temperature for different evaporator surface geometry with water as the working fluid

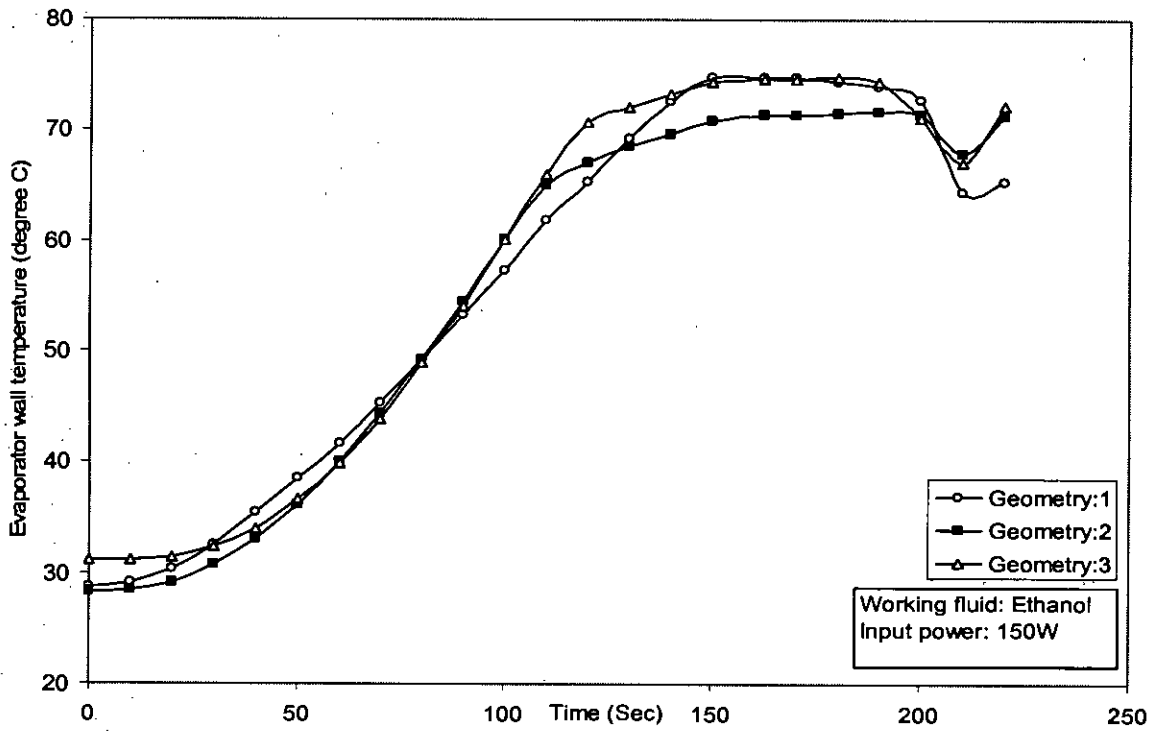


Figure 4.5: Variation of evaporator wall temperature for different evaporator surface geometry with ethanol as the working fluid

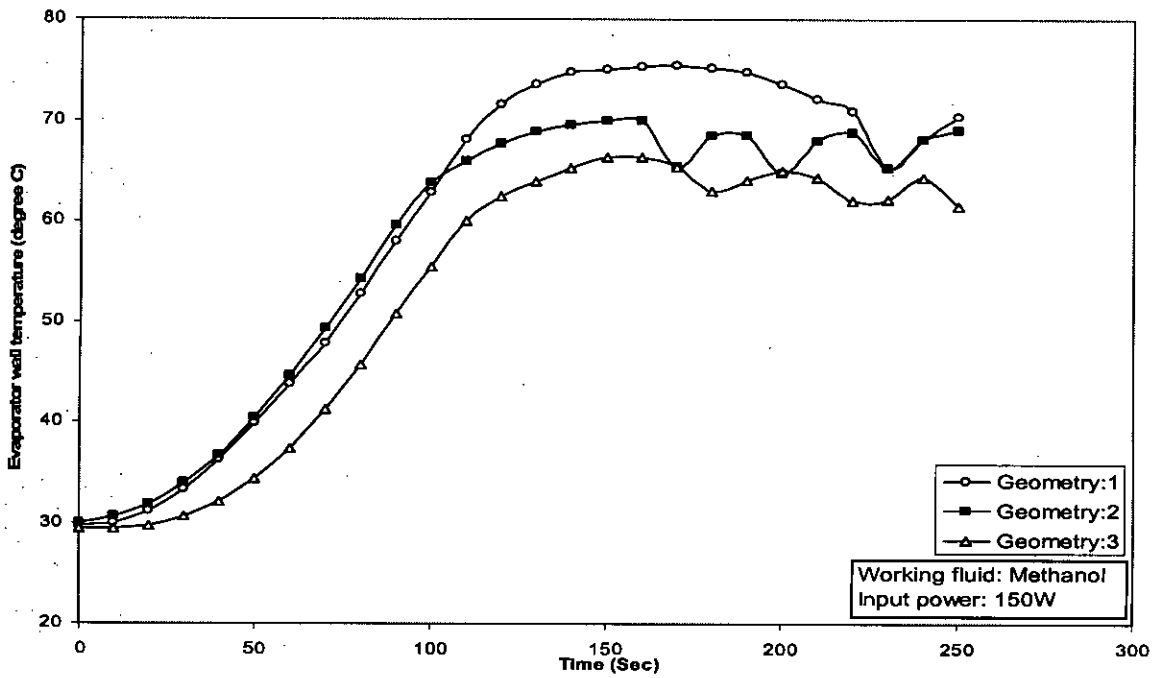


Figure 4.6: Variation of evaporator wall temperature for different evaporator surface geometry with methanol as the working fluid

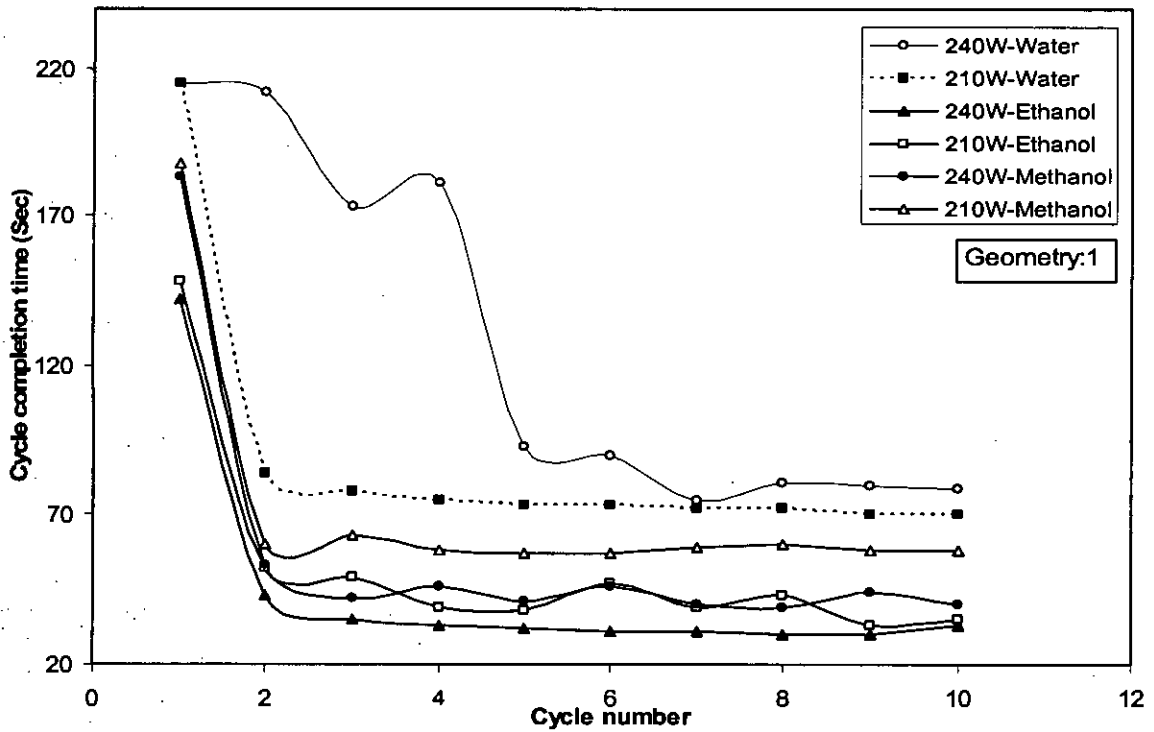


Figure 4.7: Comparison of cycle completion time for different working fluid (water, ethanol, methanol) at input powers of 210W & 240W (Geometry:1)

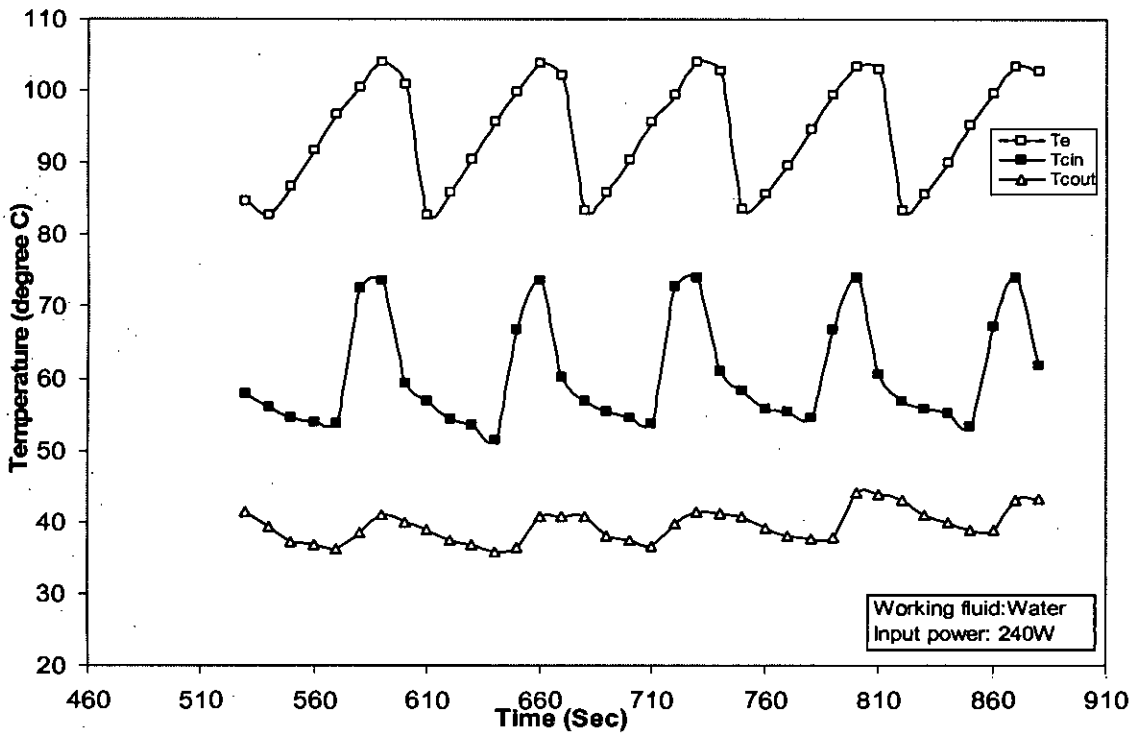


Figure 4.8: Temperatures during five consecutive cycles (6 to 10) for geometry one and water as the working fluid

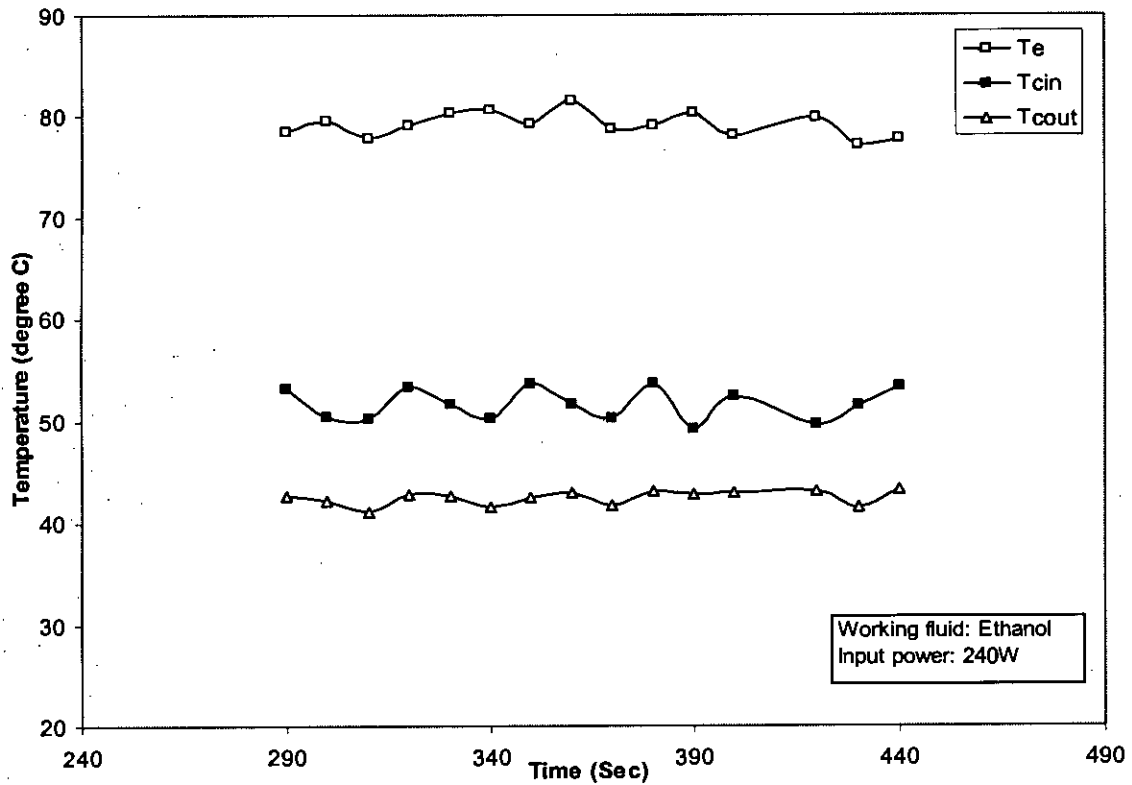


Figure 4.9: Temperatures during five consecutive cycles (6 to 10) for geometry one and ethanol as the working fluid

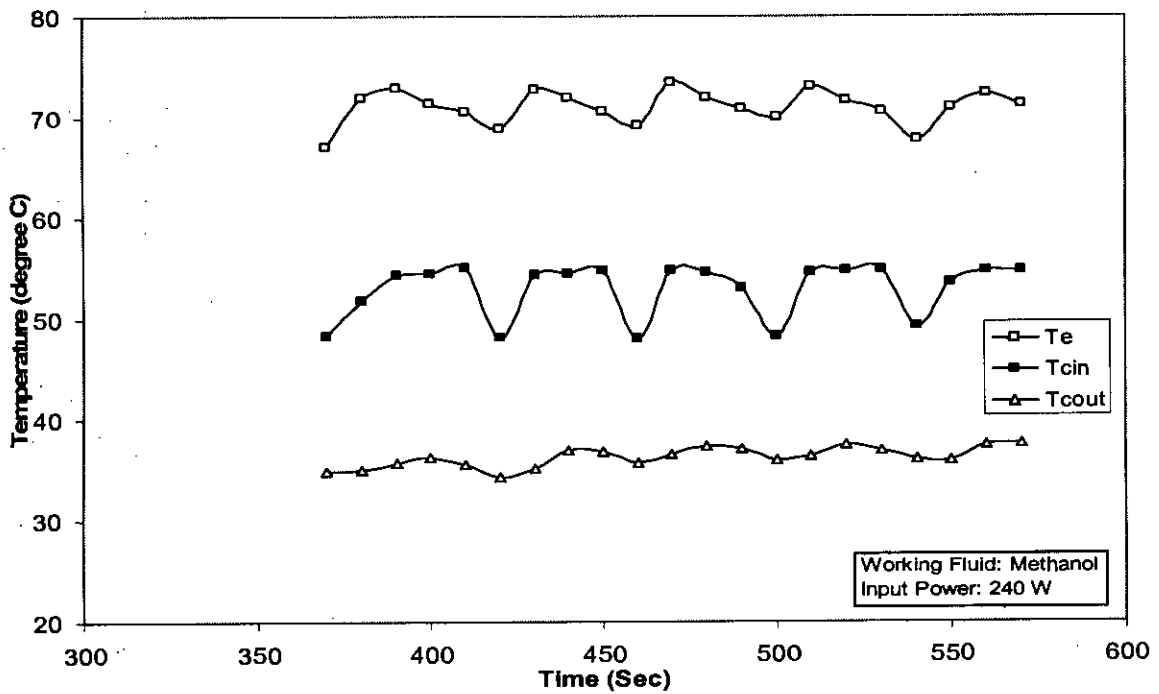


Figure 4.10: Temperatures during five consecutive cycles (6 to 10) for geometry one and methanol as the working fluid

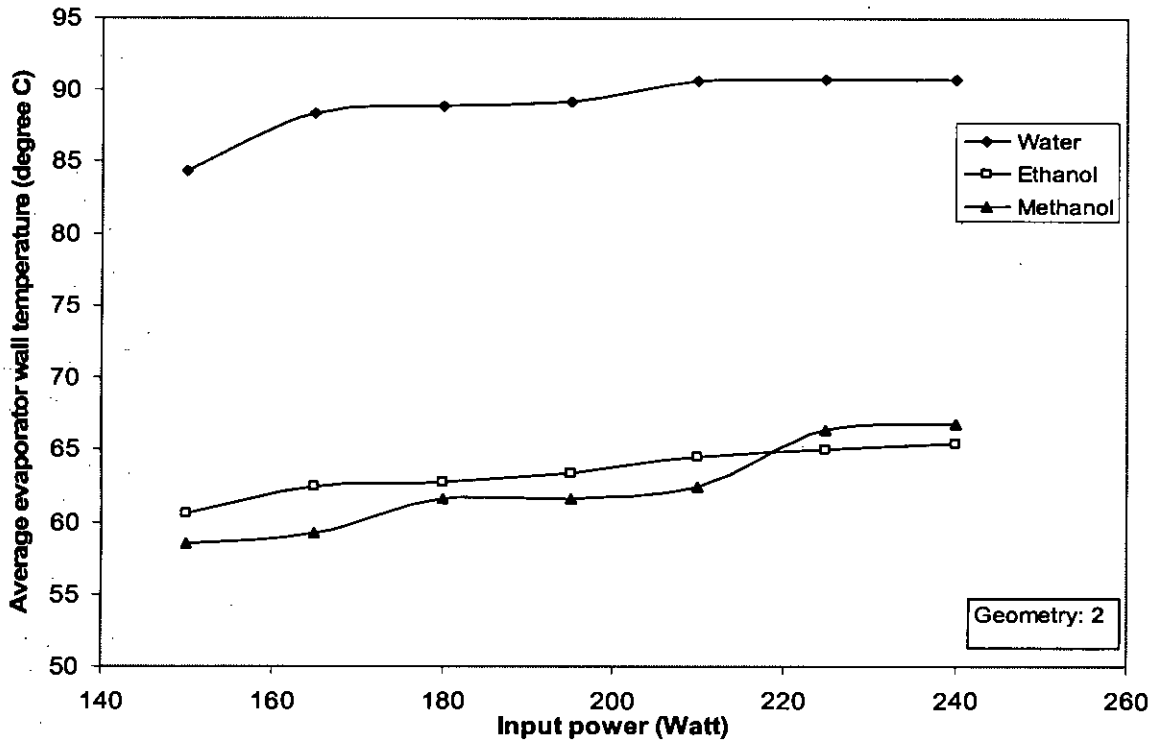


Figure 4.11: Variation of average evaporator wall temperature with input power for three working fluids (Geometry: 2)

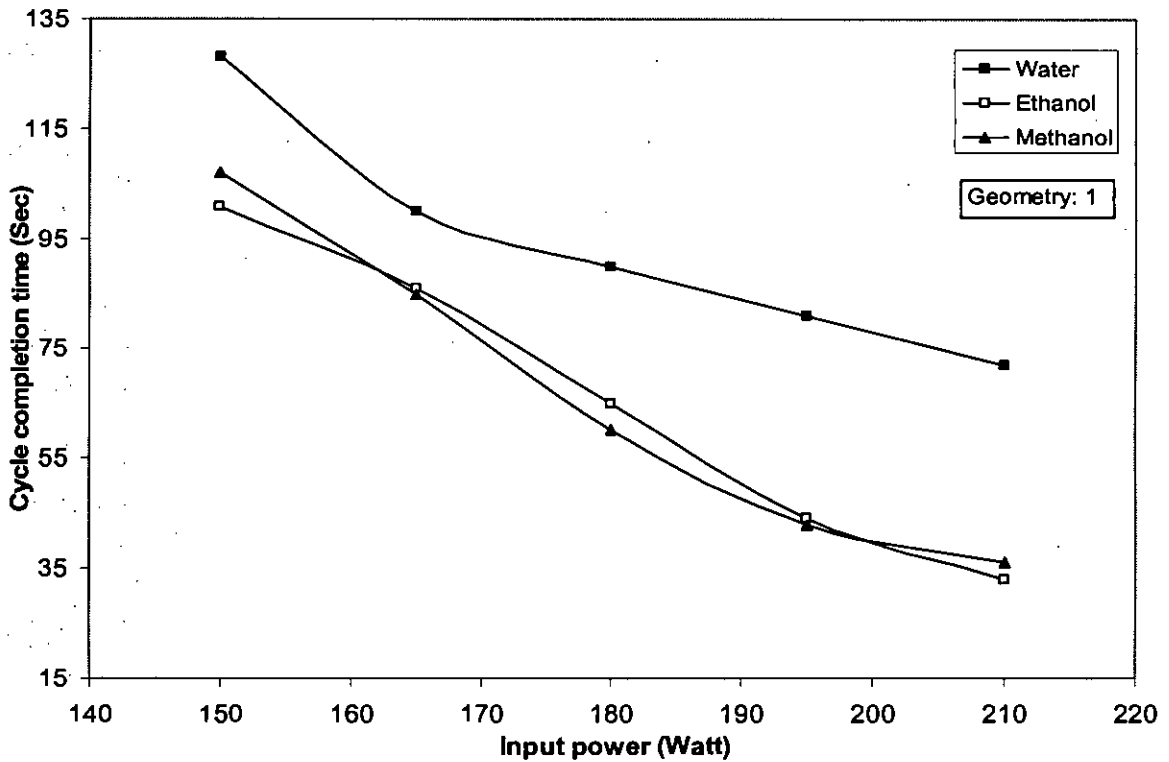


Figure 4.12: Effect of input power on cycle time for different working fluid (Geometry:1)

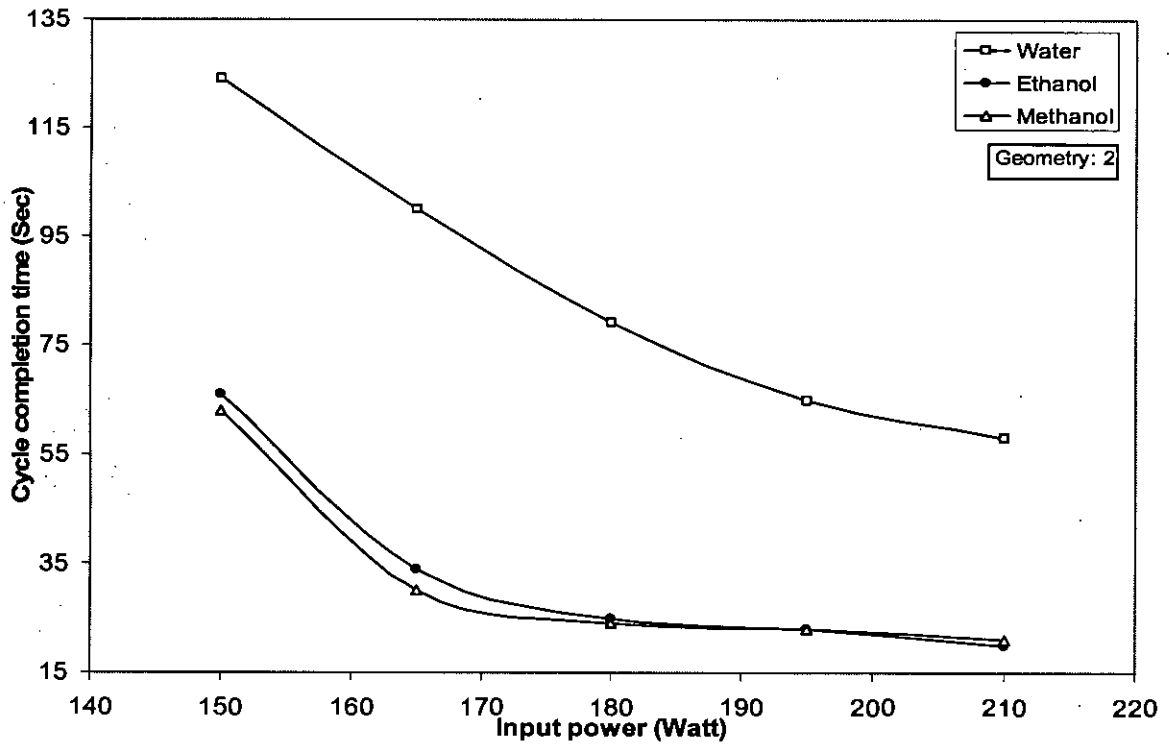


Figure 4.13: Effect of input power on cycle time for different working fluid (Geometry:2)

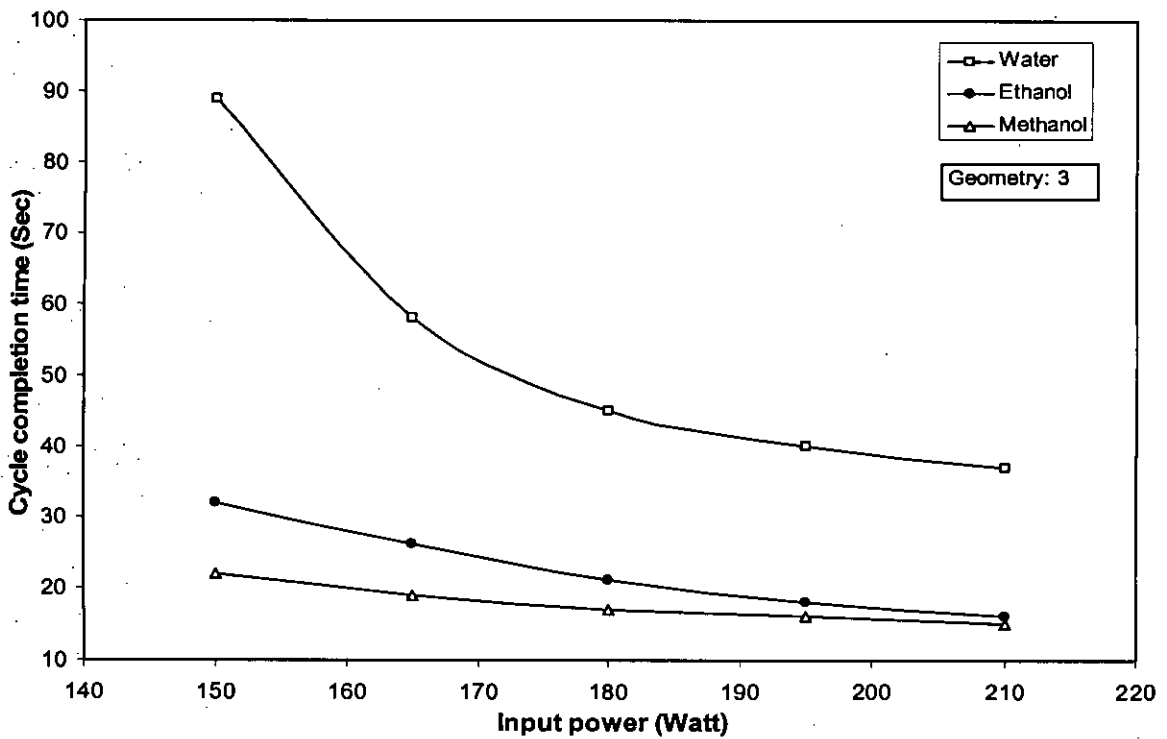


Figure 4.14: Effect of input power on cycle time for different working fluid (Geometry:3)

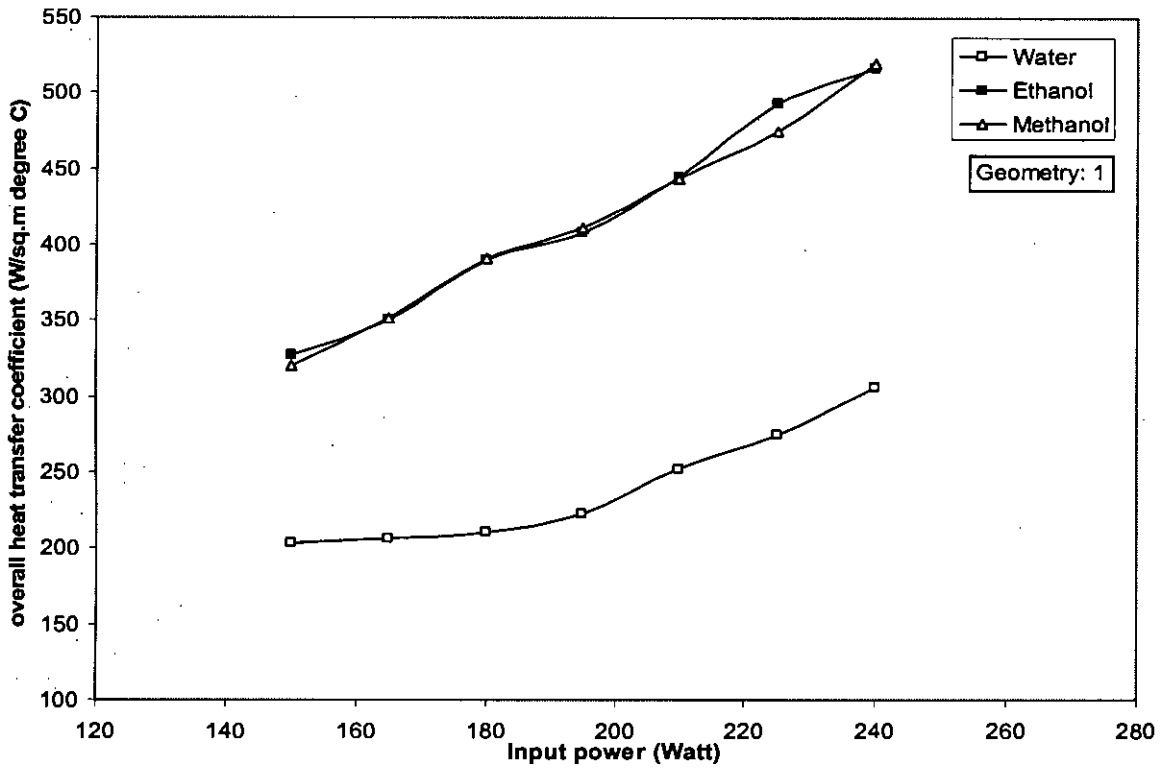


Figure 4.15: Effect of working fluid on overall heat transfer coefficient for geometry-1

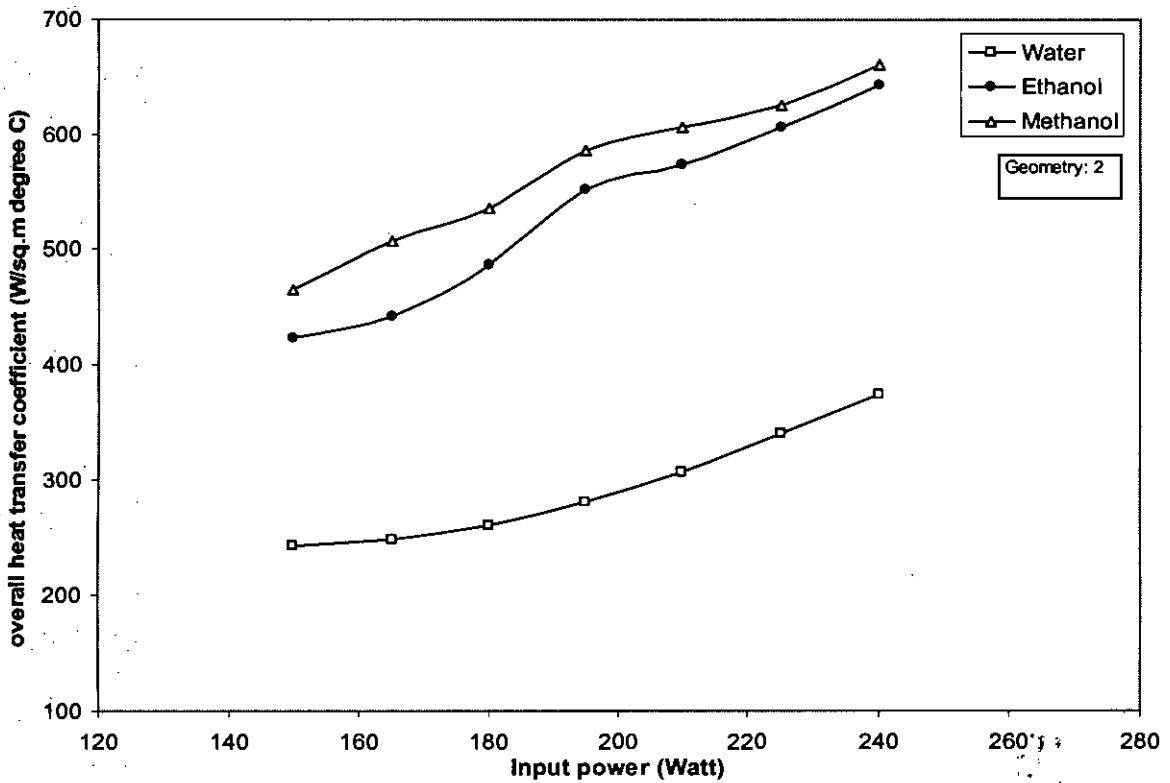


Figure 4.16: Effect of working fluid on overall heat transfer coefficient for geometry-2

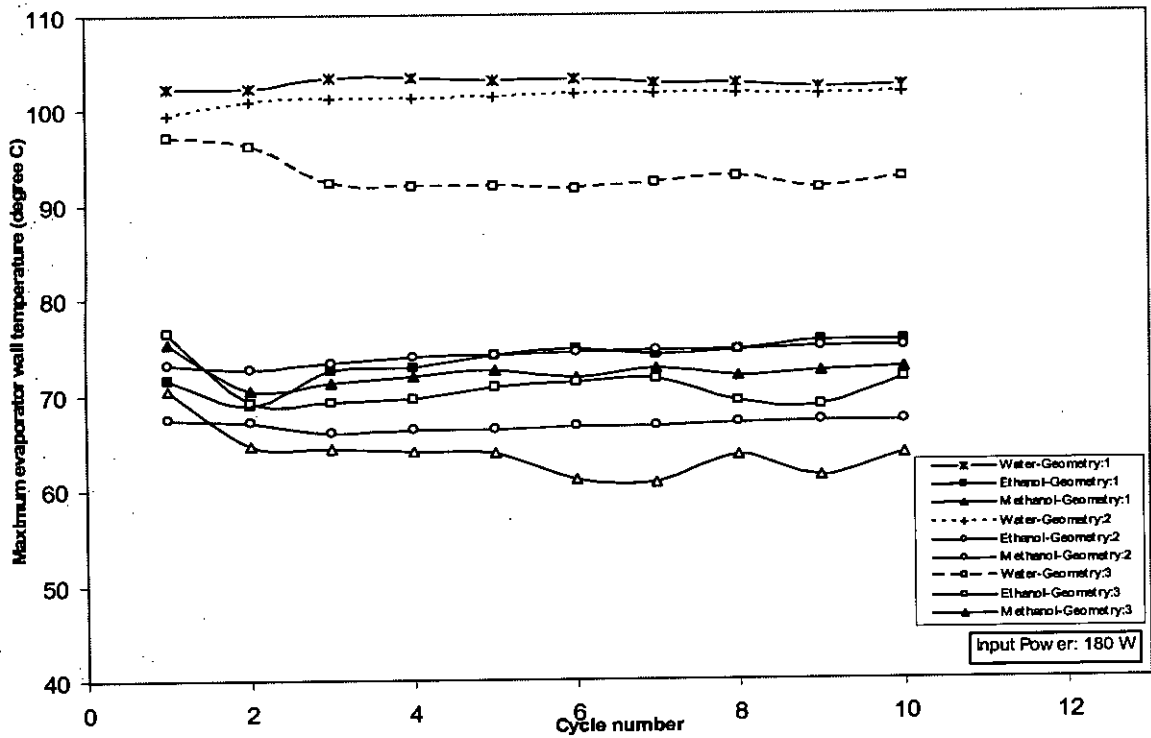


Figure 4.17: Effect of maximum evaporator wall temperature on different working fluid and different evaporator surface geometry for input power of 180W

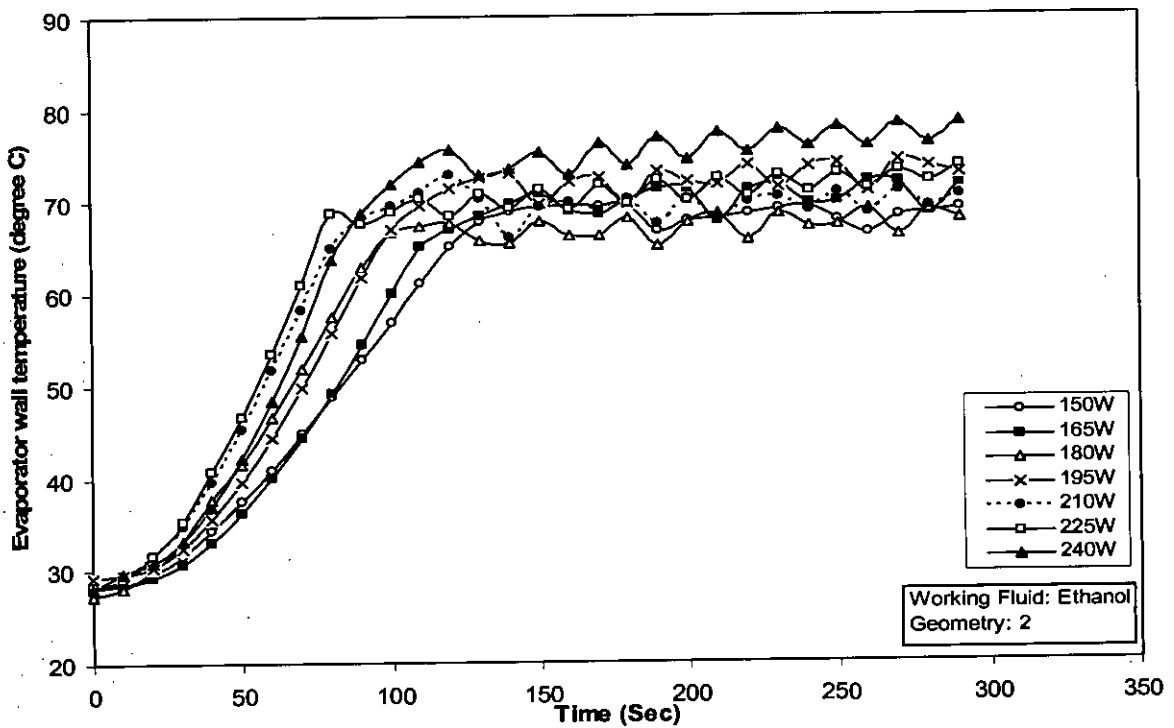


Figure 4.18: Variation of evaporator wall temperature with time for different input power with ethanol as the working fluid (Geometry:2)

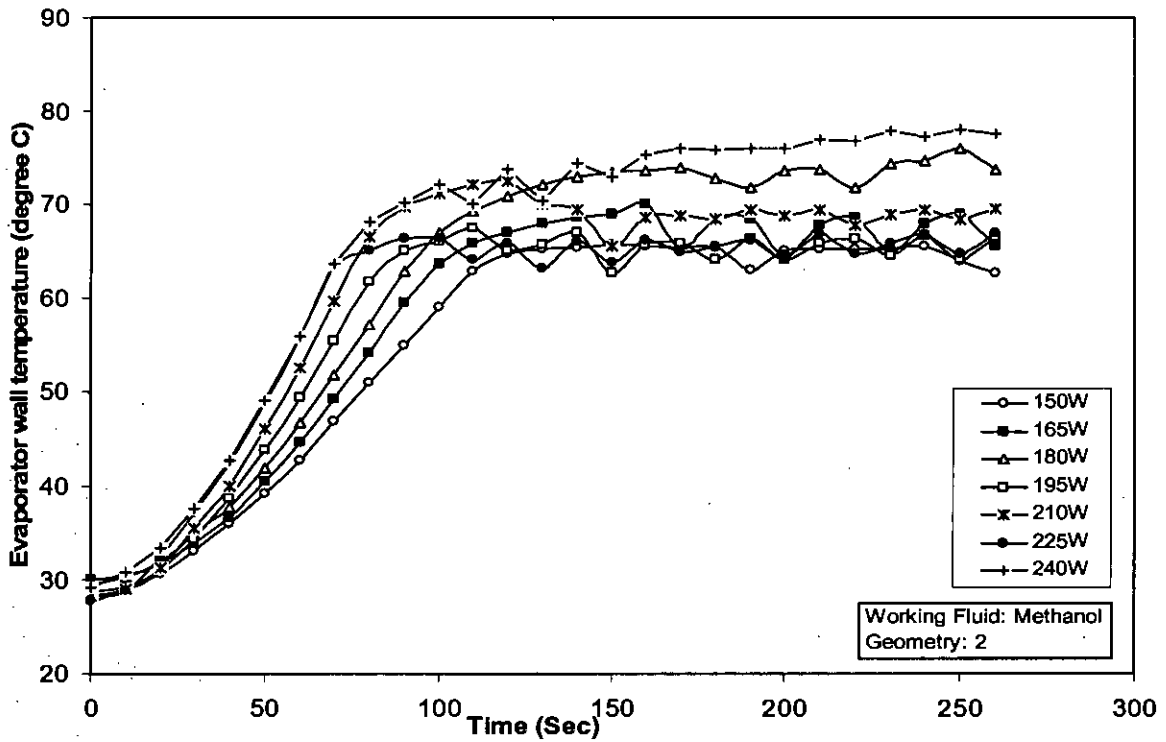


Figure 4.19: Variation of evaporator wall temperature with time for different input power with methanol as the working fluid (Geometry:2)

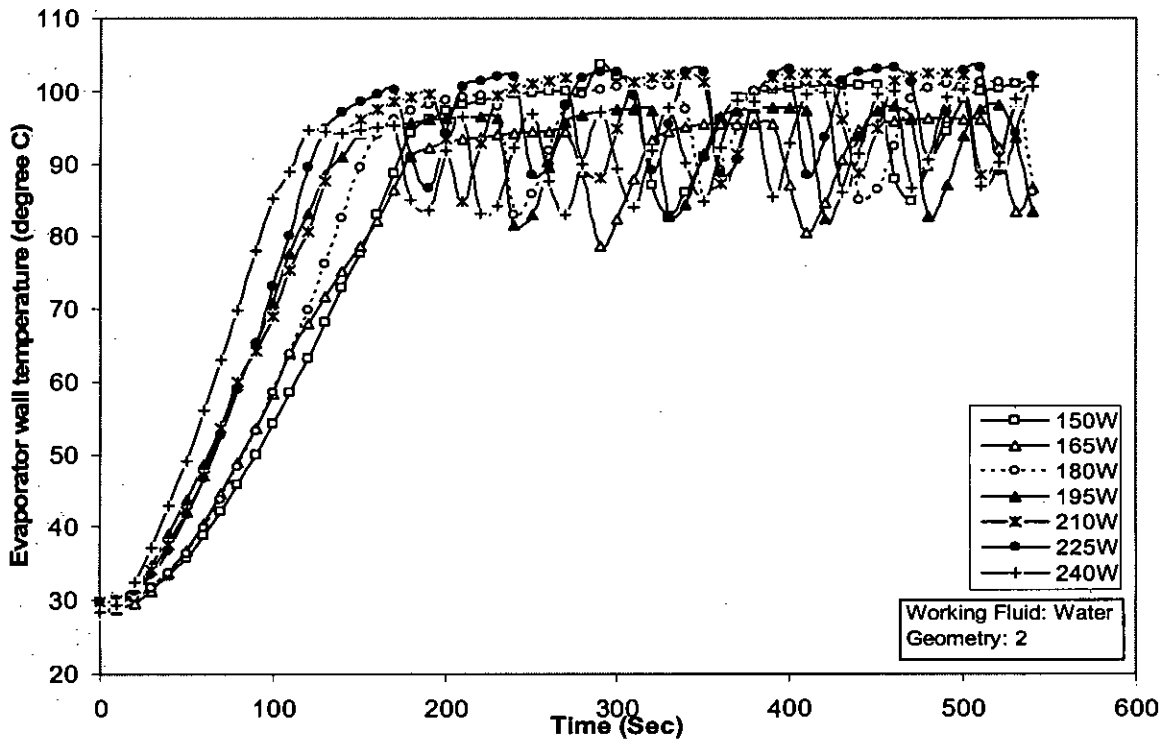


Figure 4.20: Variation of evaporator wall temperature with time for different input power with water as the working fluid (Geometry:2)

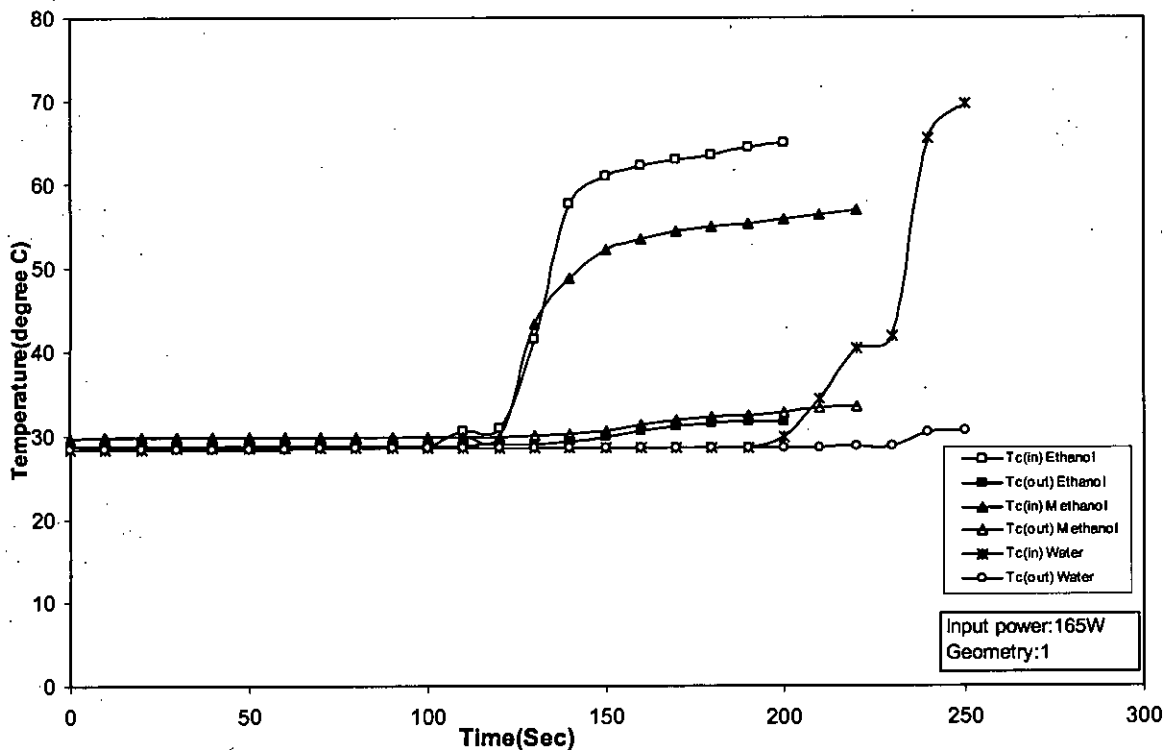


Figure 4.21: Effect of working fluid on condenser wall temperatures for geometry-1

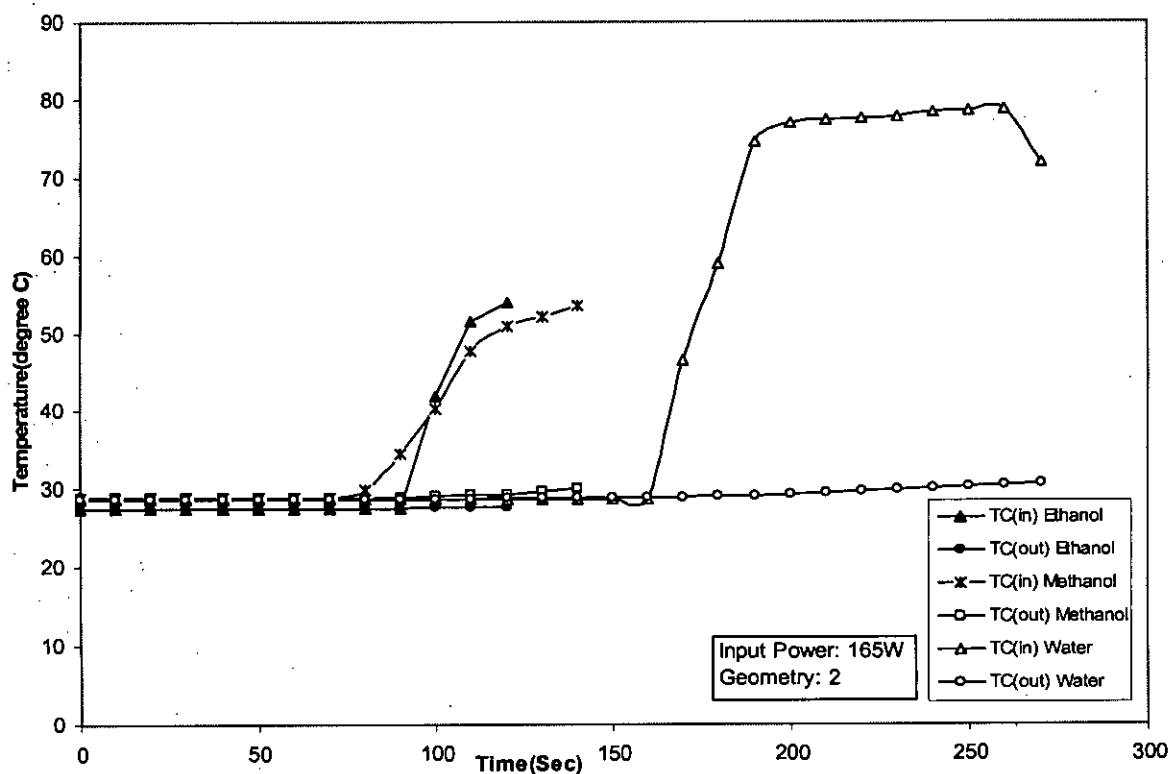


Figure 4.22: Effect of working fluid on condenser wall temperatures for Geometry-2

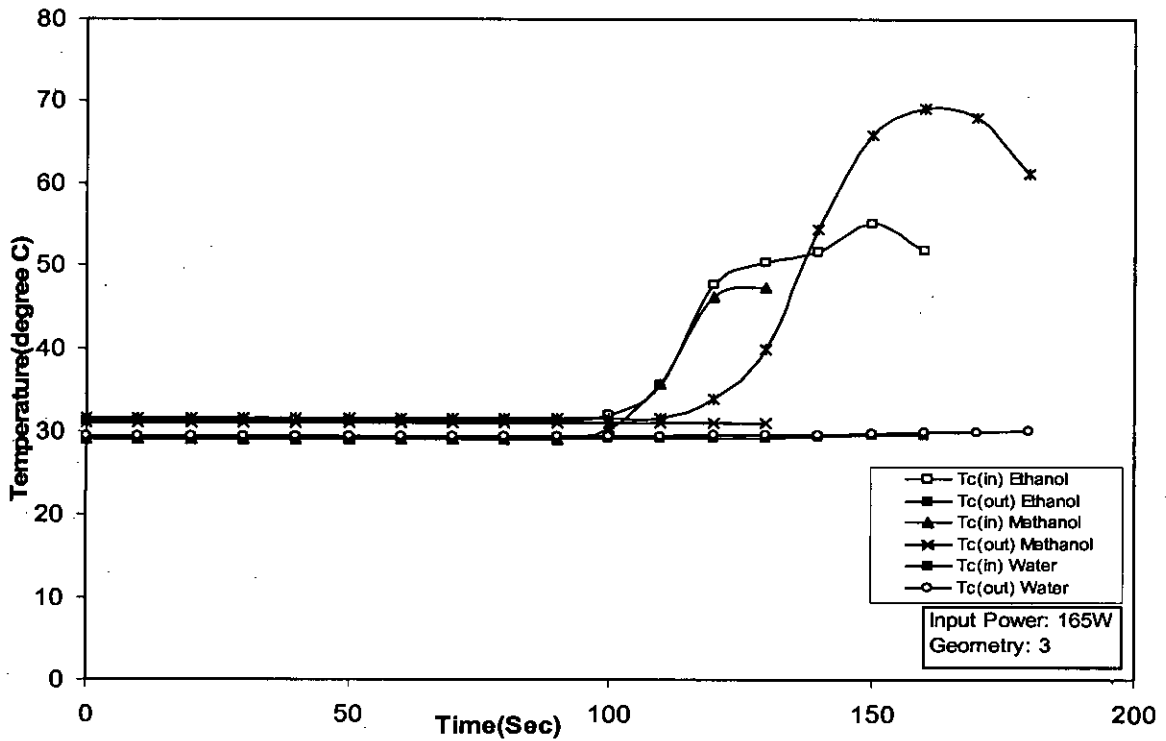


Figure 4.23: Effect of working fluid on condenser wall temperatures for geometry-3

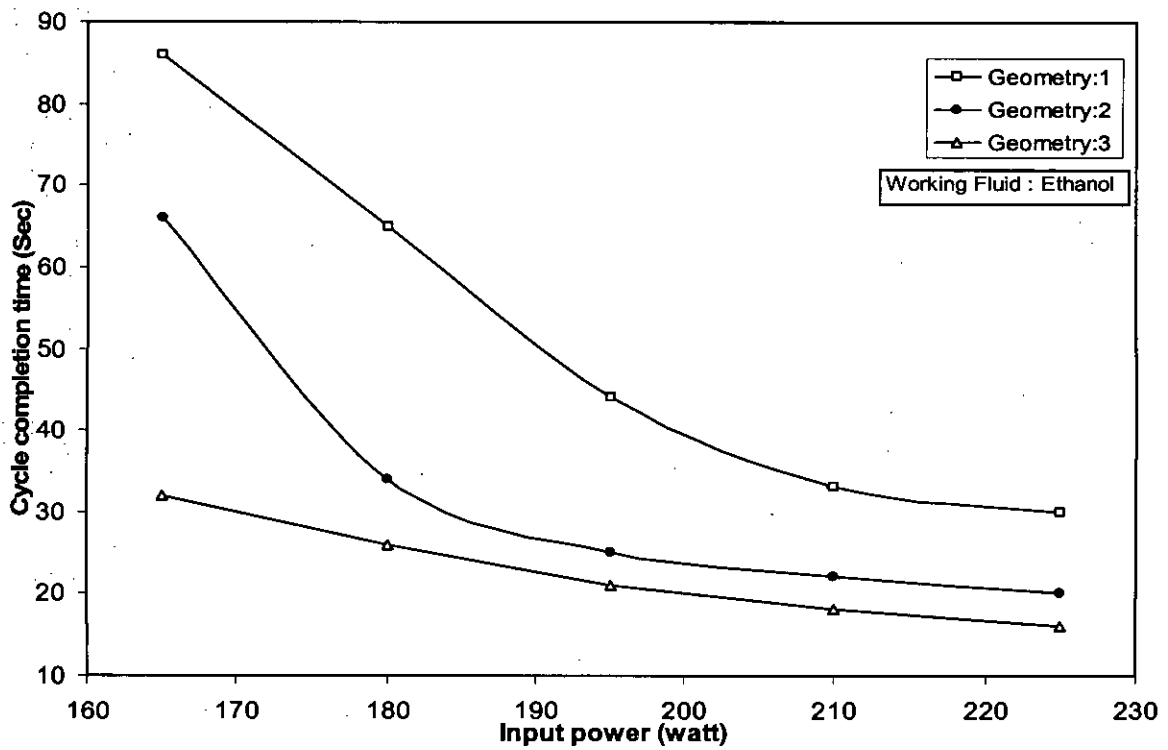


Figure 4.24: Effect of input power on cycle time for different evaporator surface geometry with ethanol as the working fluid

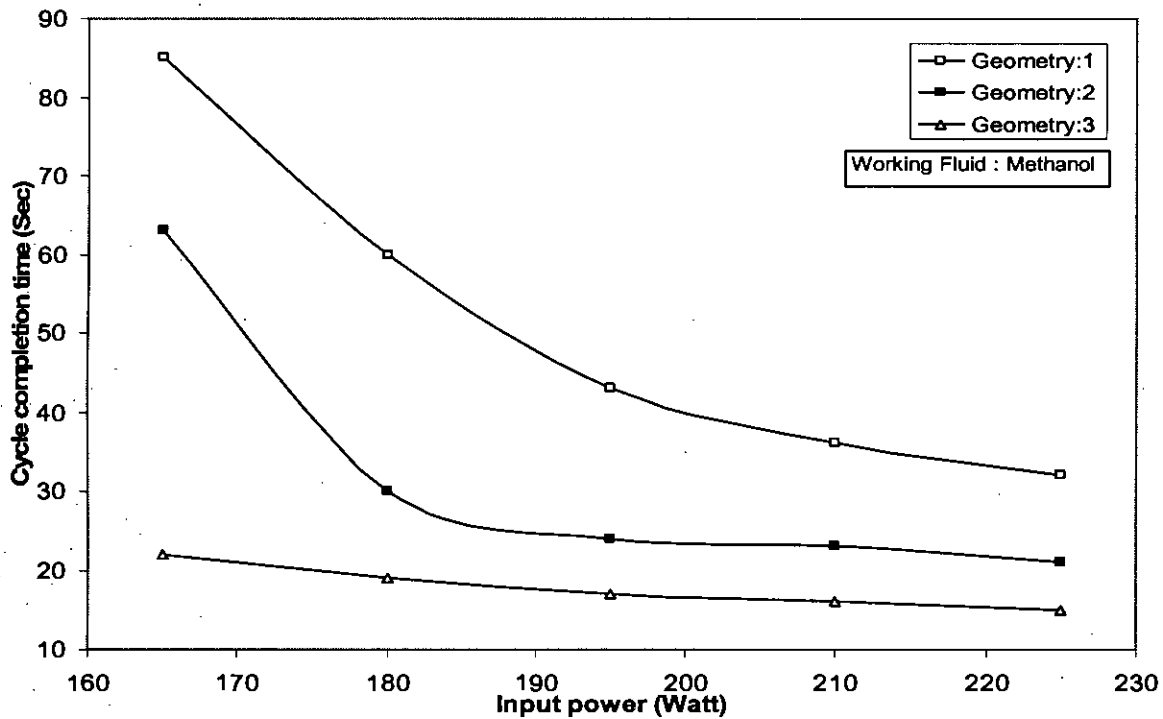


Figure 4.25: Effect of input power on cycle time for different evaporator surface geometry with methanol as the working fluid

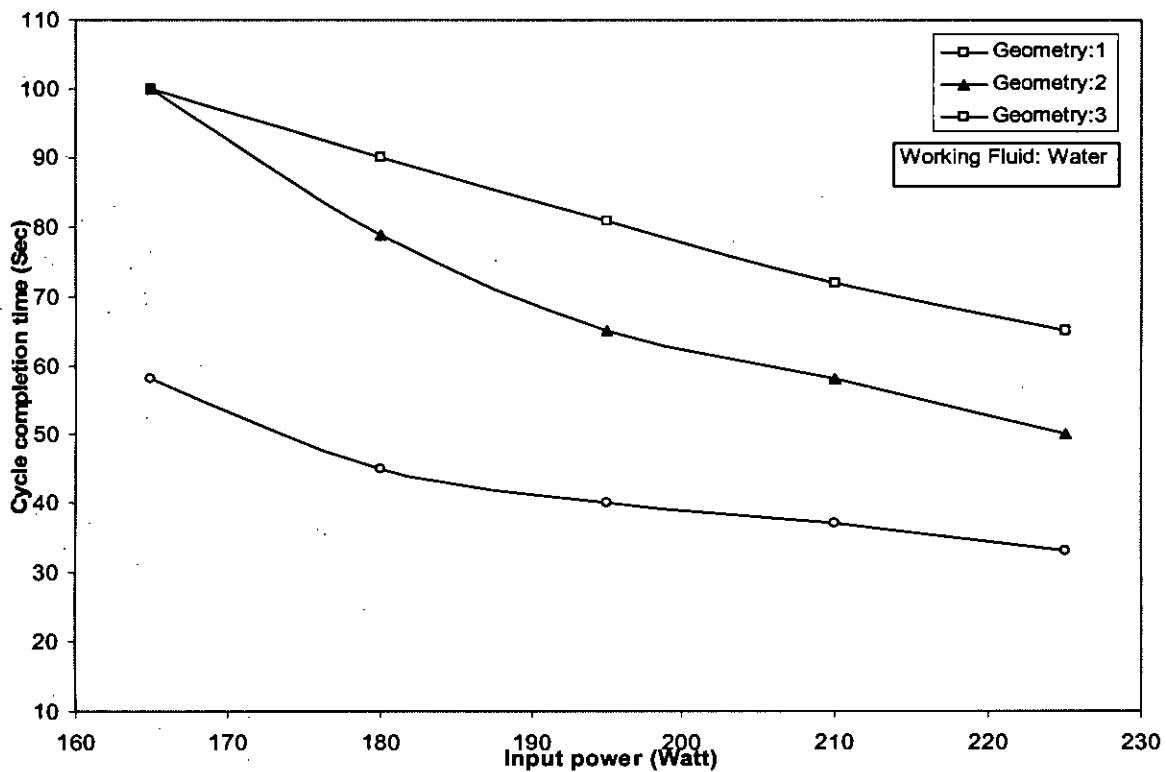


Figure 4.26: Effect of input power on cycle time for different evaporator surface geometry with water as the working fluid

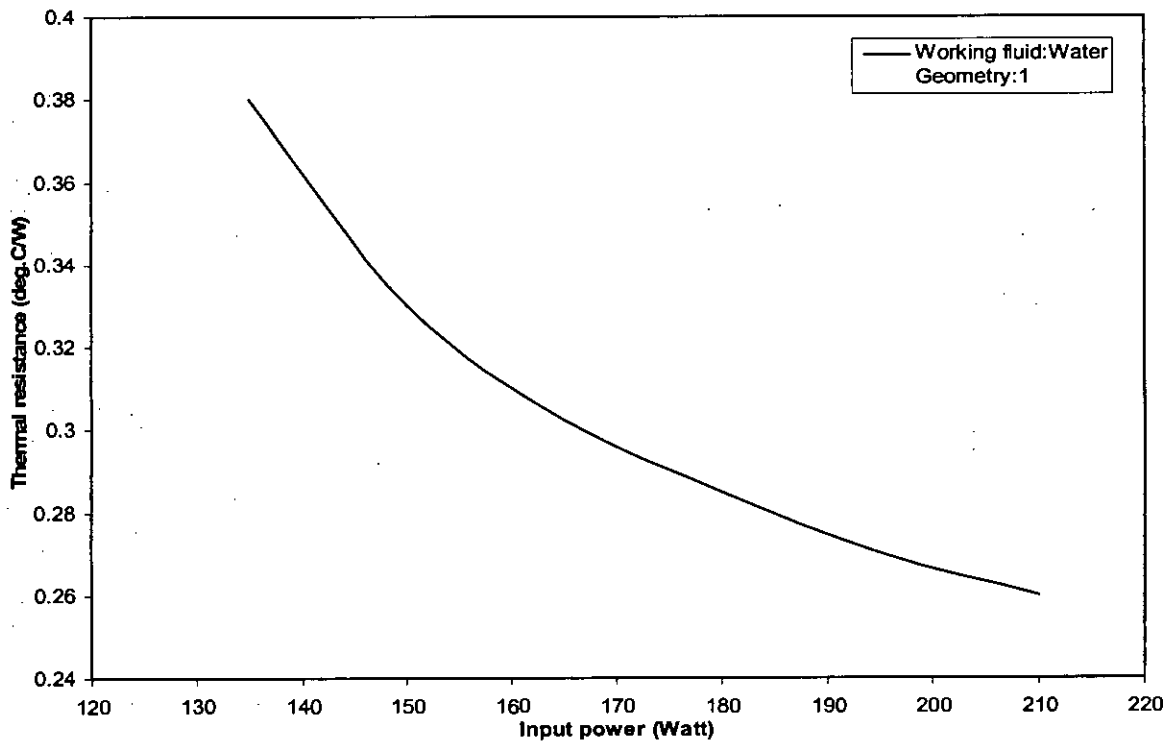


Figure 4.27: Effect of input power on thermal resistance for geometry-1 and water as the working fluid

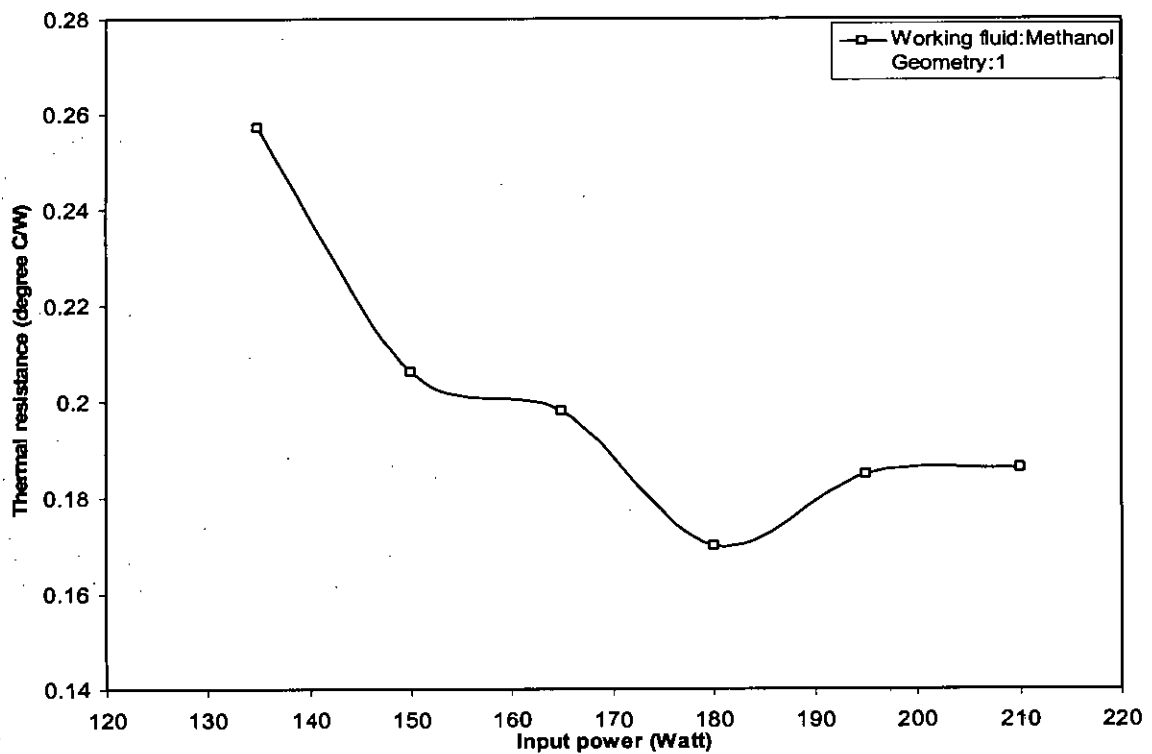


Figure 4.28: Effect of input power on thermal resistance for geometry one and methanol as the working fluid

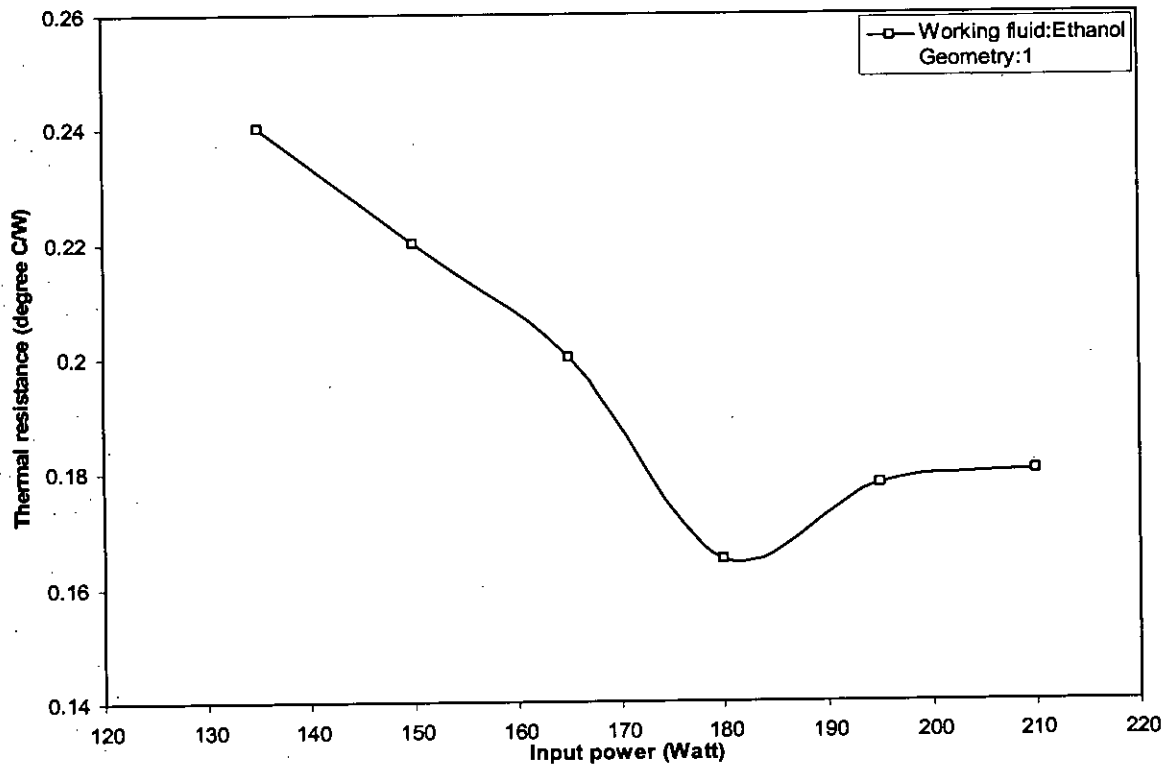


Figure 4.29: Effect of input power on thermal resistance for geometry-1 and ethanol as the working fluid

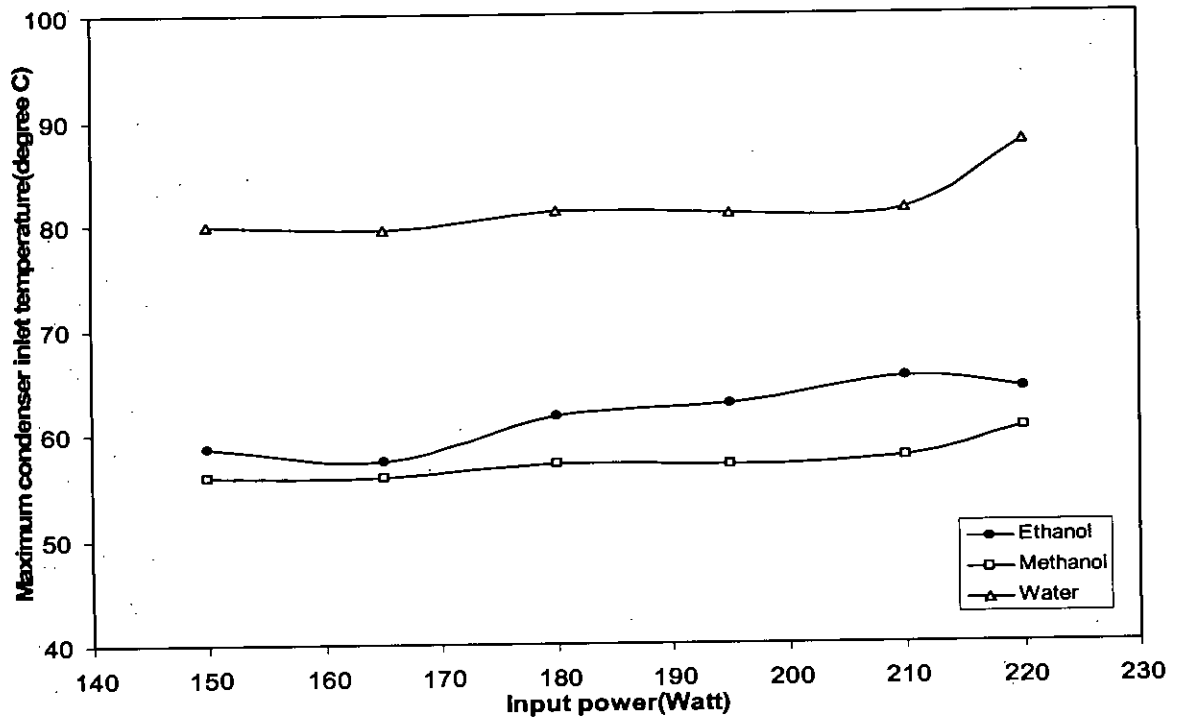


Figure 4.30: Variation in the maximum condenser inlet temperature with increasing input power for different working fluids (Geometry: 2)

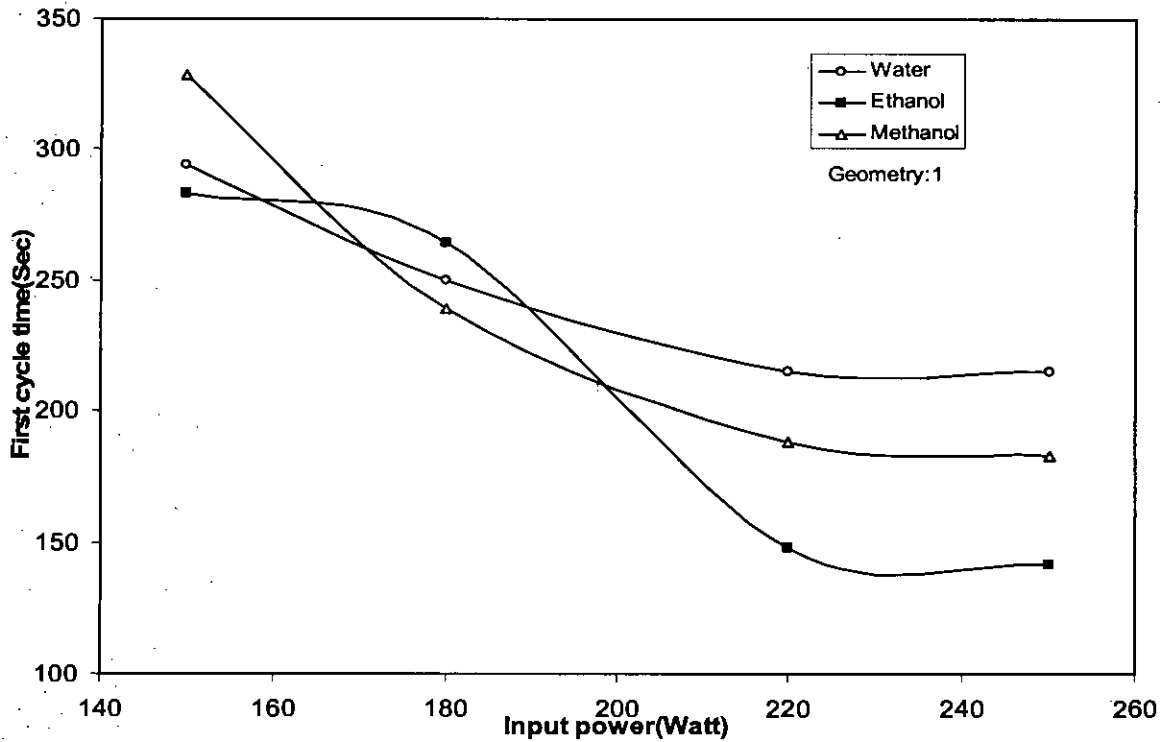


Figure 4.31: Effect of working fluids on first cycle time for geometry-1

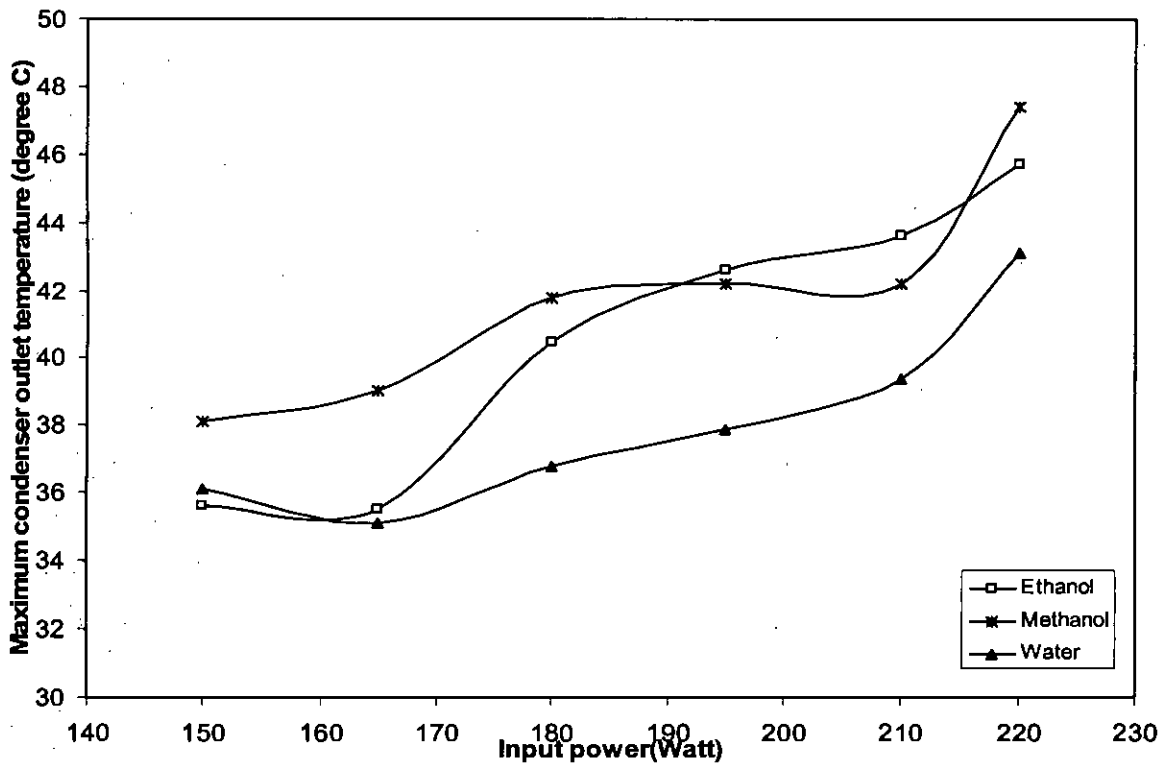


Figure 4.32: Variation in the maximum condenser outlet temperature with increasing input power for different working fluids (Geometry:2)

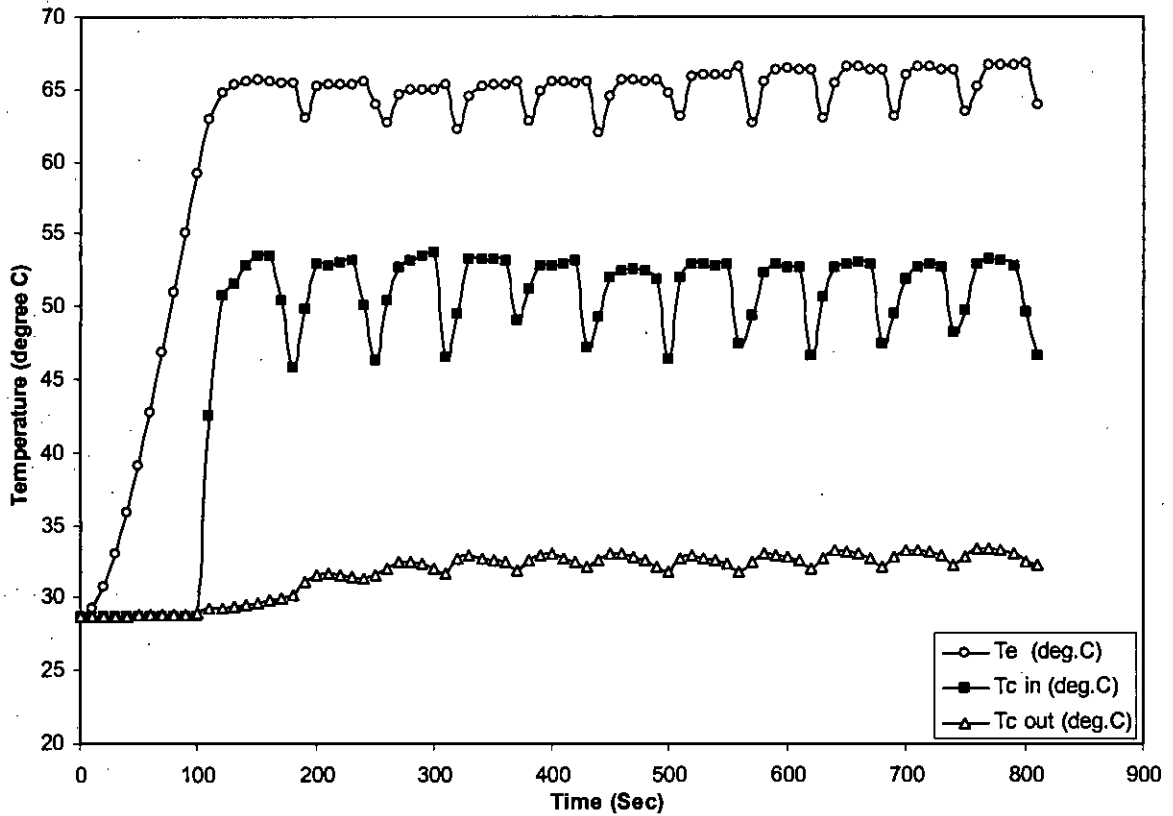


Figure 4.33: Temperature diagram for ethanol, 120W as heat power rate (Geometry: 2)

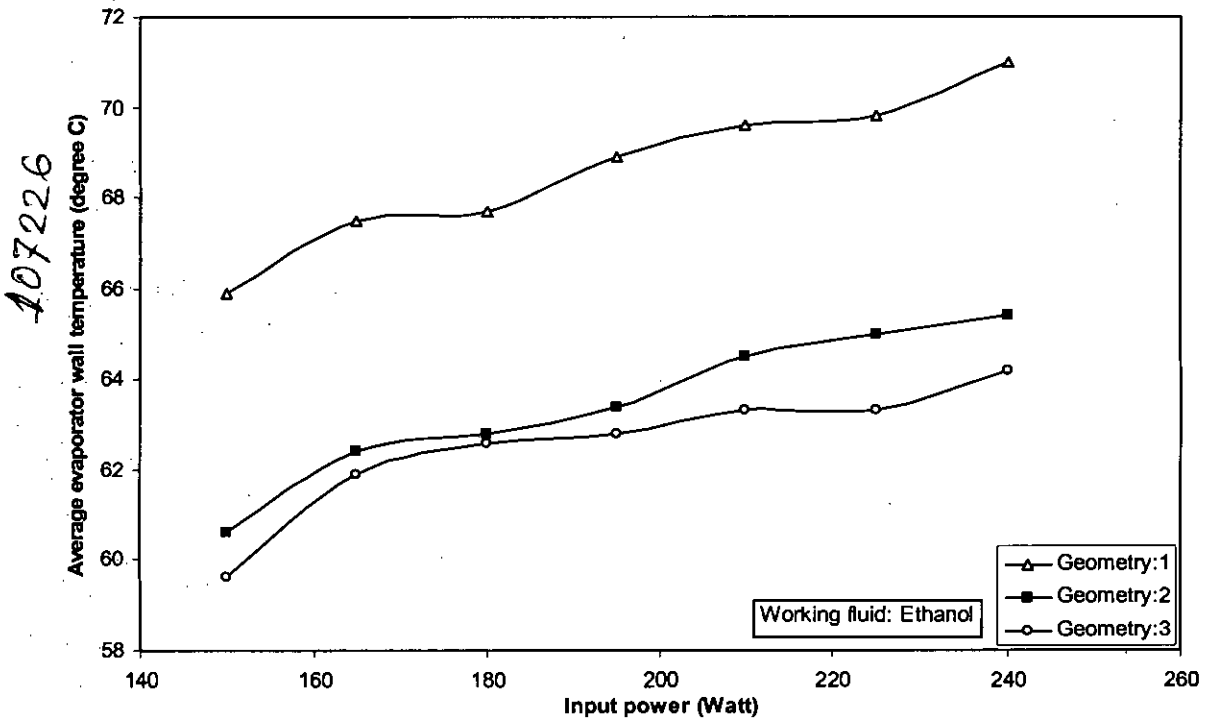


Figure 4.34: Effect of average evaporator wall temperature on different evaporator surface geometry with ethanol as the working fluid

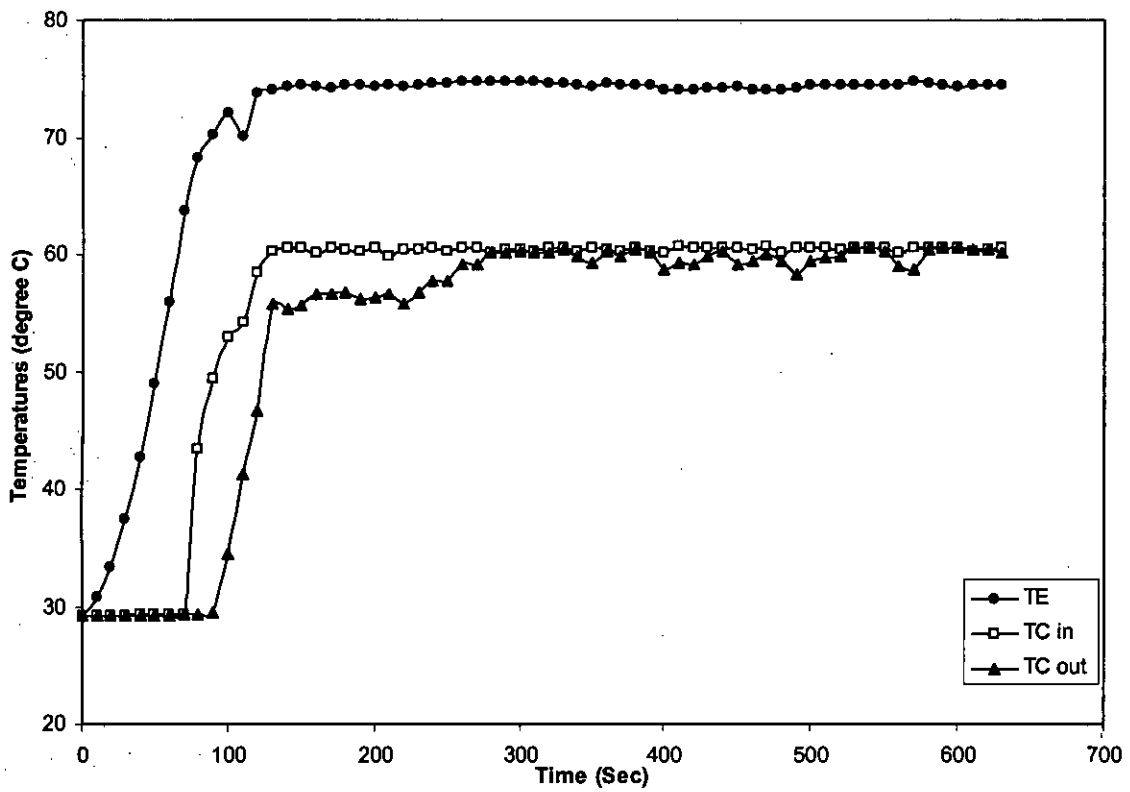


Figure 4.35: Effect of temperatures on time for working fluid methanol at a input power of 240W (Geometry:2)

CONCLUSIONS AND RECOMMENDATIONS**5.1 CONCLUSIONS**

This study demonstrates the performance evaluation of a two phase loop thermosyphon with enhanced heat transfer surfaces in the evaporator. Three different working fluids, water, ethanol and methanol have been tested for three different evaporator surface geometry of the loop thermosyphon. The experimental results support the following conclusions:

1. The evaporator surface temperature was as high as 104.4°C to transfer heat flux of 300W for water. These temperatures were 81.7°C and 74.3°C for ethanol and methanol respectively. The respective heat fluxes were 270W and 240W.
2. The maximum possible heat inputs applied for geometry-1, geometry-2 and geometry-3 are respectively 300W, 255W and 210W. Thus more heat fluxes were dissipated by evaporator surface geometry-1.
3. The response of the system with increasing thermal load was very smooth. This has considerable practical significance where the repeatability of performance is essential for a reliable system. At higher heat loads the system responds fairly quickly during start up.
4. Optimal performance of the loop thermosyphon device was found to greatly depend on the physical characteristics of the thermosyphon such as the optimal structure of the evaporator surface, as well as the fluid properties such as the type of fluid. Water is a better working fluid, as the thermal properties of water are better than that of ethanol and methanol.

5.2 RECOMMENDATIONS

The experimental tests have shown that this TPLT can be a really low cost alternative solution for the electronics cooling, but some experimental investigations had to be made in order to optimize it. For further study, the following recommendations may be made:

1. Further detailed numerical and experimental studies can be developed to accurately predict the behavior of the loop thermosyphon.
2. Future electronic applications will require dissipating heat fluxes up to $200\text{W}/\text{cm}^2$ and suitable extended and enhanced inner surfaces for the evaporator part will have to be developed.
3. For optimal performance, different working fluids such as acetone, isobutene, ethylene glycol, fluoro-carbon family etc. can be used.
4. To estimate mass flow of liquid and vapor during operation.
5. For electronics cooling, the loop thermosyphon device at a much miniature scale and at different orientation can be investigated.

REFERENCES

- [1] Ramaswamy, C., Joshi, Y., and Nakayama, W., "Combined Effects of Sub-Cooling and Operating Pressure on the Performance of a Two-Chamber Thermosyphon", IEEE Transactions on Components and Packaging Technologies, March 2000, pp. 61-69.
- [2] Rossi, L., Polasek, F., "Thermal Control of Electronic Equipment by Heat Pipes and Two-Phase Thermosyphons", 11th International Heat Pipe Conference, pp. 50-74, Tokyo 1999.
- [3] Bar-Cohen, A., and Schweitzer, H., "Thermosyphon Boiling in Vertical Channels", J. Heat Transfer, Vol. 107, pp. 772-778, 1985.
- [4] Kishimoto, T., and Harada, A., "Two-Phase Thermosyphon Cooling for Telecom-Multichip Modules", Advances in Electronic Packaging (ASME), Vol. I, pp. 135-141, 1992.
- [5] Alam, M., "Thermoloop: A Heat and Mass Transfer Technology and Device", 3rd BSME-ASME International Conference on Thermal Engineering, 20-22 December, 2006, Dhaka, Bangladesh.
- [6] Mudawar, I., and Anderson, T. M., "High Flux Electronic Cooling by Means of Pool Boiling Part-I: Parametric Investigation of the Effects of Coolant Variation, Pressurization, Sub Cooling and Augmentation", Heat Transfer in Electronics, ASME HTD-Vol. III, Ed. R. K. Shah, pp. 25-34, 1989.
- [7] Rahman, M.A., Islam, M.A., and Alam, M., "Performance Study of Thermoloop: Effect of Evaporator Fill Ratio and Condenser Condition", International Conference on Mechanical Engineering, 29-31 December, 2007, Dhaka, Bangladesh.
- [8] Palm, B., and Tengblad, N., "Cooling of Electronics by Heat Pipes and Thermosyphons, A Review of Methods and possibilities", Processing of the 31st National Heat Transfer Conference, ASME, HTD, Vol. 329, 7, 97-108, 1996.
- [9] Incropera, F. P., "Liquid Immersion Cooling of Electronic Components", Heat Transfer In Electronic And Microelectronic Equipment, Ed. A. E. Bergles, Hemisphere Publishing Corporation, pp. 407-444, 1990
- [10] Bergles, A.E., and Bar-Cohen, A., "Direct Liquid Cooling of Microelectronic Components", Advances in Thermal Modeling of Electronic Components and

- Systems- Vol. 2, Eds. A. Bar-Cohen and A. D. Kraus, ASME Press, NY, pp. 241-250, 1990.
- [11] Katto, Y., Yokoya, Y. and Teraoka, K., "Nucleate Transition Boiling in a Narrow Space Between Two Horizontal, Parallel Disc Plates", Bulletin of the JSME, Vol. 20, pp. 98-107, 1977.
- [12] Nowell, R.M., Bhavnani, S. H. and Jaedar, R.C., "Effect of Channel Width on Pool Boiling from a Microconfigured Heat Sink", Proceedings of the Inter Society Conference on Thermal Phenomena in Electronic System (I-THERM IV), pp. 3-39,1990.
- [13] Githinji, P. M. , and Sabersky, R. H., 1963, "Some Effect of the Orientation of the Heating Surface in Nucleate Boiling", Trans. ASME J. Heat Transfer, Vol. 85, n4, pp. 379.
- [14] Nishikawa, K., Fujita, Y., Uchida, S. and Ohta, H., 1984, "Effect of Surface Configuration on Nucleate Boiling Heat Transfer, Int. J. Heat Mass Transfer, Vol. 27, n9, pp. 1559-1571.
- [15] Webb, R. L. , Gilley, M. D. , and Zernescu. V., "Advanced Heat Exchange Technology for Thermoelectric Cooling Devices", Proceedings of the 31st Heat Transfer Conference, ASME HTD Vol. 329, 7, 125-133, 1996.
- [16] Yuan, L., Joshi, Y., and Nakayama, W., 2001. "Effect of Condenser Location and Tubing Length on the Performance of a Compact Two-Phase Thermosyphon". Proceedings of 2001, International Mechanical Engineering Congress and Exposition, ASME, November 11-16, 2001, New York, NY.
- [17] Peterson, G. P. "An Introduction to Heat Pipes, Modeling, Testing and Applications", John Wiley & Sons Inc., New York, 1994.
- [18] Groll, M., et al., "Thermal Control of Electronic Equipment by Heat Pipes, Rev. Gen. Du Therm, Vol. 37, 1998.
- [19] Xie, H., Ali, A., Bhatia R., "The Use of Heat Pipes in Personal Computers", Intersociety Conf. On Thermal Phenomena, IEEE Conference, 1998.
- [20] Busse, CA. A. Reay "Theory of ultimate heat transfer limit of cylindrical Heat Pipes, Int. J. Heat and Mass Transfer. Vol. 16, pp 169-186, 1973.
- [21] Khrustalev D., Faghri A., "Thermal Characteristics of Conventional and Flat Miniature Axially-Grooved Heat Pipes", Journal of Heat Transfer Vol. 117, 1995.

- [22] Kaya, T., Hoang, T.T, "Mathematical Modeling of Loop Heat Pipes", American Institute of Aeronautics and Astronautics, AIAA 99-0477, pp. 1-10, 1999.
- [23] Ponnappan R., "Non Traditional Grooved Wicks for Flat Miniature Heat Pipe", 12th IHPC Conference, Moscow, May 2002.
- [24] Peterson G.P., Babin B.R., Wu D., "Steady State modeling and testing of a micro heat pipe", Heat Transfer T. ASME, 112 vol.8, 1990.
- [25] Wu D., Peterson G.P., Chang W.S., "Transient experimental investigation of micro heat pipes", Journal of Thermophys. Heat Tr. Vol.5, 1991.
- [26] Shen D. S. et al. "Micro Heat Spreader Enhanced Heat Transfer in MCMs", IEEE Multi-chip Module Conference, Santa Cruz, 1995.
- [27] Cao Y., Faghri A., "Micro/Miniature Heat Pipes and Operating Limitations", HTD Vol.236, ASME, 1993.
- [28] Gromoll B., "Micro Cooling Systems for High Density Packaging", Rev. Gen. Du Therm., vol. 37, 1998.
- [29] Zhuang J., "Research on CPU Heat Pipe Coolers", 12th IHPC, Mosca, May 2002.
- [30] Maidanik Y.F., Pastukhov V. G., Vershinin C.V., Koruko M. A. "Miniature Loop Heat Pipes for Electronic Cooling", 12th IHPC, Mosca, May 2002.
- [31] Miyasaka A., Nakajima K., Tsunoda H., "Experimental Results for Capillary Loop Pipe Applied to Direct Cooling Method", J. Thermo-physics Heat Transfer, vol. 9, 1995.
- [32] Chen Pin-Chih, Lin Wei-Keng, "The application of capillary pumped loop for cooling of electronic components", Applied Thermal Engineering, vol. 21, 2001.
- [33] Garner, S. D., and Patel, C. D., 2001. "Loop Thermosyphons and Their Applications to High Density Electronics Cooling". Proceedings of the International Electronic Packaging Technical Conference and Exhibition, 2001.
- [34] Webb, R. L., and Yamauchi, S., 2001. "Thermosyphon Concept to Cool Desktop Computers and Servers", Proceedings of the International Electronic Packaging Technical Conference and Exhibition, 2001.
- [35] Pal, A., Joshi, Y., Beitelmal, M. H., Patel, C. D., Wenger, T., "Design and Performance Evaluation of a Compact Thermosyphon", Proceedings of the

United Engineering Foundation, Thermes, Santa Fe, New Mexico, January 2002.

- [36] Alam, M., "Thermoloop Heat Transfer Technology", 9th AIAA/ASME Joint Thermophysics and Heat Transfer Conference, 5-8 June 2006, San Francisco, California.
- [37] Rahman, M.A., 2008, "Performance Study of a Pulsated Two-Phase Loop Thermosyphon ", M. Sc. Thesis, Department of Mechanical Engineering, Bangladesh University of Engineering & Technology, Dhaka.
- [38] Sasin, V.J., Borodkin, A.A., Feodorov, V.N., Bolotin, E.M., Fantozzi, F., "The Experimental Research of an Anti-Gravity Thermosyphons for A Heating System", LII Congress ATI, Cernobbio, Italy, 1997.
- [39] Polasek, F., Zelko, M., "Thermal Control of Electronic Components by Heat Pipes and Thermosyphons", Proc. Int. Heat Pipe Conf., Stuttgart, 1997.
- [40] Mathur, M. L., Sharma, R. P., " A Course in Internal Combustion Engines", Dhanpat Rai & Sons, Delhi, 1994, pp.243.
- [41] Fantozzi, F., Filippeschi, S. and Latrofa, E. M., "Miniature pulsated loop thermosyphon for desktop computer cooling: feasibility study and first experimental tests", 5th Minsk International Seminar on Heat pipes, Heat Pumps, Refrigerators, 8-11 September, 2003.
- [42] Murthy, S. S., "Thin Two-Phase Heat Spreaders with Boiling Enhancement Microstructures for Thermal Management of Electronic Systems", Ph.D. Dissertation, Department of Mechanical Engineering, Graduate School of the University of Maryland, 2004.
- [43] Ramaswamy, C., Joshi, Y., Nakayama, W., "Performance of a Compact Two-Chamber Two-Phase Thermosyphon: Effect of Evaporator Inclination, Liquid Fill Volume and Contact Resistance", Proc. of the 11th International Heat Transfer Conference, Kyongju, South Korea, Vol. 2, pp. 127-132, 1998.

APPENDIX-A

Total Heat Supply Calculation

$$Q = VI \cos\theta \quad (A1)$$

Where, V = Voltage, Volt

I = Current, Ampere

$\cos\theta = 0.8$

Q = Total Heat Supply, W

Heat Loss Calculation

$$\text{Total Heat Loss, } q_L = q_{\text{conv}} + q_{\text{radi}} \quad (A2)$$

$$q_{\text{conv}} = h_s A (T_E - T_a) \quad (A3)$$

Where, q_{conv} = Heat Loss by Convection, W

h_s = Heat Transfer Coefficient, $\text{W/m}^2\text{ }^\circ\text{C}$

A = Evaporator Surface Area (comprising of six surfaces), m^2

T_E = Evaporator Surface Temperature, $^\circ\text{C}$

T_a = Ambient Temperature, $^\circ\text{C}$

$$q_{\text{radi}} = \sigma A (T_E^4 - T_a^4) \quad (A4)$$

Where, q_{radi} = Heat Loss by Radiation, W

σ = Stefan-Boltzmann Constant

$$= 5.669 \times 10^{-8} \text{ W/m}^2\text{K}^4$$

Wall Superheat: (ΔT_{sat})

Wall superheat calculated for three different fluids, which are

$$\Delta T_{\text{sat}} = T_E - 64.7^\circ\text{C} \text{ (for methanol)}$$

$$\Delta T_{\text{sat}} = T_E - 78.3^\circ\text{C} \text{ (for ethanol)}$$

$$\Delta T_{\text{sat}} = T_E - 100^\circ\text{C} \text{ (for water)}$$

Rohsenow Correlation:

$$\frac{C_{p,l} \Delta T_{sat}}{h_{fg} Pr_{r,l}^n} = C_{s,f} \left[\frac{q_R}{\mu_l h_{fg}} \sqrt{\frac{\sigma}{g(\rho_l - \rho_v)}} \right]^{0.33}$$

Where, $C_{p,l}$ = specific heat of saturated liquid, J/kg.K

ΔT_{sat} = wall superheat = $T_E - T_{sat}$, °C

h_{fg} = enthalpy of vaporization, J/kg

$Pr_{r,l}$ = Prandtl number of saturated liquid

$n = 1.0$ for water and 1.7 for other liquids

$C_{s,f}$ = coefficient for various liquid surface combinations

q_R = heat flux from Rohsenow correlation, W/m²

μ_l = liquid viscosity, kg/m.s

σ = surface tension of liquid-vapor interface, N/m

g = gravitational acceleration, m/s²

ρ_l = density of saturated liquid, kg/m³

ρ_v = density of saturated vapor, kg/m³

Heat Flux from Rohsenow Correlation is calculated in the following way

$$q_R = \mu_l h_{fg} \left[\frac{g(\rho_l - \rho_v)}{\sigma} \right]^{\frac{1}{2}} \left[\frac{C_{p,l} \Delta T_{sat}}{C_{s,f} h_{fg} Pr_{r,l}^n} \right]^3 \quad (A5)$$

For Water:

$$\mu_l = 277.53 \cdot 10^{-6} \text{ kg/m.s}$$

$$h_{fg} = 2256.7 \cdot 10^3 \text{ J/kg}$$

$$g = 9.81 \text{ m/s}^2$$

$$\rho_l = 958.3 \text{ kg/m}^3$$

$$\rho_v = 0.597 \text{ kg/m}^3$$

$$\sigma = 58.91 \cdot 10^{-3} \text{ N/m}$$

$$C_{p,l} = 4.22 \cdot 10^3 \text{ J/kg.K}$$

$$C_{s,f} = 0.013$$

$$Pr_{r,l} = 1.72$$

$$n = 1.0$$

Putting the above value in equation (A5), we have

$$q_R = 277.53 \times 10^{-6} \times 2256.7 \times 10^3 \left[\frac{9.81(958.3 - 0.597)}{58.91 \times 10^{-3}} \right]^{\frac{1}{2}} \left[\frac{4.22 \times 10^3 \times \Delta T_{sat}}{0.013 \times 2256.7 \times 10^3 \times 1.72^1} \right]^3$$

$$q_R = 146.29(\Delta T_{sat})^3 \text{ W/m}^2$$

$$\therefore q_R = 0.0146(\Delta T_{sat})^3 \text{ W/cm}^2$$

For Ethanol:

$$\mu_l = 428.7 \times 10^{-6} \text{ kg/m.s}$$

$$h_{fg} = 963 \times 10^3 \text{ J/kg}$$

$$g = 9.81 \text{ m/s}^2$$

$$\rho_l = 757 \text{ kg/m}^3$$

$$\rho_v = 1.435 \text{ kg/m}^3$$

$$\sigma = 17.7 \times 10^{-3} \text{ N/m}$$

$$C_{p,l} = 3 \times 10^3 \text{ J/kg.K}$$

$$C_{s,f} = 0.002$$

$$Pr_{l,1} = 8.37$$

$$n = 1.7$$

Putting the above value in equation (A5), we have

$$q_R = 428.7 \times 10^{-6} \times 963 \times 10^3 \left[\frac{9.81(757 - 1.435)}{17.7 \times 10^{-3}} \right]^{\frac{1}{2}} \left[\frac{3 \times 10^3 \times \Delta T_{sat}}{0.002 \times 963 \times 10^3 \times 8.37^{1.7}} \right]^3$$

$$q_R = 19.87(\Delta T_{sat})^3 \text{ W/m}^2$$

$$\therefore q_R = 1.98 \times 10^{-3}(\Delta T_{sat})^3 \text{ W/cm}^2$$

For Methanol:

$$\mu_l = 428.7 \times 10^{-6} \text{ kg/m.s}$$

$$h_{fg} = 963 \times 10^3 \text{ J/kg}$$

$$g = 9.81 \text{ m/s}^2$$

$$\rho_l = 757 \text{ kg/m}^3$$

$$\rho_v = 1.435 \text{ kg/m}^3$$

$$\sigma = 17.7 \times 10^{-3} \text{ N/m}$$

$$C_{p,l} = 3 \times 10^3 \text{ J/kg.K}$$

$$C_{s,f} = 0.002$$

$$P_{r,1} = 8.37$$

$$n = 1.7$$

Putting the above value in equation (A5), we have

$$q_R = 428.7 \times 10^{-6} \times 963 \times 10^3 \left[\frac{9.81(757 - 1.435)}{17.7 \times 10^{-3}} \right]^{\frac{1}{2}} \left[\frac{3 \times 10^3 \times \Delta T_{sat}}{0.002 \times 963 \times 10^3 \times 8.37^{1.7}} \right]^3$$

$$q_R = 19.87(\Delta T_{sat})^3 \text{ W/m}^2$$

$$\therefore q_R = 1.98 \times 10^{-3} (\Delta T_{sat})^3 \text{ W/cm}^2$$

Thermal Resistance:

$$R = \frac{T_e - T_c}{Q_c} \quad (A6)$$

Where, R = Thermal Resistance, °C/W

Te = Average Evaporator Wall Temperature, °C

Tc = Average Condenser Outlet Temperature, °C

Qc = Heat Dissipated by Condenser, W

For Water:

$$Q = 225 \text{ W}$$

$$Q_c = 163.3 \text{ W}$$

$$T_e = 84.6 \text{ } ^\circ\text{C}$$

$$T_c = 31.8 \text{ } ^\circ\text{C}$$

From equation (A6), we have

$$\therefore R = 0.3233 \text{ } ^\circ\text{C/W}$$

For Ethanol:

$$Q = 225 \text{ W}$$

$$Q_c = 163.3 \text{ W}$$

$$T_e = 60.6 \text{ } ^\circ\text{C}$$

$$T_c = 31.1 \text{ } ^\circ\text{C}$$

From equation (A6), we have

$$\therefore R = 0.1794 \text{ } ^\circ\text{C/W}$$

For Methanol:

$$Q = 225 \text{ W}$$

$$Q_c = 163.3 \text{ W}$$

$$T_e = 58.5 \text{ }^\circ\text{C}$$

$$T_c = 31.6 \text{ }^\circ\text{C}$$

From equation (A6), we have

$$\therefore R = 0.1647 \text{ }^\circ\text{C/W}$$

Overall Heat Transfer Coefficient:

$$U_t = \frac{Q_c}{A_e(T_e - T_c)} \quad (\text{A7})$$

Where, U_t = Overall Heat Transfer Coefficient, $\text{W/m}^2 \text{ }^\circ\text{C}$

Q_c = Heat Dissipated by Condenser, W

A_e = Evaporator Surface Area, m^2

T_e = Average Evaporator Wall Temperature, $^\circ\text{C}$

T_c = Average Condenser Outlet Temperature, $^\circ\text{C}$

For Water:

$$Q = 225 \text{ W}$$

$$Q_c = 163.3 \text{ W}$$

$$A_e = 0.012 \text{ m}^2$$

$$T_e = 88.4 \text{ }^\circ\text{C}$$

$$T_c = 33.1 \text{ }^\circ\text{C}$$

From equation (A7), we have

$$\therefore U_t = 246.08 \text{ W/m}^2 \text{ }^\circ\text{C}$$

For Ethanol:

$$Q = 225 \text{ W}$$

$$Q_c = 163.3 \text{ W}$$

$$A_e = 0.012 \text{ m}^2$$

$$T_e = 62.4 \text{ }^\circ\text{C}$$

$$T_c = 31.3 \text{ }^\circ\text{C}$$

From equation (A7), we have

$$\therefore U_t = 437.56 \text{ W/m}^2 \text{ } ^\circ\text{C}$$

For Methanol:

$$Q = 225 \text{ W}$$

$$Q_c = 163.3 \text{ W}$$

$$A_e = 0.012 \text{ m}^2$$

$$T_e = 59.2 \text{ } ^\circ\text{C}$$

$$T_c = 32.1 \text{ } ^\circ\text{C}$$

From equation (A7), we have

$$\therefore U_t = 502.15 \text{ W/m}^2 \text{ } ^\circ\text{C}$$

APPENDIX-B

RAW SAMPLE DATA

Working fluid: Ethanol

Date: 01/09/08

Input power: 150W, Geometry:1

CycleNo.	tct(Sec)	Time(sec)	TE(0C)	TCin(0C)	TCout(0C)
1	283	0	28.2	28.2	28.2
		10	29.6	28.2	28.2
		20	31.1	28.1	28.2
		30	32.8	28.1	28.1
		40	35	28.1	28.1
		50	37.6	26.9	28
		60	40.4	26.9	28
		70	41.8	26.9	30.4
		80	42.9	27	30.4
		90	44.8	27	30.5
		100	46.8	27.1	30.5
		110	49.2	27.1	30.5
		120	52.6	27.1	30.5
		130	56	27.1	30.6
		140	59.9	27.1	30.6
		150	62.5	27.1	30.6
		160	65.3	30.6	30.6
		170	66.1	45.3	30.7
		180	68	48.6	30.9
		190	69.1	50.4	31.1
		200	70.3	51.1	31.3
		210	70.1	51.6	31.6
		220	71.8	52.1	31.8
		230	70.8	52.3	31.9
		240	71	52.7	32.1
		250	71	53.2	32.3
		260	69.7	53.6	32.5
		270	69.8	54.2	32.7
		280	69.2	54.4	32.7
290	69.1	47.2	32.7		
2	111	300	67.1	44.5	32.7
		310	67	46.1	32.8
		320	67.2	51.4	33.5
		330	68.7	52.3	33.6

		340	69.6	52.8	33.8
		350	70.6	53.1	33.9
		360	69.4	53.4	33.9
		370	70.9	53.9	33.8
		380	70.7	54.2	33.7
		390	71.2	54.9	33.6
		400	71.2	49.4	33.6
		410	69.4	45.5	33.5
		420	70.8	50.3	33.4
		430	71.1	52.1	33.8
		440	71	52.5	34
		450	70.4	52.9	34.2
		460	69.5	53	34.2
		470	69.7	53.3	34.2
		480	68.9	53.8	34.1
		490	69	54.3	33.9
		500	68.5	54.4	33.8
		510	66.8	48.3	33.6
		520	67.2	45.7	33.6
		530	69.4	52	33.7
		540	71.2	52.5	33.9
		550	70.2	52.8	34.2
		560	69	53.3	34.3
		570	68.6	53.4	34.1
		580	67.9	54	33.9
		590	68	54.2	33.9
		600	68.8	54.4	33.6
		610	68.8	49.4	33.5
		620	66.9	46.1	33.6
		630	68.6	49.3	34
		640	69	52	34.3
		650	70.2	52.4	34.4
		660	69.2	52.9	34.5
		670	69.5	53.2	34.5
		680	70	53.4	34.3
		690	69.7	53.9	34.1
		700	68.9	54.4	34.1
		710	70.6	54.7	33.8
		720	67.5	48.2	33.7
		730	67.2	45	33.8
		740	69.2	51.5	34
		750	70.6	52.5	34.3

		760	69.8	53	34.4
		770	70.9	52.4	34.3
		780	71.3	53.6	34.3
		790	71	53.8	34.2
		800	70.6	54.4	34
		810	69.3	54.7	34
		820	68.4	48.1	33.8
		830	68.5	46.1	34
7	101	840	69	51.2	34.2
		850	70.1	52.2	34.5
		860	69.3	52.7	34.6
		870	69.9	53.1	34.5
		880	68.3	53.4	34.4
		890	68	53.7	34.3
		900	68	54.2	34.2
		910	68.8	54.7	34.2
		920	67.3	47.1	33.8
		930	66.5	45	33.8
		940	67.7	50.9	34.1
		950	68.7	52.4	34.5
		960	68.6	52.7	34.6
8	101	970	68.3	53	34.6
		980	68.7	53.5	34.4
		990	69	53.9	34.3
		1000	68.5	54.3	34.2
		1010	68.4	54.6	34.1
		1020	66	50.5	33.9
		1030	68.5	45	33.8
		1040	69.4	51	34
		1050	71	52.2	34.2
		1060	70.8	52.8	34.4
		1070	69.7	53.1	34.3
		1080	71	53.4	34.3
		1090	71	53.7	34.2
		1100	70.9	54.1	34.1
		1110	70.8	54.4	34
		1120	69.3	50.5	33.9
9	100	1130	69.7	48.1	33.9
		1140	71.6	44.5	33.8
		1150	70.9	49.5	34.1
		1160	69.7	52.1	34.2
10	104	1170	68.7	52.9	34.4

		1180	69.4	53.3	34.3
		1190	69.5	53.8	34.3
		1200	69.7	54.1	34
		1210	69.8	54.4	34
		1220	69.6	52.6	33.9
11	103	1230	68.1	45.7	33.7
		1240	68.9	47.1	33.8
		1250	69	52	34.1
		1260	69.2	52.4	34.3
		1270	69.4	53	34.3
		1280	71.4	53.2	34.2
		1290	71.1	53.5	34.2
		1300	69.2	53.8	34.1
		1310	69	54.1	34
		1320	68.6	54.4	34
		1330	67.1	50.3	33.8
12	103	1340	66.4	46.6	33.8
		1350	66.4	46.3	33.9
		1360	65.9	51.7	34.1
		1370	67.3	52.7	34.4
		1380	67.3	53	34.4
		1390	67.7	53.3	34.3
		1400	66.1	53.5	34.3
		1410	67.9	54.1	34.2
		1420	66.8	54.5	34.1

Working fluid: Ethanol

Date:30/08/08

Input power: 210W, Geometry:1

CycleNo.	tct(Sec)	Time(sec)	TE(0C)	TCin(0C)	TCout(0C)
1	148	0	28.4	28.4	28.4
		10	35.4	28.4	28.5
		20	37.7	28.4	28.6
		30	41.6	28.4	28.6
		40	45.9	28.4	28.6
		50	50	28.4	28.6
		60	55.1	28.4	28.6
		70	61	28.4	28.6
		80	67.3	28.5	28.6
		90	71.3	39.8	28.7

		100	74	50.6	28.8
		110	77	53.8	29.7
		120	78.6	55.4	30.8
		130	78.6	56.6	31.4
		140	77.1	57.9	31.8
2	52	150	76.5	51.8	32.2
		160	73.9	46.9	33.4
		170	75.3	54	35
		180	75.2	55.9	36.6
		190	75.7	57	36.8
		200	74.8	58	36.6
3	49	210	73.7	49.5	36.1
		220	76.5	55.6	36.8
		230	77.3	56.4	38.2
		240	76.7	57.1	38.2
4	39	250	77.9	57.6	37.8
		260	75.7	50.3	36.8
		270	77.3	56.1	37.6
		280	77.6	56.8	39.2
5	38	290	76.1	52.3	38.9
		300	75.6	49.8	38.2
		310	76.6	56.2	38.5
		320	76.5	56.7	40.3
6	47	330	75.4	52.2	39.6
		340	76	51.6	39.7
		350	77.4	56.6	39.5
		360	78.4	57	40.5
		370	76.3	58.2	40
7	39	380	74.9	51.8	38.8
		390	75.4	55.6	38.9
		400	76.2	56.7	40.6
		410	76.3	57.3	40.6
8	43	420	76	50.9	39.2
		430	75.5	55.8	38.9
		440	75.3	56.7	40.7
		450	76	57.4	40.7
9	33	460	75.8	52	39.9
		470	75.8	54.5	38.9
		480	76.1	56.6	40.7
10	35	490	76.4	54	41.1
		500	75.1	50.6	40.6
		510	75.6	56.5	40.9

		520	74.6	57.1	41.8
11	32	530	73.5	52.6	40.6
		540	73.8	54.3	41.2
		550	75.2	56.5	41.8
12	38	560	75	51.7	41.5
		570	75.4	51.7	41.1
		580	75.7	56.4	41
		590	75.6	57.1	41.1

Working fluid: Ethanol

Date:30/08/08

Input power: 210W, Geometry:1

CycleNo.	tct(Sec)	Time(sec)	TE(0C)	TCin(0C)	TCout(0C)
1	148	0	28.4	28.4	28.4
		10	35.4	28.4	28.5
		20	37.7	28.4	28.6
		30	41.6	28.4	28.6
		40	45.9	28.4	28.6
		50	50	28.4	28.6
		60	55.1	28.4	28.6
		70	61	28.4	28.6
		80	67.3	28.5	28.6
		90	71.3	39.8	28.7
		100	74	50.6	28.8
		110	77	53.8	29.7
		120	78.6	55.4	30.8
		130	78.6	56.6	31.4
2	52	140	77.1	57.9	31.8
		150	76.5	51.8	32.2
		160	73.9	46.9	33.4
		170	75.3	54	35
		180	75.2	55.9	36.6
		190	75.7	57	36.8
3	49	200	74.8	58	36.6
		210	73.7	49.5	36.1
		220	76.5	55.6	36.8
		230	77.3	56.4	38.2
4	39	240	76.7	57.1	38.2
		250	77.9	57.6	37.8
		260	75.7	50.3	36.8
		270	77.3	56.1	37.6
		280	77.6	56.8	39.2

5	38	290	76.1	52.3	38.9
		300	75.6	49.8	38.2
		310	76.6	56.2	38.5
		320	76.5	56.7	40.3
6	47	330	75.4	52.2	39.6
		340	76	51.6	39.7
		350	77.4	56.6	39.5
		360	78.4	57	40.5
		370	76.3	58.2	40
7	39	380	74.9	51.8	38.8
		390	75.4	55.6	38.9
		400	76.2	56.7	40.6
		410	76.3	57.3	40.6
8	43	420	76	50.9	39.2
		430	75.5	55.8	38.9
		440	75.3	56.7	40.7
		450	76	57.4	40.7
9	33	460	75.8	52	39.9
		470	75.8	54.5	38.9
		480	76.1	56.6	40.7
10	35	490	76.4	54	41.1
		500	75.1	50.6	40.6
		510	75.6	56.5	40.9
		520	74.6	57.1	41.8
11	32	530	73.5	52.6	40.6
		540	73.8	54.3	41.2
		550	75.2	56.5	41.8
12	38	560	75	51.7	41.5
		570	75.4	51.7	41.1
		580	75.7	56.4	41
		590	75.6	57.1	41.1

